PE&RS

November 2024 Volume 90, Number 11

PHOTOGRAMMETRIC ENGINEERING & REMOTE SENSING

The official journal for imaging and geospatial information science and technology

A

New-Generation Spaceborne Hyperspectral Sensors Ushering in a New Era in Remote Sensing

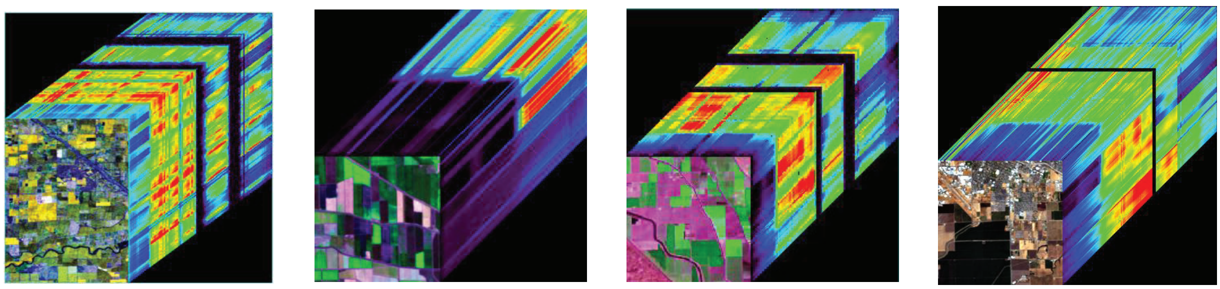

Hyperion **DESIS** **PRISMA** **EnMAP**

B

Spectral Library of California's Cotton Crop using Hyperspectral Data

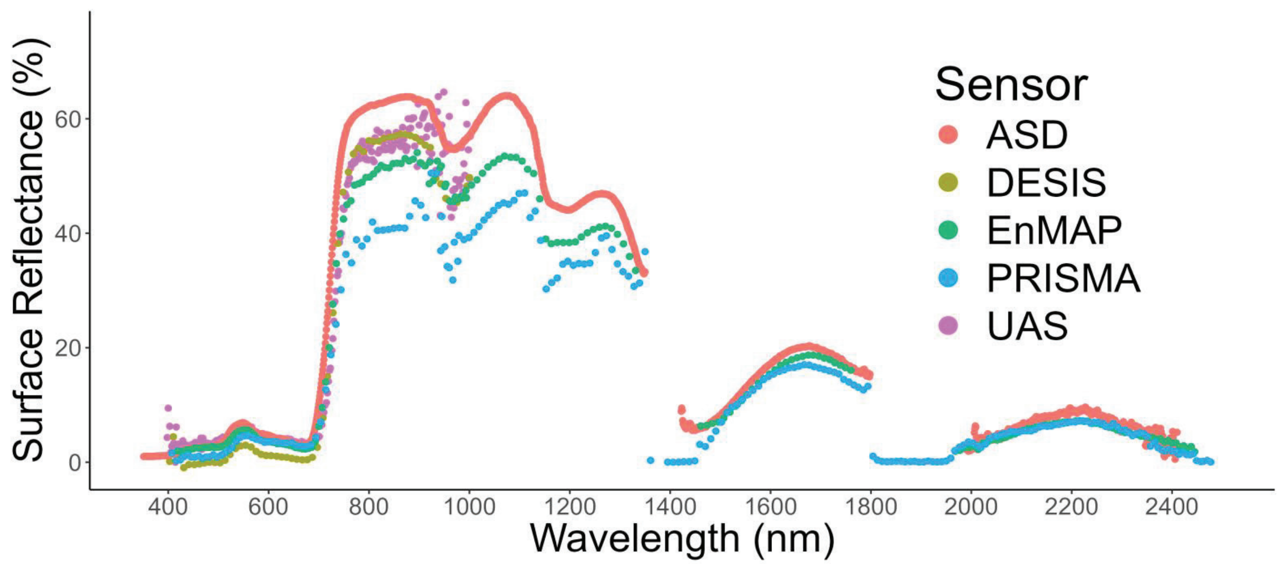

C

Crop Classification Using DESIS Hyperspectral data and Machine Learning Algorithms (MLAs)

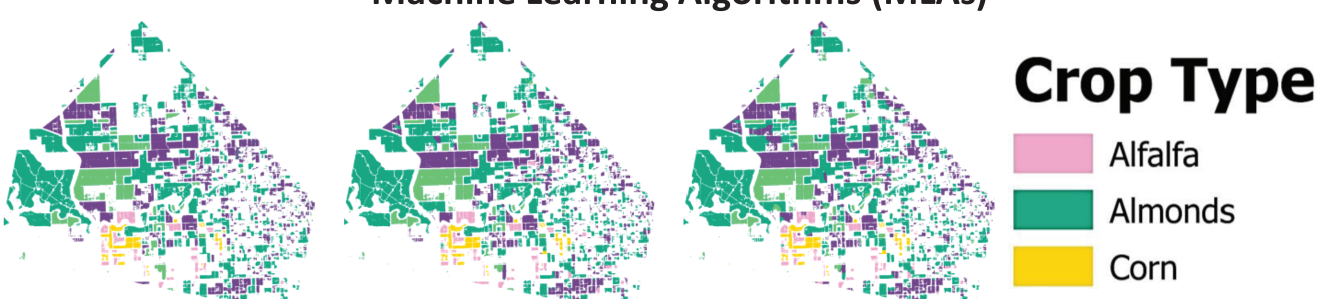

USDA NASS CDL
Reference Data

DESIS SVM
Full Spectral Analysis (FSA)

DESIS SVM
Optimal Hyperspectral Narrowbands (OHNBs)

asprs THE IMAGING & GEOSPATIAL INFORMATION SOCIETY

ASPRS MEMBERSHIP

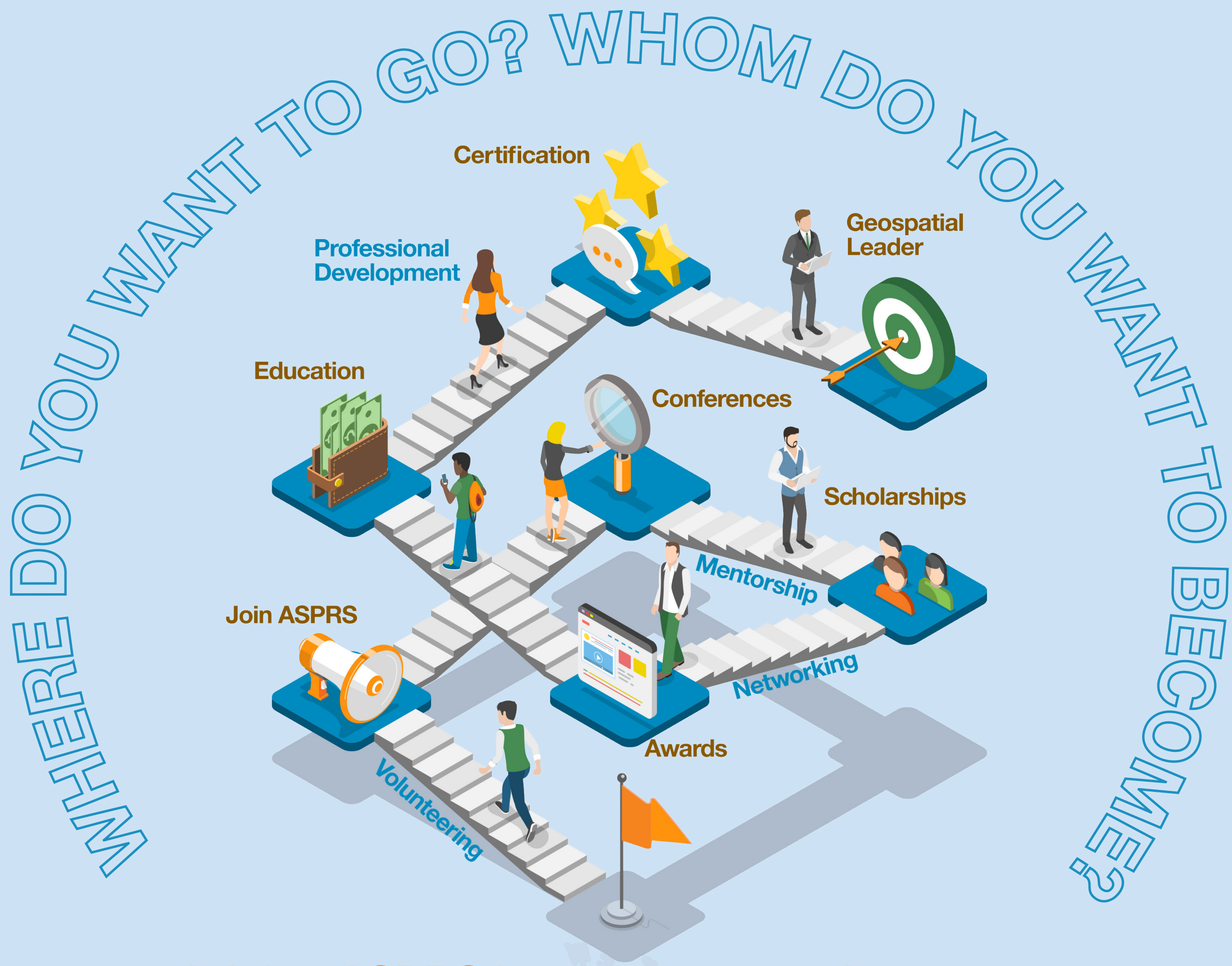

Joining ASPRS is a great way to boost your resume and learn valuable life lessons

WHY GET INVOLVED WITH ASPRS?

- Develop leadership skills
- Experience working on a team
- Gain valuable soft skills
- Network
- Learn about yourself
- Have fun!

Scholarships

The many ASPRS scholarships are only available to student members

Certification

The ASPRS certification program for mapping scientists, photogrammetrists and technologists is the only fully Accredited certification program in the geospatial sciences

Continuing Education

Earn professional development hours and CEUs by attending workshops at our conferences and on-line as well as our monthly on-line geobytes series

PE&RS

Our monthly journal, is packed with informative and timely articles designed to keep you abreast of current developments in your field. Now available in e-format.

Get Connected

facebook.com/ASPRS.org

linkedin.com/company/asprs/about/

twitter.com/ASPRSorg

youtube.com/user/ASPRS

Image and text courtesy the ASPRS Florida Region

asprs FLORIDA REGION THE IMAGING & GEOSPATIAL INFORMATION SOCIETY

To have your press release published in *PE&RS*, contact Rae Kelley, rkelley@asprs.org.

INDUSTRYNEWS

ANNOUNCEMENTS

During the opening session of GIS-Pro 2024, URISA (Urban and Regional Information Systems Association) officially announced its rebranding as the Geospatial Professional Network (GPN). This change reflects the organization's evolution to better serve the global geospatial community. The announcement, made by URISA President Thomas Fisher, AICP, GISP, and President-Elect John Nolte, GISP, signifies a major milestone in the organization's legacy of leadership in GIS.

A New Name for a Broader Mission — The transition to the Geospatial Professional Network marks a significant shift from URISA's original focus on urban information systems. While still serving urban and regional geospatial professionals, the new name represents a broader mission to unite GIS professionals across all sectors and regions, providing enhanced opportunities for career development, networking, and education.

"We've known for some time that we needed a brand that invited professionals in, saying, 'Come and join us right now,'" said Thomas Fisher, URISA President. "This rebranding is a pivotal step in ensuring that our organization continues to empower GIS professionals globally while staying relevant to the diverse and expanding field of geospatial technology."

Sara Thompson, 2023-2024 Vanguard Cabinet Chair, echoed the importance of the rebrand: "The urban and regional aspect is definitely a misnomer. That wasn't where I came from, and for years, URISA wasn't relevant to my GIS work at a nonprofit. The old name gave the impression that the organization was for urban planners. This rebrand clears up that confusion and positions us to connect with a much broader community of GIS professionals."

A Thoughtful Rebranding Process — The rebranding initiative was driven by extensive research, including interviews with leadership and a comprehensive survey of the membership. The feedback clearly indicated a desire for an identity that better reflects the organization's growing role in supporting professionals at all stages of their GIS careers, from recent graduates to seasoned experts.

"The power of this network—whether it's solving problems, building connections, or advancing careers—cannot be overstated," said John Nolte, President-Elect. "We're deeply passionate about GIS, and we believe this new identity will help us reach an even larger and more diverse community of geospatial professionals."

As the Geospatial Professional Network, the organization will continue providing renowned programs, such as the GIS Leadership Academy, and foster partnerships with local and regional GIS groups. With this new identity, GPN is poised to become an even more integral part of the global geospatial landscape, offering tools, resources, and a supportive community for GIS professionals everywhere.

Visit www.geospatialprofessionalnetwork.org/ for more information.

The GIS Certification Institute (GISCI) is thrilled to announce the appointment of a new president and several outstanding board members, highlighting its unwavering commitment to elevating the geospatial profession and driving innovation in the field.

Effective immediately, Chief Executive Officer of Cultivate Geospatial Solutions LLC Allen Ibaugh, GISP, will step into the role of President of the GISCI Board. With extensive experience in the geospatial industry, Ibaugh is dedicated to enhancing the value of the GISP certification and promoting high professional standards across the sector. He previously served as the Vice President and represented URISA. Jochen Albrecht, Ph.D., GISP, who served as President from 2022-2024, will continue to contribute his expertise as a Director on the GISCI Board and representative to UCGIS.

Additionally, the GISCI Board of Directors welcomes several new members who bring a wealth of knowledge and expertise to the organization. Demetrio P. Zourarakis, Ph.D., GISP, CMS, and Karen Schuckman, PLS, CP, CMS-Lidar, will serve as the ASPRS Representatives for 2024-2027, further strengthening the partnership between GISCI and ASPRS. Tripp Corbin, GISP, also joins as a URISA Representative for the 2024-2027 term. Together, these new members will play a vital role in advancing the geospatial profession and supporting GIS practitioners.

The GISCI Board also extends their gratitude to Martin Roche for his twelve years of dedicated service to the organization. His leadership and contributions have been instrumental in the growth and success of GISCI over the past decade.

As the organization continues to evolve, GISCI remains committed to fostering the professional development of GIS practitioners and advancing the geospatial field. The newly appointed board members bring new perspectives and expertise that will further enhance GISCI's mission. For more information about GISCI and its initiatives, visit www.gisci.org.

NV5 Global, Inc., www.nv5.com, a provider of technology, certification, and consulting solutions, announced today that it has been awarded a prime contract with the National

Geospatial-Intelligence Agency (NGA) to provide unclassified commercial geospatial intelligence (GEOINT)-derived computer vision and analytic services under the Luno A program.

"We are pleased to have been selected by NGA to support the national intelligence community through GEOINT-derived analytics," said Dickerson Wright, PE, Executive Chairman of NV5. "NV5 has built a reputation supporting NGA's mission for over 20 years, and we look forward to expanding our relationship with NGA and the value we deliver to the agency through the Luno A program."

The $290 million contract is a five-year, multiple-award indefinite delivery, indefinite quantity contract to monitor global economic and environmental activity, as well as military capabilities. The contract will leverage commercial computer vision and artificial intelligence capabilities and will integrate into analytic workflows for the national security community's operational use. NV5 anticipates that it will receive approximately $30 million in revenue over the term of the Luno A contract.

Esri, www.esri.com, the global leader in location intelligence recently entered into a cooperative research and development agreement (CRADA) with the National Oceanic and Atmospheric Administration (NOAA) to increase the accessibility of ocean and coastal data. This partnership will create a first-of-its-kind open data platform that will empower decision-makers and communities with equitable, actionable, and ready-to-use information. By combining NOAA's world-class data with Esri's geospatial technology, the online hub will provide timely, relevant, user-friendly information that helps support sustainable development while also protecting and restoring marine ecosystems.

Currently, vital ocean and coastal data exist across a patchwork of disconnected sources. This data often requires significant translation before stakeholders can make use of it.

"This collaboration could not come at a more important time in helping our coastal communities remain vibrant now and in the future," said NOAA Administrator Rick Spinrad, Ph.D. "Combining NOAA's ocean and coastal expertise with Esri's long history of user-centered successes will unlock the true value of this data in the hands of the communities that need it most."

As part of the agreement NOAA will build a prototype ocean and coastal data hub demonstration project using Esri technology that turns overwhelming amounts of data into local, issue-relevant information. The resulting hub will serve as a proof of concept for a new publicly accessible resource. Ocean community organizations, NGOs, academia, and the private sector will be able to use the hub make NOAA data an actionable tool for accomplishing their goals. The aim for the hub is a site where different visitors can find answers to wide-ranging questions like "Where can I fish?", "Where can I lay an underwater cable?", "What are the latest nautical charts?", or "How is climate change impacting vital marine ecosystems?"

"The ocean covers 70 percent of our planet, and yet its terrain and ecosystems remain some of the most unknown on the planet," said Jack Dangermond, Esri president. "We are happy to collaborate with NOAA to help make their comprehensive and authoritative ocean and coastal data a mapping resource for decision-making, conservation, and education. By combining our expertise, we can unlock the full potential of this data and empower users to make informed decisions that contribute to a thriving blue economy while safeguarding our oceans and coasts for future generations."

NOAA and Esri have a long history of collaborating on tools aimed at bringing understanding of ocean, weather, and climate data to users of all types. This includes the creation of Heat.gov as well as the Climate Mapping for Resilience and Adaptation (CMRA) portal. Both websites provide easily accessible and interactive geospatial information for decision-makers and stakeholders about climate hazards impacting their communities.

After six months and the completion of the demonstration project, NOAA and Esri will reevaluate their agreement and decide how to move forward.

To learn more about how Esri's is helping advance the field of ocean science through GIS, visit esri.com/en-us/about/science/initiatives/ocean-science**.**

CALENDAR

- 18-22 November, **URISA GIS Leadership Academy**, Fort Worth, Texas; https://urisa.org/page/URISA_AdvancedGLA.
- 2-6 December, **URISA GIS Leadership Academy**, virtual; https://urisa.org/page/URISA_AdvancedGLA.
- 29-31 January, 2025, **ISPRS, EARSeL & DGPF Joint Istanbul Workshop**, Istanbul, Turkey; https://isprsistanbul2025.org/
- 10-12 February 2025, **Geo-Week**, Denver, Colorado; www.geo-week.com/

PE&RS

PHOTOGRAMMETRIC ENGINEERING & REMOTE SENSING

The official journal for imaging and geospatial information science and technology

November 2024 Volume 90 Number 11

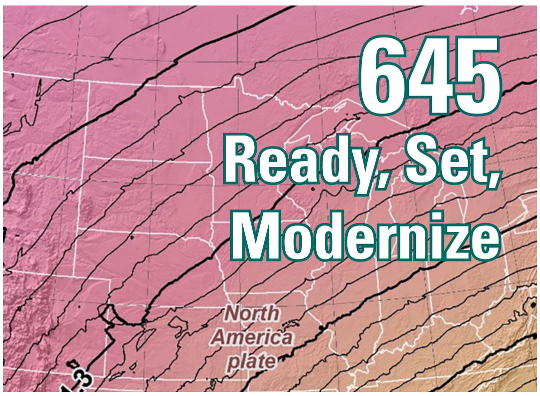

HIGHLIGHT ARTICLE

COLUMNS

ANNOUNCEMENTS

DEPARTMENTS

See the Cover Description on Page 644

COVER DESCRIPTION

The front cover page depicts the new generation of spaceborne hyperspectral sensors ushering in a new era in satellite remote sensing of the Earth.

A. Images depict hyperspectral data cubes of the German DESIS sensor onboard the International Space Station (ISS) acquiring data in 235 hyperspectral narrow bands (HNBs) over 400-1000 nm spectral range in 2.55 to 10 nm bandwidths, polar-orbiting Italian PRISMA acquiring data in 238 HNBs over 400-2500 nm spectral range and 10 to 12 nm bandwidth, and polar-orbiting German EnMAP acquiring data in 222 HNBs over 400-2500 nm spectral range and 10 nm bandwidth. This is compared with old-generation NASA's polar-orbiting Hyperion acquiring data in 242 HNBs over 400-2500 nm spectral range and 10 nm bandwidth.

B. Spectral libraries of the irrigated cotton crop of California's Central Valley for August 2023 acquired for a ground-based ASD spectroradiometer (400-2500 nm, in 1 nm bandwidth), spaceborne DESIS, and drone acquired hyperspectral data (400-2500 nm, in 2 nm bandwidth). Spaceborne PRISMA and EnMAP spectra from September 2022 and September 2023 respectively.

C. Crop type classification of a study area using DESIS hyperspectral data and the Machine Learning Algorithm (MLA) Support Vector Machines (SVM) based on full spectral analysis involving HNBs (except one omitted noisy band) and 9 optimal HNBs (OHNBs) and compared to the USDA NASS Cropland Data Layer (CDL) reference data.

Cover page credits
Dr. Itiya Aneece, United States Geological Survey (USGS)
Dr. Prasad Thenkabail, United States Geological Survey (USGS)
Dr. Pardhasarathi Teluguntla, Bay Area Environmental Research Institute @ USGS

asprs
THE IMAGING & GEOSPATIAL INFORMATION SOCIETY

PHOTOGRAMMETRIC ENGINEERING & REMOTE SENSING

JOURNAL STAFF

Publisher ASPRS
Editor-In-Chief Alper Yilmaz
Director of Publications Rae Kelley
Electronic Publications Manager/Graphic Artist
Matthew Austin

Photogrammetric Engineering & Remote Sensing is the official journal of the American Society for Photogrammetry and Remote Sensing. It is devoted to the exchange of ideas and information about the applications of photogrammetry, remote sensing, and geographic information systems. The technical activities of the Society are conducted through the following Technical Divisions: Geographic Information Systems, Photogrammetric Applications, Lidar, Primary Data Acquisition, Professional Practice, Remote Sensing Applications, and Unmanned Autonomous Systems. Additional information on the functioning of the Technical Divisions and the Society can be found in the Yearbook issue of *PE&RS*.

All written correspondence should be directed to the American Society for Photogrammetry and Remote Sensing, PO Box 14713, Baton Rouge, LA 70898, including general inquiries, memberships, subscriptions, business and editorial matters, changes in address, manuscripts for publication, advertising, back issues, and publications. The telephone number of the Society Headquarters is 225-408-4747; the fax number is 225-408-4422; web address is www.asprs.org.

PE&RS. *PE&RS* (ISSN0099-1112) is published monthly by the American Society for Photogrammetry and Remote Sensing, 8550 United Plaza Blvd, Suite 1001, Baton Rouge, Louisiana 70809 . Periodicals postage paid at Bethesda, Maryland and at additional mailing offices.

SUBSCRIPTION. *PE&RS* is available as an e-Subscription (single-site and multi-site licenses) and an e-Subscription with print add-on (single-site license only). PE&RS subscriptions are on a calendar-year, beginning in January and ending in December.

The rate for a single-site e-Subscription for the USA/Non-USA is $1040 USD, for Canadian* is $1092 USD.

The rate for a multi-site e-Subscription for the USA/Non-USA is $1040 USD plus $250 USD for each additional license, for Canadian* is $1092 USD plus $263 for each additional license.

The rate for e-Subscription with print add-on for the USA is $1546 USD, for Canadian* is $1637 USD, and for Non-USA is $1596 USD.

*Note: Subscription prices for Canada includes 5% of the total amount for Canada's Goods and Services Tax (GST #135123065). **PLEASE NOTE: All Subscription Agencies receive a 20.00 USD discount.**

POSTMASTER. Send address changes to PE&RS, ASPRS, PO Box 14713, Baton Rouge, LA 70898. CDN CPM #(40020812).

MEMBERSHIP. Membership is open to any person actively engaged in the practice of photogrammetry, photointerpretation, remote sensing and geographic information systems; or who by means of education or profession is interested in the application or development of these arts and sciences. Membership is for one year, with renewal based on the anniversary date of the month joined. Membership Dues include a 12-month electronic subscription to *PE&RS*. Annual Individual Membership dues are $175.00 USD and Student Membership dues are $50.00 USD. A tax of 5% for Canada's Goods and Service Tax (GST #135123065) is applied to all members residing in Canada.

READY, SET, MODERNIZE

ASPRS Takes on Preparing the Geospatial Industry for the Modernized National Spatial Reference System (NSRS)

ASPRS NSRS MODERNIZATION WORKING GROUP

Christopher Parrish *Oregon State University*
Qassim Abdullah *Woolpert, Inc.*
Linda Foster *ESRI & NSPS*
Stephen White *NOAA National Geodetic Survey*
Jenna Borberg *Oregon State University*

Context

The National Geodetic Survey (NGS) is modernizing the National Spatial Reference System (NSRS) in the United States. The modernization involves significant updates to the official reference frames and vertical datum used across the country, affecting the entire geospatial industry. Key benefits of the Modernized NSRS will include improved accuracies and enhanced interoperability and sustainability of geospatial data and systems.

The ASPRS NSRS Modernization Working Group produced this paper to help prepare the geospatial industry for the upcoming changes. It serves as a guide for industry professionals to understand the implications of the Modernized NSRS and recommendations to begin preparing for it. It emphasizes the importance of proactive measures to ensure a smooth transition to the new reference frames and vertical datum.

Your Input Wanted!

The ASPRS NSRS Modernization Working Group wants to hear your Success Stories. Please submit short news articles describing how the Modernized NSRS will benefit your work and how your organization is working to transition to the Modernized NSRS. To share your messages and success stories, please contact the Working Group through the ASPRS NSRS Modernization Working Group community page at: https://community.asprs.org/wg-nsrs/home.

Photogrammetric Engineering & Remote Sensing
Vol. 90, No. 11, November 2024, pp. 645-651.
0099-1112/22/645-651

doi: 10.14358/PERS.90.11.645

Introduction

The geospatial industry is on the brink of a major advance that will affect all facets of our work. For the first time in over four decades, the official reference frames and geopotential (vertical) datum of the U.S., including territories, are scheduled to be updated. The primary reasons for the updates include the non-geocentricity of the current North American Datum of 1983 (NAD 83) frames, bias and tilt of the North American Vertical Datum of 1988 (NAVD 88), multiple vertical datums, sea level change, the dynamic movements of geodetic control marks, and vast improvements in survey technologies and accuracies since the 1980s.[1] As large volumes of existing maps and geospatial data are referenced to NAD 83 and NAVD 88, these updates are a significant undertaking with broad-reaching implications.

The agency leading these updates is the National Geodetic Survey (NGS), a program office within the National Oceanic and Atmospheric Administration (NOAA), National Ocean Service (NOS). NGS is mandated to define, maintain, and provide access to the National Spatial Reference System (NSRS), the official system that defines latitude, longitude, gravity, scale, orientation, and height throughout the nation.

This paper highlights the main upcoming changes, the impacts to existing maps and geospatial data, and the benefits of NSRS Modernization for the geospatial industry, including those working in photogrammetry, lidar, sonar, remote sensing, mobile mapping, surveying and GIS, among others. We then present recommendations for geospatial firms in preparing for NSRS Modernization. These recommendations are separated into those for geospatial service providers, software manufacturers, and the entire industry. We conclude with a look ahead at the anticipated NSRS Modernization schedule and opportunities for getting involved in ongoing efforts to assist with the integration of the Modernized NSRS into geospatial infrastructure and workflows.

1. NOAA Technical Report NOS NGS 67 "Blueprint for the Modernized NSRS, Part 3: Working in the Modernized NSRS"; https://www.ngs.noaa.gov/library/pdfs/NOAA_TR_NOS_NGS_0067.pdf

Key Changes and What Happens to Existing Geospatial Data

Key changes in the Modernized NSRS are summarized in Table 1. It should be noted that the information in this table is intended only as a high-level synopsis. Full details on the changes can be found in NGS's Blueprint documents for the Modernized NSRS.[2]

Terrestrial Reference Frames: NAD 83→NATRF2022

- NSRS Modernization will include the replacement of the current three NAD 83 datums (frames) with four new terrestrial reference frames (TRFs):
  - North American Terrestrial Reference Frame of 2022 (NATRF2022)
  - Pacific Terrestrial Reference Frame of 2022 (PATRF2022)
  - Mariana Terrestrial Reference Frame of 2022 (MATRF2022)
  - Caribbean Terrestrial Reference Frame of 2022 (CATRF2022)
- These four reference frames are sometimes collectively abbreviated NAT/PAT/MAT/CATRF2022. They will replace NAD 83(2011) for North America and the Caribbean, NAD 83(PA11) for the Pacific, and NAD 83(MA11) for Guam and the Northern Mariana Islands.
- NATRF2022 will be the primary terrestrial reference frame covering the contiguous U.S. and Alaska. Within this region, NATRF2022 is what will be entered in a field that, in geospatial software, is often labeled "horizontal datum." However, it should be noted that NAT/PAT/MAT/CATRF2022 are more precisely referred to as "reference frames," and like the current three NAD 83 datums (also often called "frames"), will support measurements of latitude, longitude, and ellipsoid height, such that "horizontal" is a misnomer.
- The new TRFs are "plate fixed." This means that each is tied to a specific tectonic plate and accounts for that plate's rigid motion, maintaining a higher level of coordinate

2. NOAA NGS. Blueprint for Modernized NSRS, Parts 1, 2 and 3: https://geodesy.noaa.gov/datums/newdatums/policy.shtml

Table 1. Summary of changes from the current NSRS to Modernized NSRS.

Current NSRS	Modernized NSRS	Summary of key benefits
Three datums (frames): NAD 83(2011) NAD 83(PA11), and NAD 83(MA11)	Four frames: NATRF2022, PATRF2022, CATRF2022, and MATRF2022	Improved accuracies supporting current geospatial requirements and survey technologies; correct Earth's geocenter by ~2.24 m (Figure 1); support time-dependency of coordinates
NAVD 88 (and other vertical datums on islands and for the Great Lakes)	NAPGD2022	More accurate heights; better predict water flow; eliminate reliance on physical survey marks; replace multiple vertical datums with a single geopotential datum
GEOID18 (and GEOID12b and previous hybrid GEOID models)	GEOID2022	Better model, incorporating nearly 16 million square kilometers of new gravity data; not a "hybrid" model warped to match leveled bench marks
SPCS 83	SPCS2022	Reduce distortion; provide many more zones, incorporating stakeholder input

consistency over time. The three NAD 83 frames are also plate fixed, but the plate rotation will be more accurately modeled for the new TRFs.

- NATRF2022 will be aligned to ITRF2020 at epoch 2020.00 and then will diverge from ITRF2020 based on plate motion modeled as an Euler pole rotation. The same will be true of the three other TRFs, and each will have its own Euler pole.
- NAD 83 will remain valid datums, and not all existing maps and geospatial data will need to be transformed. This is directly analogous to the many historic maps that are referenced to the now long-superseded North American Datum of 1927 (NAD 27).
- For data that need to be transformed to the new reference frames, practitioners should be aware of the anticipated magnitudes of coordinate shifts and the uncertainty that this transformation will add. The Earth's origin will shift by ~2.24 meters (Figure 1); with this, in the conterminous U.S., transformed data will undergo shifts of up to several meters horizontally (Figure 2) and up to 1.7 meters in ellipsoid height (Figure 3). All transformations introduce some level of uncertainty, which must be accounted for when assessing the accuracy of transformed coordinates.
- In some cases, a preferred alternative to transforming coordinates will be to reprocess or readjust the original survey data in the new reference frames, or to create entirely new datasets with new observations.

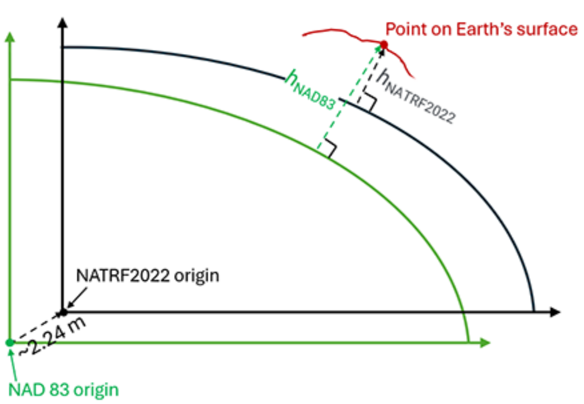

Figure 1. Simplified difference in origins of NAD 83 and NATRF2022 (adapted from NGS).

Vertical Datums: NAVD 88→NAPGD2022

- NAVD 88 will be replaced by the new geopotential (vertical) datum, **North American-Pacific Geopotential Datum of 2022 (NAPGD2022)**. It will also replace four existing vertical datums on islands (Puerto Rico, U.S. Virgin Islands, Guam, and the Northern Mariana Islands), and the International Great Lakes Datum of 1985.
- NAVD 88 will remain a valid datum, and not all existing maps and geospatial data will need to be transformed.
- Data that need to be transformed will undergo shifts of up to approximately 1.5 meters vertically in the conterminous

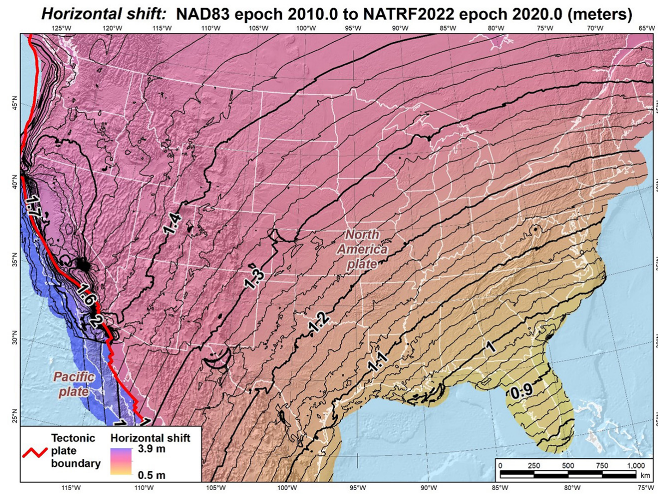

Figure 2. Estimated horizontal shift from NAD 83(2011) epoch 2010.0 to NATRF2022 epoch 2020.0 (courtesy of NGS).

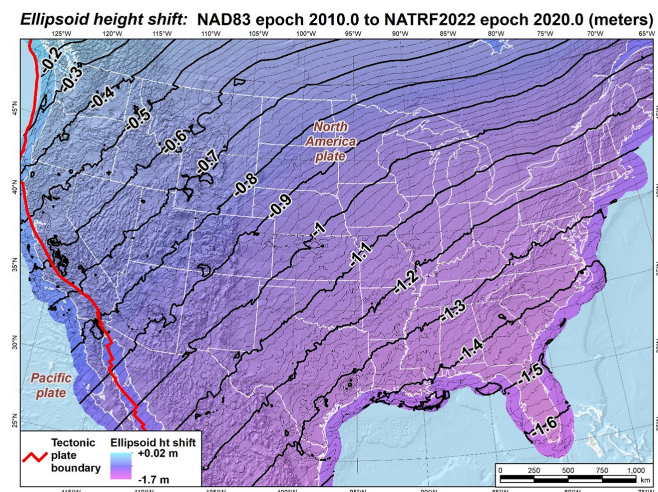

Figure 3. Estimated ellipsoid height shift from NAD 83(2011) epoch 2010.0 to NATRF2022 epoch 2020.0 (courtesy of NGS).

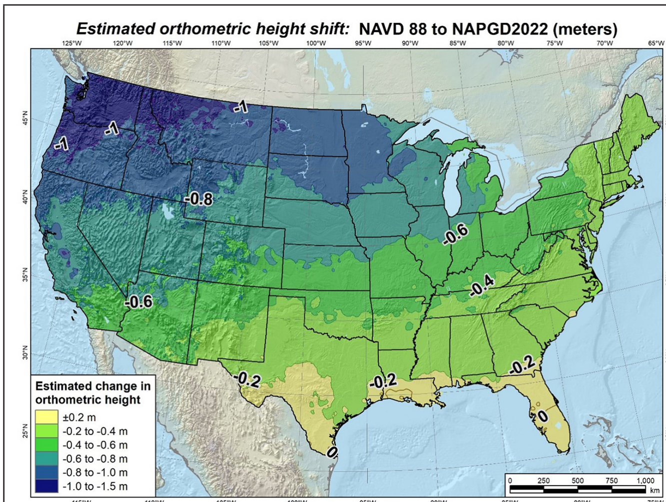

Figure 4. Estimated orthometric height shift from NAVD 88 (epoch undefined) to NAPGD2022 epoch 2020.0 (courtesy of NGS).

U.S., depending on location (Figure 4). Again, all transformations introduce some level of uncertainty, which must be accounted for in assessing the accuracy of transformed coordinates, and in some cases, a preferred alternative will be to reprocess the original survey data in the new datum, or to make new observations.
- Orthometric heights (heights above the geoid along a plumbline) in NAPGD2022 will be defined through NATRF2022 ellipsoidal heights and a new geoid model, GEOID2022.

Geoid Models: GEOID18→GEOID2022

- GEOID18, as well as previous geoid models, will be replaced with **GEOID2022**.
- GEOID2022, which incorporates the latest airborne and terrestrial gravity data acquired by NGS in its Gravity for the Redefinition of the American Vertical Datum (GRAV-D) program**,** will be defined in a manner that best fits global mean sea level at the epoch of NAPGD2022. When global sea level changes by some threshold level, a new geoid model, and thus new geopotential datum, will likely need to be released.
- GEOID2022 will be a purely gravimetric geoid model. Unlike "hybrid" models such as GEOID18, it will not be warped to match leveled heights on bench marks that were observed using GNSS. Thus GEOID2022 will be a more consistent and stable model.

State Plane Coordinate System: SPCS 83→SPCS2022

- The current State Plane Coordinate System of 1983 (SPCS 83) will be replaced by **SPCS2022** in the Modernized NSRS.
- The main change is that linear distortion (scale error) is minimized at the topographic surface rather than the reference ellipsoid surface. Additionally, SPCS2022 is designed to minimize distortion in areas of high usage or populated areas. States can have zone "layers." By incorporating zone layers and allowing state contributions, SPCS2022 represents a customer-driven evolution of SPCS, intended to meet the wide-ranging needs of the nation's diverse geospatial community (Figures 5 and 6).
- Another critical difference between the current SPCS 83 and upcoming SPCS2022 is that only the international foot (1 foot = 0.3048 meter, exactly) will be supported. This differs from the current SPCS 83, in which there are two different definitions of the foot, the international foot and the U.S. survey foot (1 foot = 1200/3937 meters, exactly), with states differing in which is officially adopted. Although these two definitions of the foot differ by only 2 parts per million, the difference in State Plane coordinates can reach tens of feet. In addition, only the international foot definition will be supported in all other components of the Modernized NSRS (such as orthometric heights).

Benefits of a Modernized NSRS for the Geospatial Industry

The improved accuracies and data interoperability that will be enabled through NSRS Modernization will provide tremendous benefits across all segments of the geospatial landscape. The Modernized NSRS will better support data sustainability, meaning that geospatial data will remain useful over longer time periods and across multiple applications. Just a few examples of specific applications that stand to benefit tremendously from the Modernized NSRS include:

- Floodplain modeling
- Coastal storm inundation modeling
- Improved hydrodynamic modeling (e.g., in support of salmon migration protection on the Columbia River)
- Precision navigation (including autonomous vehicles)
- Marine navigation safety, including computation of real-time under-keel clearance
- Infrastructure positioning and monitoring
- Transportation and engineering projects construction and maintenance

Also of importance, NGS is building in mechanisms to support time-dependent coordinates through the use of reference epoch coordinates (RECs), which will be computed by NGS every 5 or 10 years, and survey epoch coordinates (SECs), which will provide the position at the time of survey.

Preparing for NSRS Modernization in the Geospatial Industry: ASPRS Working Group Recommendations

To prepare to take full advantage of the benefits enabled by NSRS Modernization, it is imperative that geospatial service firms and software providers take certain steps now. The following are ASPRS Working Group recommendations for geospatial firms, separated into those that apply mainly to geospatial service providers, those that apply mainly to geospatial software manufacturers, and those that apply to the entire profession. A critical aspect of these recommendations is ensuring forwards and backwards compatibility of coordinates.

Working Group Recommendations for Geospatial Service Providers

Geospatial Service Providers - including those who collect, process and provide aerial and satellite imagery, lidar, sonar, hyperspectral imagery and other forms of geospatial data - are advised to take the following steps:

1. Ensure that all metadata for all archived data (not just final deliverables) is complete and correct, paying particular attention to reference frames, coordinate epochs, units (if feet, be sure to document whether international feet or U.S. survey feet), geoid models applied (e.g., GEOID12b, GEOID18), and acquisition dates and times.
2. For all **control points** and **checkpoints**, archive the survey report and store the **observation data files** (for example, RINEX raw observation files, processed GNSS

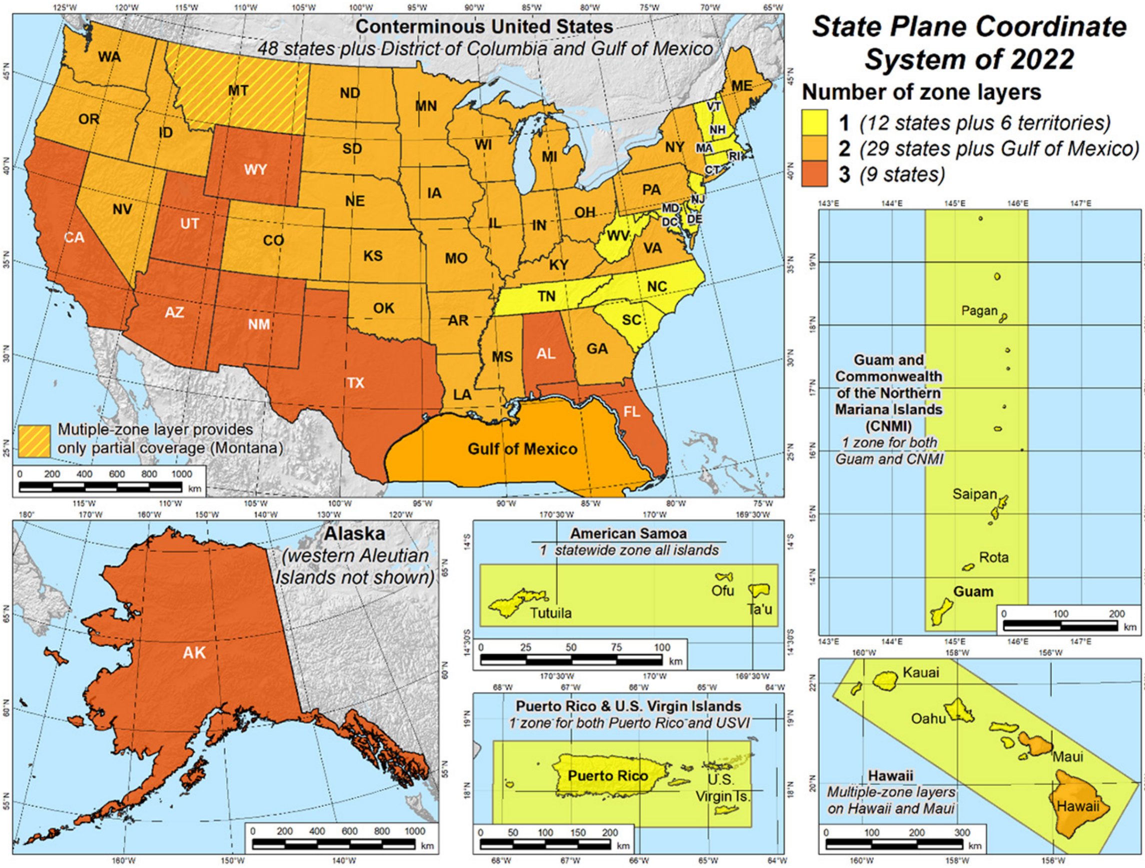

Figure 5. Preliminary SPCS2022 design: number of zone layers per state (courtesy of NGS).

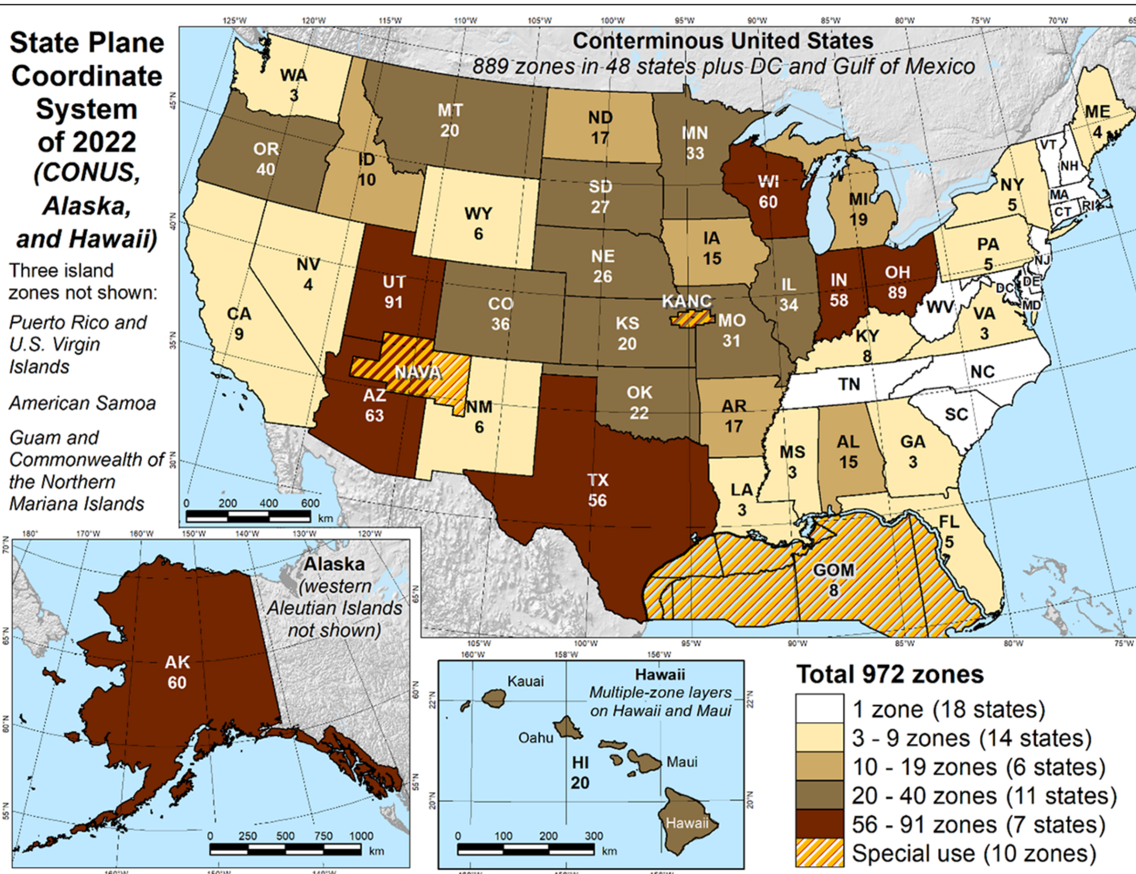

Figure 6. Preliminary SPCS2022 design: number of zones per state (courtesy of NGS).

vector solutions, or total station observation files), so that they can be reprocessed later relative to the Modernized NSRS. To the extent possible, store data using the NGS standard file formats (https://www.ngs.noaa.gov/web/science_edu/presentations_library/files/Gillins_FileFormats.pdf). Reprocessing or readjusting the raw data or processed observations (such as GNSS vectors) are the most accurate forms of relating legacy data to the new datums. Users can also transform data, but the transformed coordinates will not be as accurate as if the raw data are reprocessed in the new datums.

3. For all data deliverables (and possibly important intermediate products), store versions with **geodetic coordinates (latitudes, longitudes, and ellipsoid heights)** relative to the current NSRS (e.g., NAD 83(2011) epoch 2010.00), even if the project deliverables call for, say, SPCS 83 northings, eastings, and NAVD 88 heights.
4. Document the full project **workflows** with particular attention to any **coordinate transformations** or **conversions**.
5. Work with **software manufacturers** for all steps in your end-to-end project workflow to ensure they are aware of and preparing for NSRS Modernization.
6. Assess and document the **uncertainty of spatial coordinates** in all geospatial data products. This will enable additional uncertainties associated with transformations to be accounted for and used in assessing whether transformed products still meet requirements.

Working Group Recommendations for Geospatial Software Manufacturers

Geospatial software manufacturers are advised to take the steps listed below. As a note on terminology, many of these recommendations refer to handling of what are widely (if somewhat loosely) referred to as “Coordinate Reference Systems” or “CRSs” in geospatial software. Ideally, a CRS provides a complete definition of the reference frame (e.g., NAD 83, ITRF2020, or, in the future, NATRF2022), the realization (e.g., 2011), and epoch (date for which coordinates are valid), and, if applicable, the map projection system (e.g., Universal Transverse Mercator (UTM) or SPCS 83), zone, units (e.g., international feet, or meters), and vertical datum. (Unfortunately, current methods of storing CRS do not allow specifying the epoch, except in the remarks, but this is anticipated to be addressed in future standards revisions.)

- If your software uses **European Petroleum Survey Group (EPSG) codes or International Organization for Standardization (ISO) Geodetic Registry (ISOGR)** to define CRSs internally and/or in exported data products, ensure that the EPSG codes or ISOGR entries for new terrestrial reference frames and NAPGD2022 and SPCS2022 are supported. (Side note: the intent is for EPSG to be replaced with ISOGR, although the timeline is yet to be determined.)
- Ensure **SPCS2022** coordinates can be computed in units of both **meters and international feet** (1 international foot = 0.3048 meter, *exactly*)
- Ensure **coordinate conversions and transformations** (if provided in your software) are consistent with those of NGS
- Ensure **proper and consistent use of geoid models**. Importantly, any geoid model is designed for and valid for only a specific reference frame (and often also a specific realization of the frame) and region. For example, in the current NSRS, NGS’s GEOID18 is designed only for coordinates in the North American Datum of 1983 (2011) epoch 2010.00 and will convert ellipsoid heights to orthometric heights in the following datums: NAVD 88 (in the conterminous U.S. only, not Alaska), the Puerto Rico Vertical Datum of 2002 (PRVD02), or the Virgin Islands Vertical Datum of 2009 (VIVD09). Applying GEOID18 geoid heights to WGS84 ellipsoid heights is invalid and does not provide heights in any recognized system. Similarly, applying Earth Gravitational Model 2008 (EGM08) geoid heights to NAD 83(2011) ellipsoid heights is invalid and does not provide heights in any recognized system. Other examples of geoid models designed for specific reference frames include GEOID09 associated with NAD 83 (NSRS 2007) and GEOID99 or GEOID96 with NAD 83 (HARN). When a geoid model is used to compute heights relative to a particular datum, it is important to **document the specific geoid model** (e.g., GEOID12b, GEOID18, etc.). In some software and metadata, the geoid model is included in parentheses after the datum, such as NAVD 88 (GEOID18).
- Provide **uncertainties in output geospatial data products**, accounting for uncertainties associated with coordinate transformations. Note that NGS is planning to provide uncertainties for transformations between current and modernized reference frames conducted using NGS’s software utilities. This is already done in the existing NGS Coordinate Conversion and Transformation (NCAT) software for transformations between all frames and datums, and that will continue in the Modernized NSRS.

Working Group Recommendations for the Entire Geospatial Industry

A recommendation on terminology is to avoid using the term “height above mean sea level” or “MSL height” when referring to NAPGD2022 orthometric heights. The correct term for height above the geoid, measured along a plumbline, is “**orthometric height**.” To explain, local mean sea level (MSL) is a tidal datum that varies along the coast, not only in response to changes in geopotential, but also to currents, local hydrodynamics and other variables. For example, if one were to set a series of benchmarks along the coast, each adjacent to a tide gauge and each set at MSL = 0.000 m, differential levels run between these marks would show them to be at different NAVD 88 (or, in the future, different NAPGD2022) orthometric heights. Future versions of NOAA’s vertical datum transformation tool, VDatum, will enable transformation between NAPGD2022 and tidal datums, such as MSL, mean lower low water (MLLW), and mean high water (MHW).

A final, and most important, recommendation for everyone in the geospatial industry is to take advantage of NSRS Modernization educational materials and opportunities. NGS, as well as university partners, have developed training modules, workshops, and short courses related to coordinate transformations, geoid models, map projections and distortion (including overviews of SPCS2022), and geodesy. A list (although not intended to be comprehensive) of recommended training modules and continuing education resources is below:

- NGS Educational Videos: https://geodesy.noaa.gov/corbin/class_description/NGS_Video_Library.shtml
- NGS Webinar Series: https://geodesy.noaa.gov/web/science_edu/webinar_series/index.shtml
- NGS Online Lessons: https://geodesy.noaa.gov/web/science_edu/online_lessons/index.shtml
- Geospatial Center for the Arctic and Pacific Workshop Series: https://gcapgeospatial.org/education/

Additional Resources

- NGS Presentations Library: https://geodesy.noaa.gov/web/science_edu/presentations_library/
- Bojan Šavrič (Esri) blog: Prepare your data for the National Spatial Reference System modernization of 2022 in the U.S.: https://www.esri.com/arcgis-blog/products/arcgis-pro/data-management/prepare-your-data-for-the-nsrs-2022/#:~:text=To%20prepare%20for%20the%20NSRS,2011)%20Epoch%202010.0%20and%20NAVD88.
- NGS's Modernized National Spatial Reference System (NSRS) presentations: https://geodesy.noaa.gov/training/nsrs-modernization/index.shtml
- NGS's Blueprint Documents for the Modernized NSRS: https://geodesy.noaa.gov/datums/newdatums/policy.shtml
- NGS's "Get Prepared" page: https://geodesy.noaa.gov/datums/newdatums/GetPrepared.shtml
- NGS SPCS2022: https://alpha.ngs.noaa.gov/SPCS/

Acknowledgements

We would like to express our gratitude to Dr. Dana Caccamise, NGS, for a very thorough review of an early draft of this article and Dr. Michael Dennis, NGS, for both editing the manuscript and providing the current versions of Figures 2-6.

How to Get Involved

For those interested in contributing to preparing the geospatial industry for NSRS Modernization, there are many opportunities to get involved. ASPRS recently launched an NSRS Modernization Working Group, which is seeking new members. Both NGS and commercial geospatial software manufacturers will be seeking beta testers and early adopters during the rollout of the Modernized NSRS. Serving as an early adopter or beta tester will provide an opportunity to stay ahead of the curve on NSRS Modernization and also to benefit the entire geospatial community by finding and reporting issues in early releases. The NGS Alpha (Preliminary Products) website (https://alpha.ngs.noaa.gov/) and Beta (Beta Products Release) website (https://beta.ngs.noaa.gov/) are important starting points for early adopters.

GIS
Tips & Tricks

By Shira A. Ellenson and Al Karlin, Ph.D., CSM-L, GISP

Mapping the Aurora Borealis

November in Alaska ushers in dark, cold winter nights, but it also marks the peak season for aurora viewing. As we embrace the magic of the northern lights and cozy up for the colder months, it's the perfect time to map this celestial wonder. Last year during the holidays, we crafted a wonderful snowy basemap to showcase Anchorage's cross-country ski trails.To continue on with our winter theme, we'll first start by recreating the custom basemap.

This month, Shira Ellenson, from the Dewberry-Alaska office, returns to the Tips & Tricks column to bring the aurora borealis to our mapping community in a step-by-step workflow for the winter season.

Tip #1 — Creating the Basemap in ArcGIS Pro 3.2 or Later Release

Step 1
Open a new map

Step 2
Change the Basemap to "Human Geography Dark Map" and remove "Human Geography Dark Base" and "Human Geography Dark Label".

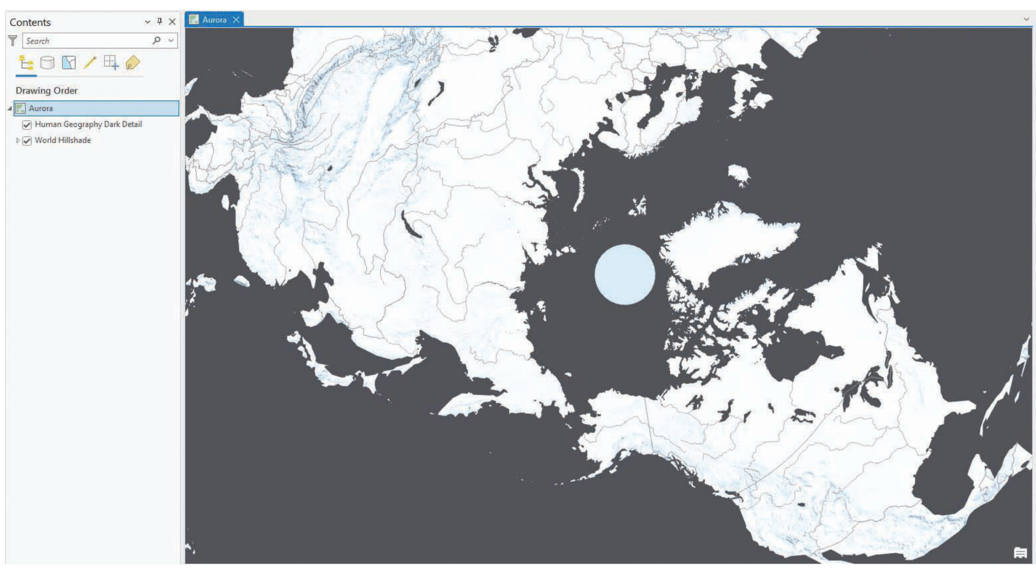

Figure 1. The Northern Winter Basemap (notice the blue hole in the center).

Under Catalog > Portal > Living Atlas > search for "World Hillshade" and add it to your map.

Under Map Properties > General, change the background color to Power Blue, #D9ECFF. Remember to use the "Color Properties" and to set the HEX Number. This will add a blue background to your map.

Step 3
With World Hillshade selected, adjust the Effects settings under the "Tile Layer" tab. Select "Luminosity" as the Layer Blend mode. This preserves the color of the background while maintaining the texture of the Hillshade.

Step 4
With the "Human Geography Dark Detail" layer selected, set the transparency to 10%. This will give your map more of a nighttime feel.

Step 5
Let's change the coordinate system to shift our attention to the North Pole. Under Polar projections, select "WGS 1984 North Pole LAEA Atlantic".

Zoom in and take a look around! You've quickly made a wonderful winter basemap!

Now what should we do about the basemap gap in the middle of your map? Time for a hack!

Photogrammetric Engineering & Remote Sensing
Vol. 90, No. 11, November 2024, pp. 653-656.
0099-1112/22/653-656

doi: 10.14358/PERS.90.11.653

TIP #2 — A Hack to fix the North Pole Hole

Step 6

On the Map tab on the ribbon, in the Layer Group, select Add a Graphics Layer. Then under the Graphics tab, insert a circle.

Step 7

Place the circle over the center.

Step 8

With the circle selected, adjust the fill and to match the map background color using the Eyedropper (Figure 2). Repeat using the eyedropper for the “Stroke” and…. Voila…,it’s like it was never there (Figure 3)!

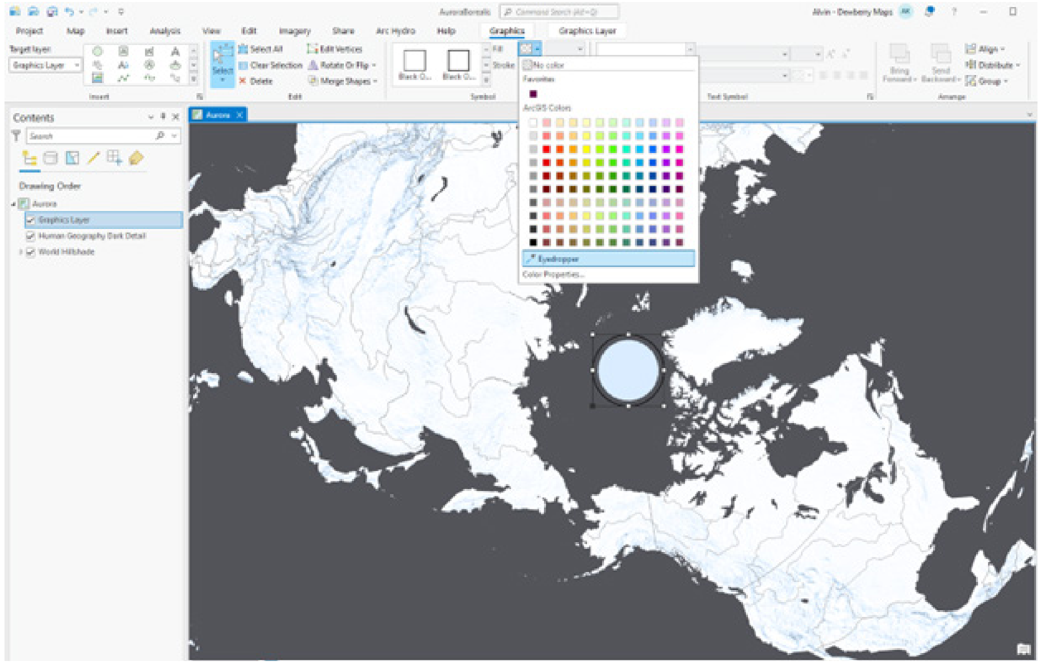

Figure 2. The Winter Basemap with a graphic circle and the eye-dropper on the color chart used to fill the hole.

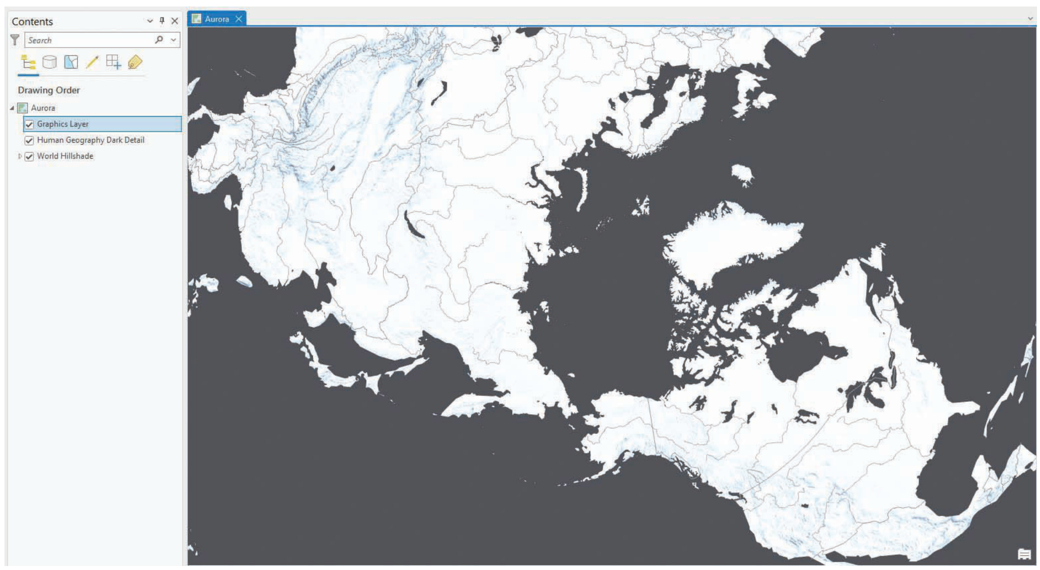

Figure 3. The filled hole on the Winter Basemap.

TIP #3 — Finding Aurora Borealis Data

Trying to find Aurora data was surprisingly difficult! Eventually, I stumbled across this great StoryMap which details how to extract data from the Oval Variation, Assessment, Tracking, Intensity, and Online Nowcasting (OVATION) Aurora model run by NOAA. It involved; (1) turning a JSON file filled with integers representing latitude, longitude, and aurora strength, into point data, and (2) then using the Spline interpolation tool to turn the point data into a raster surface. I experimented with the symbology stretch to match an ethereal holiday feel and made this data publicly available on ArcGIS Online under “Aurora OVATION Model”. Please feel free to use this layer and adjust the symbology to your liking!

TIP #4 — Now it’s Time to Turn this into a Map

Step 9

Sign into ArcGIS On-line, Search for and Add the Aurora OVATION Model layer to your map.

Step 10

Add a Layout to your project (I chose a Tabloid in Landscape mode). Center the Map Frame to your choosing.

Step 11

Add a Graticule to the map. With the Layout activated, choose the Insert tab, then in the Map Frames group, select the Grid dropdown. Choose Gray Horizontal Label Graticule.

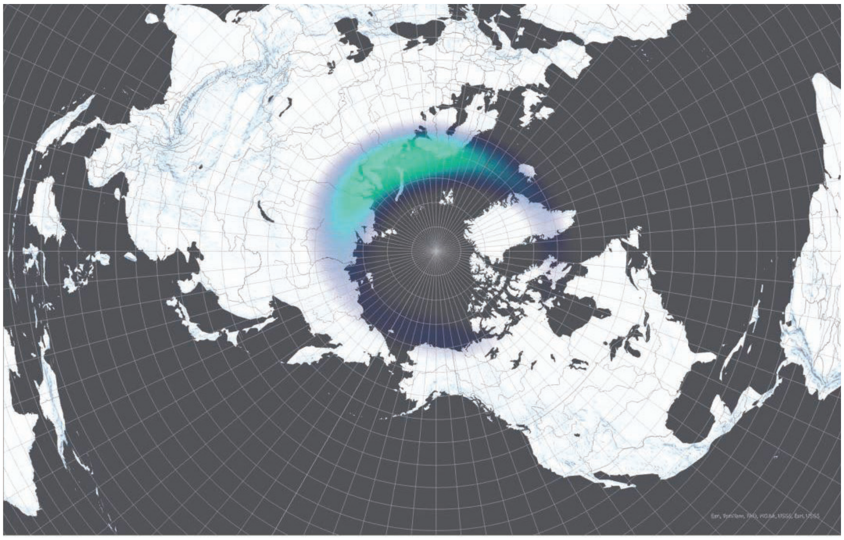

Figure 4. The Winter Basemap, Aurora OVATION Model layer from ArcGIS Online and a custom graticule.

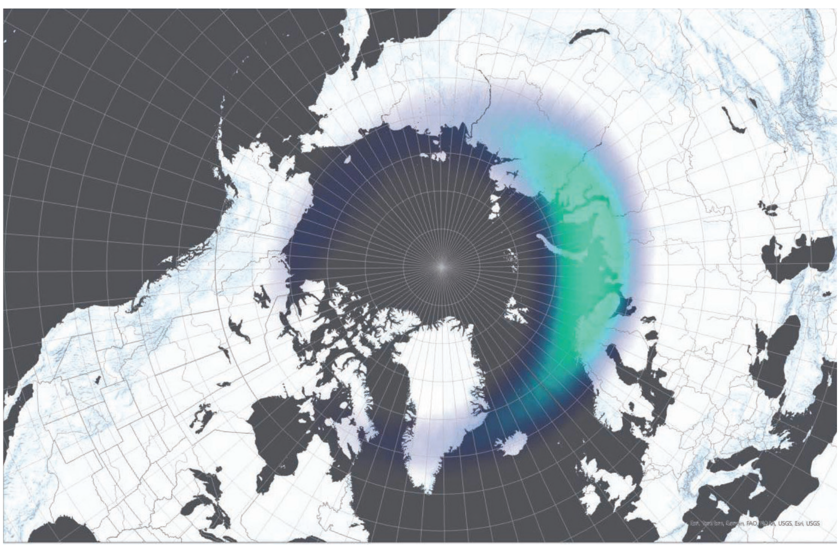

Figure 5. The map zoomed and rotated to focus attention on the northern latitudes.

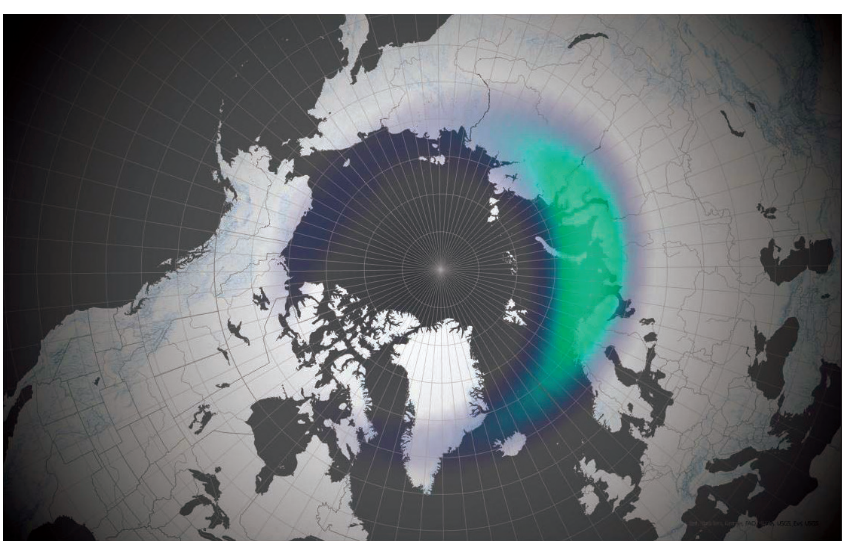

Figure 6. The map with a circular vignette.

Step 12

Customize the Graticule (Figure 4). With the Gray Horizontal Label Graticule selected, right-click on Properties to open the Element dialog. Then on the Components Tab, move the Labels, Ticks, and Ticks 1, leaving only gridlines at a 20° interval. You may need to uncheck "Automatically adjust" under Interval in the Options tab.

Step 13

Change the appearance of the gridlines to a more subdued look by using a gradient stroke stacking method. To do this, open the Properties (again), select the Map Grid tab, select the Neatline symbol on the Neatline tab and go to the Structures Pane (the wrench). Under Layers, duplicate the layer three more times (Add symbol layer | stroke layer).

Back under Layers, adjust,

- the first solid stroke Width to 0.5 and Color to White,the second Solid stroke, set the Width to 1, Color to #BEAC8C, and Transparency to 60.,
- the third Solid stroke, set the Width to 2.0, Color to #374665, and Transparency to 85%,and
- the fourth and final Solid stroke, set the Width to 4.0, Color to #374665, and Transparency to 85%,
- and Apply the modifications.

Step 14

Activate the Layout, ZOOM-IN and Rotate (Left-mouse+A) the map to focus on the Aurora (Figure 5).

Step 15

The final thing we'll add is a radial vignette to draw the reader in to the center of the map. To do this, insert a rectangle to match the extent of the entire map layout. With the rectangle selected, open the Properties Symbol and on the Layers tab, choose the gradient fill from semi-transparent black (10%) to fully transparent black (100%). Set the Direction to Circular, Type to Continuous, Extent to Relative, and Size to 99% (Figure 6).

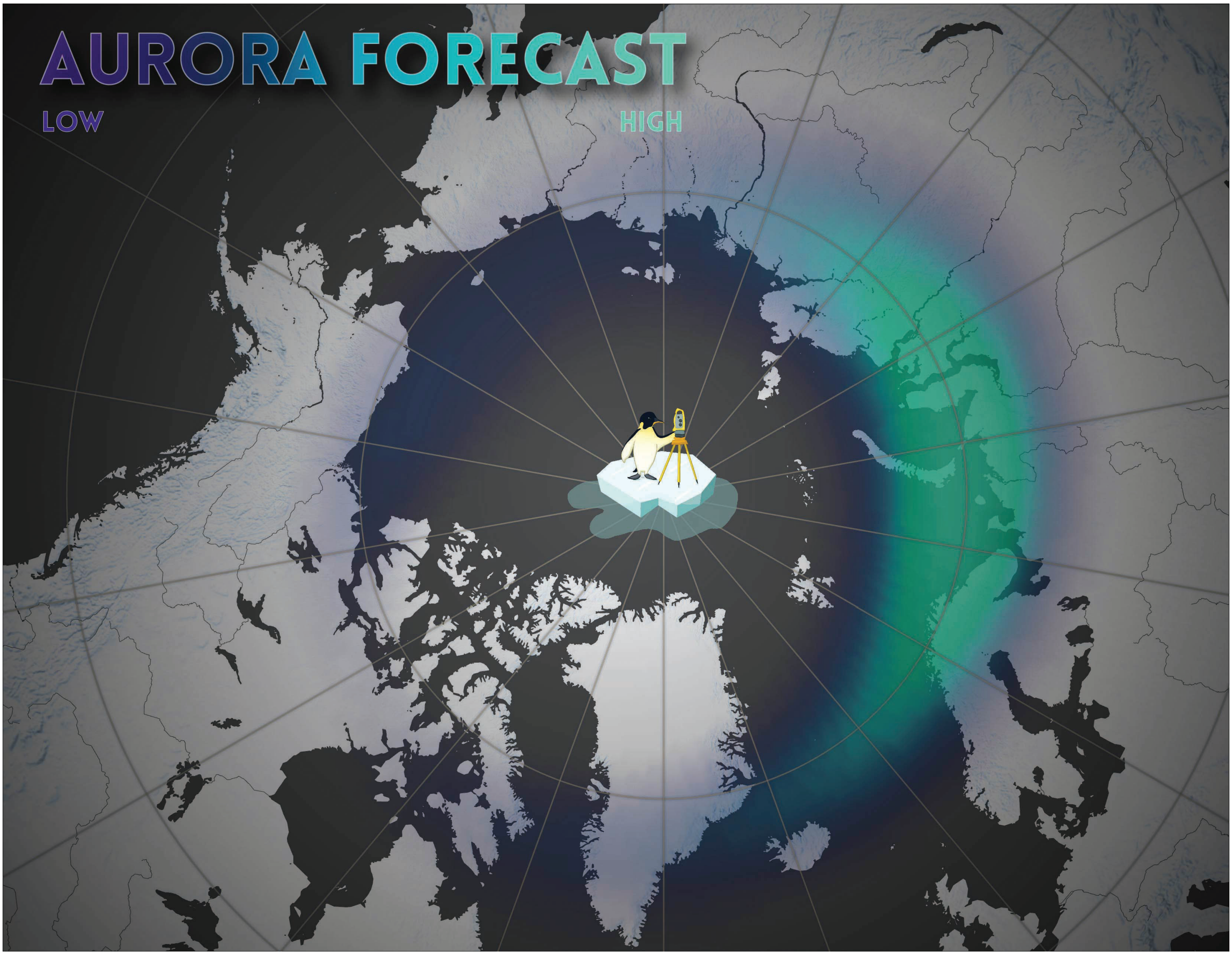

Figure 7. The final product with some **Illustrator** additions. (Note: Please be respectful of copyright limitations on the added graphics.) Penguin graphic courtesy of Yolani Martin.

After a few more graphic additions in Adobe Illustrator, there it is! Happy Holidays (Figure 7)!

Send your questions, comments, and tips to GISTT@ASPRS.org.

Shira Ellenson is a senior geospatial analyst with Dewberry's Anchorage, AK office. She specializes in remote sensing and cartography.

Al Karlin, Ph.D., CMS-L, GISP is with Dewberry's Geospatial and Technology Services group in Tampa, FL. As a senior geospatial scientist, Al works with all aspects of lidar, remote sensing, photogrammetry, and GIS-related projects.

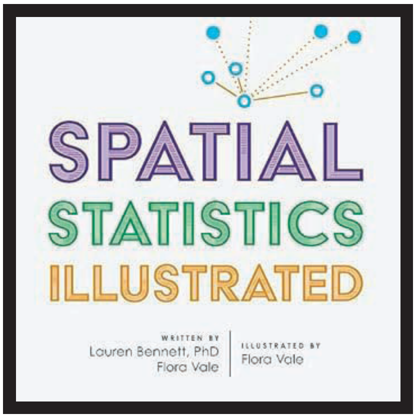

Spatial Statistics Illustrated

Lauren Bennett and Flora Vale. Esri Press, Redlands, CA. 2023. 165 pp., illustrations. Paperback $44.99. ISBN 9781589485716.

Reviewed by Kat Rocheford, PhD, Research Archaeologist, Department of Archaeology, Minnesota Historical Society, Saint Paul, Minnesota.

Spatial Statistics Illustrated by Bennett and Vale (2023) is intended for a broad audience from those beginning to learn about spatial statistics to the seasoned spatial analyst who wants to better explain spatial statistics and their results to peers and stakeholders. The authors begin with a review of statistical fundamentals and expand with a description of how spatial statistics build on the fundamentals but are different. Further, each statistical concept is described and uses specific real-world examples making the concept more accessible. For example, the description of a standard deviation ellipse may leave a reader asking why/how would this be used? Which the real-world example explains: to understand the direction of an invasive species spread. For more complex concepts that have multiple methods such as density-based clustering, the authors go the extra mile by summarizing and comparing the methods and providing examples of when each method may be preferred. I especially appreciated the reminder that statistical analysis is an iterative process and there is not one “right” method.

For many, the mere mention of statistics is intimidating, never mind understanding when to use which statistic or even understanding what the output means. Expand this to “spatial statistics” and I often see glazed over expressions from students, the general population, as well as some peers. From the design choices to the presentation and illustrations of the concepts, this book obliterates the intimidation factor. Through the subconscious mind, at 165 pages and the 16.5 x 16.5 cm dimensions, (smaller than a mouse pad), the size whittles away at what some might consider a daunting subject. The illustrations are plentiful and enhance comprehension of the concepts. The color choices for the illustrations give the book a playful feel. This book also tackles some challenging statistical methods like **spatiotemporal pattern mining**, in the same fashion, grounded in fundamentals, explained with real-world examples, and beautifully illustrated. Finally, the scholarly references are a brilliant addition for those that want to dig a little deeper.

Bennet and Vale are experts in this field and have taught many courses on the subject. Their ability to apply to provide real-world examples, across disciplines, demonstrates their thorough understanding of the subject. Anyone that has attended one of these courses will recognize their style in this book.

Photogrammetric Engineering & Remote Sensing
Vol. 90, No. 11, November 2024, pp. 657.
0099-1112/22/657

doi: 10.14358/PERS.90.11.657

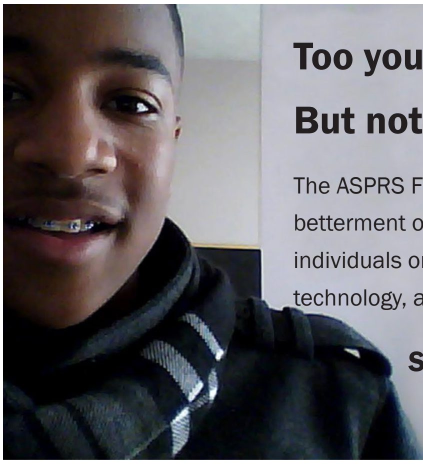

DR. ALPER YILMAZ IS RETIRING AS *PE&RS* EDITOR-IN-CHIEF

In 2016, Dr. Yilmaz because editor-in-chief of *PE&RS* because he felt compelled to share his knowledge with the next generation. At the time, Dr. Yilmaz was an Associate Professor of Civil, Environmental and Geodetic Engineering, and Associate Professor of Computer Science and Engineering at The Ohio University. He was published in over 80 journals and conference proceedings, and had received awards from The Ohio State University, IEEE, and many others.

When asked why he wanted to be Editor-in-Chief, Dr. Yilmaz noted, "ASPRS is a very vibrant community with a mission to connect at all levels. I am very honored to be a part of this mission and to serve as the editor-in-chief for *PE&RS*. We will take PE&RS to new heights by increasing subscriptions, impact factor, and quality."[1]

> "I would like to improve the overall recognition and impact factor of *PE&RS*."

Dr. Yilmaz transitioned *PE&RS* to an online management system with KGL (formally Allen Press). This aligned with the manuscript submission processes being used by other journals. It also streamlined the submission process for authors. He encouraged manuscript submission from industry professionals from outside of the US and increased *PE&RS*' impact factor. In 2022, Dr. Yilmaz was instrumental in creating an open-access policy that allows authors to publish without a large financial impact. "Due to Alper's guidance, open-access publishing in *PE&RS* is now easier for all authors," Rae Kelley, Director of Publications.

ASPRS extends its gratitude to Professor Alper Yilmaz for his leadership over the past eight years as Editor in Chief of *Photogrammetric Engineering and Remote Sensing*. Among Dr. Yilmaz's many contributions were new initiatives that increased open-access publishing and enhanced the visibility and impact of the journal.

1. An Interview – Alper Yilmaz. 2016. *PE&RS*. 82(5):313-314.

DR. RONGJUN QIN NAMED EDITOR-IN-CHIEF OF PE&RS

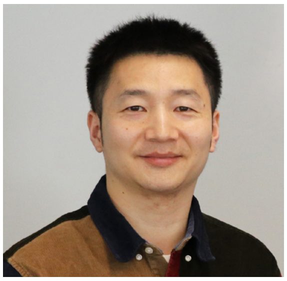

Dr. Rongjun Qin has been named Editor-in-Chief of *Photogrammetric Engineering and Remote Sensing* (*PE&RS*), the journal of the American Society for Photogrammetry and Remote Sensing (ASPRS). Dr. Qin replaces Dr. Alper Yilmaz, who has performed outstanding service in that role since 2016. The transition of responsibilities begins October 1st with receipt of new manuscripts for review.

Dr. Qin is a tenured Associate Professor of Photogrammetry and Remote Sensing (P&RS) at The Ohio State University (OSU). Dr. Qin earned a Ph.D. in Photogrammetry and Remote Sensing from ETH Zurich in 2015. He also spent time as a visiting scientist in the Department of Photogrammetry and Image Analysis at the German Aerospace Center. His research interests include both the theoretical foundations and practical applications of photogrammetry, remote sensing, computer vision, and geospatial sciences.

At OSU, he leads a research group of over 15 members, including research scientists, Ph.D. students, Master's students, and undergraduates. Their work spans diverse subfields within P&RS and computer vision, including satellite photogrammetry, UAS and mobile mapping, image-based localization, semantic segmentation, land-cover change analysis, 3D modeling, scene representation, structure from motion, and object detection.

"As a close colleague, I am thrilled about the appointment of Prof. Qin as the new Editor-in-Chief of our flagship journal. I see a bright future under his leadership, and as a community, we eagerly anticipate new initiatives to enhance the impact of Photogrammetric Engineering and Remote Sensing. We look forward to efforts to expand open access, streamline the peer-review process, and highlight key advancements in our field," Charles Toth, The Ohio State University.

Over the past 15 years, Dr. Qin has authored/co-authored 78 journal papers and 55 conference papers, including publications in prestigious Q1 and Q2 journals such as the *ISPRS Journal of Photogrammetry and Remote Sensing*, *Remote Sensing of Environment*, and *IEEE Transactions on Geoscience and Remote Sensing*. He also has extensive editorial experience, served as an Associate Editor (AE) for PE&RS since 2017, and as a member of the ASPRS Publication Committee since 2022.

Additionally, Dr. Qin has been an AE for the *ISPRS Journal of Photogrammetry and Remote Sensing* (a Q1 journal) and a member of the editorial board for *The Photogrammetric Record Journal* for nearly three years. Served as a guest editor for seven special issues of these and other journals and, over the past few years, handled about 200 manuscripts as an AE.

We are very pleased that Dr. Qin has agreed to join our outstanding *PE&RS* editorial staff, said ASPRS Director of Publications Rae Kelley in announcing the appointment. Dr. Qin's experience and professional credentials will enable us to continue to serve the Society readership, as well as the broader geospatial community of *PE&RS* subscribers, with the highest journalistic standards.

NEW ASPRS MEMBERS

ASPRS would like to welcome the following new members!

Ayodele Oduwole	Elizabeth Carroll	Manasha Arunachalam	Prince Lartey Lawson
Azka Ramzan	Emily Cranston	Max Blaustein	Rahul Kumar Ghose
Brandon Elia	Esi Dadzie	Miss Sahar Kamalou	Rasmoni Karak
Christine Karugu	Ghaith Kouki	Mohammad Sohail	Rayan Afsar
Christopher Scott Jackson	Gül Nur KARAL NESIL	Mr. Faisal Hussain	Rodolfo Asch, Jr.
Dana Lind	Himanjali Mylapalli	Muhammed Rasit Çevikalp	Russell Dodge
Deanna Renee Foster	Jennifer Kirkland	Nandini Kuppala	Ryan Carter
Deepika Sharma	JONATHAN MEYERS	Nasem Badreldin	Samuel Frank Landry
Diego Cortes	Jorge Carlos Gibert	Navya Bharathi	Tomas Genatios
Dorcas Twumwaa Gyan	Krishna Chaitanya Mummadi	Patricia Ojonoka Idakwo	
Elise Piazza	Lori Garrison	Peng Yuan	

FOR MORE INFORMATION ON ASPRS MEMBERSHIP, VISIT **HTTP://WWW.ASPRS.ORG/JOIN-NOW**

SPECIAL ISSUE INTRODUCTION

New Generation Hyperspectral Data for Quantum Leap in Remote Sensing Science for Agriculture

Dr. Prasad S. Thenkabail, Dr. Itiya Aneece, Dr. Pardhasaradhi Teluguntla

The November 2024 issue of the *Photogrammetric Engineering and Remote Sensing* (*PE&RS*) is the second special issue on the topic of "Ushering a New Era of Hyperspectral Remote Sensing to Advance Remote Sensing Science in the Twenty-first Century." The first was the August 2024 special issue of *PE&RS* (Thenkabail *et al.*, 2024). Great advances are taking place in remote sensing science (Thenkabail, 2024 a,b,c,d,e,f) especially in hyperspectral remote sensing (Thenkabail et al., 2024, Aneece and Thenkabail, 2022, Aneece et al., 2022, Thenkabail *et al.*, 2018) science with advent of new generation of spaceborne hyperspectral sensors such as:

1. Planet Lab's Tanager-1 acquiring data in 420 hyperspectral narrow bands (HNBs) over 400-2500 nm spectral range in 5 nm bandwidths,
2. German Space Agency's DESIS (DLR Earth Sensing Imaging Spectrometer) onboard the International Space Station (ISS) acquiring data in 235 hyperspectral narrow bands (HNBs) over 400-1000 nm spectral range in 2.55 to 10 nm bandwidths,
3. German Space Agency's EnMAP (Environmental Mapping and Analysis Program) acquiring data in 222 HNBs over 400-2500 nm spectral range and 10 nm bandwidth,
4. Italian Space Agency's PRISMA (PRecursore IperSpettrale della Missione Applicativa, Hyperspectral PRecursor of the Application Mission) acquiring data in 238 HNBs over 400-2500 nm spectral range and 10 to 12 nm bandwidth.

Many others such as NASA's SBG (Surface Biology and Geology) hyperspectral sensor as well as numerous others from space agencies of various governments as well as hyperspectral micro-satellite contellations from private enterprises like Pixxel and Orbital Sidekick (Global Hyperspectral Observation Satellite of or GHOSt) to be launched in the coming years. NASA's SBG will acquire data in about 242 HNBs over 400-2500 nm (visible and short-wave infrared or VSWIR) spectral range and 10 nm bandwidth and at least 5 bands in 4000-12,000 nm bandwidth. All sensors have global coverage with the ability to cover the planet at least every 20 days, have 30 m spatial resolution (1 pixel = 0.09 hectares) and a signal to noise ratio greater than 400 in the visible and near-infrared (VNIR; 400-1100 nm) region and ≥250 in the shortwave infrared (SWIR; 1000-2500 nm) region. In addition, drones/uncrewed aircraft systems or UASs, airborne, ground-based spectroradiometers are proliferating and acquiring data frequently in many regions of the world. The new generation hyperspectral data are propelling remote sensing science with a gigantic leap (Thenkabail *et al.*, 2021a) in global spectral data facilitating newer applications, and advances in existing applications using multispectral broadband (MBB) data. Nevertheless, HNB data bring with them their own challenges of understanding, characterizing, and analyzing them. These challenges include developing capacity in people's expertise, and advanced analysis methods and techniques to overcome data volumes and redundancies. In addition, new hyperspectral vegetation indices (HVIs) can be used to model and map specific quantities hitherto not feasible through MBB data, or to provide significant advances over MBB data in terms of mapping and modeling.

Given the above context, we have established two special issues of *PE&RS* focused on hyperspectral remote sensing of agriculture using new generation hyperspectral sensors, big-data analytics, machine learning (ML), deep learning (DL), cloud computing, and artificial intelligence (AI). Solicitation of papers brings papers not only on the topic, but also closely related topics that help in methods and approaches of analyzing massive quantities of data. A total of 9 papers are published in the two *PE&RS* special issues: five in August 2024 and four in November 2024 (this issue) for which we have provided overviews (Thenkabail *et al.*, 2024 in August 2024 special issue of *PE&RS* and this article in November 2024 special issue of *PE&RS*).

The strength of HNB data is the ability to acquire information in hundreds or even thousands of spectral bands. This provides tremendous advantages in discerning subtle differences in objects or features on Earth. For example, one can find specific HNBs to observe carotenoids, chlorophyll, plant moisture, plant health, and various plant biophysical and biochemical quantities (Thenkabail *et al.*, 2021b). However, when we acquire HNB data (e.g., <10 nm bandwidth), simultaneously obtaining a sufficiently high spatial resolution of imagery while maintaining high signal-to-noise (SNR) ratio is challenging. This is a limitation of the optic design and other mechanical issues in sensor design. As a result, HNB data may often have low spatial resolution. In contrast, acquiring high spatial resolution multispectral images is much easier. Obtaining HNB data with high spatial resolution requires great advances in sensor design such as optics. More recently, this issue was addressed by software solutions using machine learning techniques to combine high spectral resolution images with high spatial resolution images into hyperspectral imaging super-resolution (HSI SR) imagery. The paper by Lang *et al.* proposes and implements a spatial-spectral middle cross-attention (CA) fusion network (MCAFN) for this HSI SR task.

This special issue also includes a paper by Chen and Huang on vehicle detection using Synthetic Aperture Radar (SAR) data because the future of remote sensing will involve the integration of data from multiple sensors to extract the best possible information. Like hyperspectral data, SAR data are unique. Whereas hyperspectral data are acquired in passive mode (measuring sun energy reflected off objects) in hundreds or thousands of HNBs, SAR data are acquired in active mode (measuring pulses of energy generated by the instrument reflected off objects). There are also many new generation SAR sensors such as the European Space Agency's Sentinel-1, NASA's TerraSAR-X, Canada's

Dr. Prasad S. Thenkabail is with U. S. Geological Survey (USGS), Flagstaff, Arizona, USA (pthenkabail@usgs.gov)

Dr. Itiya Aneece is with U. S. Geological Survey (USGS), Flagstaff, Arizona, USA (ianeece@usgs.gov)

Dr. Pardhasaradhi Teluguntla is with Bay Area Environmental Research Institute (BAERI) @ USGS, California, USA (pteluguntla@usgs.gov)

Photogrammetric Engineering & Remote Sensing
Vol. 90, No. 11, November 2024, pp. 661–663.
0099-1112/22/661–663

doi: 10.14358/PERS.90.11.661

RADARSAT-2, and China's GF-3. The paper by Chen and Huang demonstrated vehicle detection using SAR and methods such as convolutional neural networks (CNNs). Hyperspectral data also provide a powerful mechanism for target detection (Chen *et al.*, 2023) For example, spectral signatures from hyperspectral data help detect plant types or crop types, their growth stages, their structure, and help assess their biophysical and biochemical content (Annece and Thenkabail, 2022). The fusion of hyperspectral data with other types of data such as SAR and LiDAR enhance classification accuracies of land cover types in applications such as agriculture, wetlands, or forestry (Kumar *et al.*, 2023, Norton *et al.*, 2022, Yuan *et al.*, 2022). Further, the methods such as the CNNs used in the paper by Chen and Huang have applications across data types, especially in hyperspectral data.

The paper by Aneece *et al.* utilizes two new-generation sensors (PRISMA and DESIS) to model, map, and study irrigated agricultural crops in a study area of California's Central Valley (CCV). The paper touches upon many key issues of hyperspectral data analysis, including generating spectral libraries of crops, developing inter-sensor relationships, building machine learning algorithms for crop classifications, and establishing major philosophies of hyperspectral data analysis. The ability to generate spectral libraries throughout the crop growing seasons (e.g., Figure 1) offers many new advances such as creating an ideal spectral data bank, and providing unique signatures of crops across growing seasons, an option to use spectral libraries to train DL/ML/AI algorithms as well as to use them in testing and validating products. Strong inter-sensor relationships (R-square = 0.97) between PRISMA and DESIS were developed. Three machine learning algorithms (support vector machines [SVMs], random forest [RF], and spectral angle mapper [SAM]) were applied for crop classification, with RF and SVM providing high levels of overall, producer's and user's accuracies. Crop types were classified using full spectral analysis (FSA) and optimal hyperspectral narrowband (OHNB) analysis. About 15-20 OHNBs provide optimal classification accuracies for crops. Both approaches have strengths. The FSAs are required for spectral matching (e.g., Figure 2), creating an ideal spectral data bank, and for use in AI models. The OHNBs help reduce data volumes and make classification computationally less intensive.

The massive volumes of hyperspectral data require DL/ML/AI methods to process and analyze data on cloud platforms such as Google Earth Engine (GEE) and Amazon Web Services (AWS). In this regard, neural networks are becoming popular, especially for handling hyperspectral data. CNNs are widely used for analyzing hyperspectral data for a wide array of applications such as crop type classification, plant disease detection, tree species mapping, and so on. In this issue, Kong *et al.* utilize CNN learning models and apply them on two well-known publicly available hyperspectral datasets: Jasper Ridge and Cuprite datasets, to demonstrate the ability of CNN models to extract endmembers and estimate abundance.

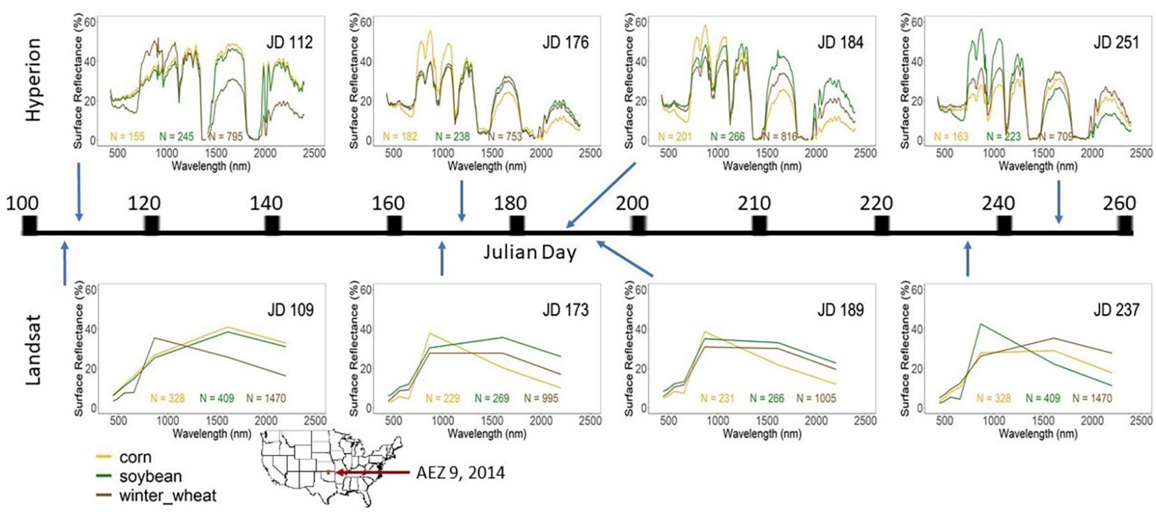

Figure 1. Spectral libraries of agricultural crops from hyperspectral vs. multispectral. Spectral libraries of agricultural crops generated by hyperspectral narrowband (HNB) data from Earth Observing-1 Hyperion hyperspectral sensor and compared with the Landsat 8 multi-spectral broadband (MBB) data.

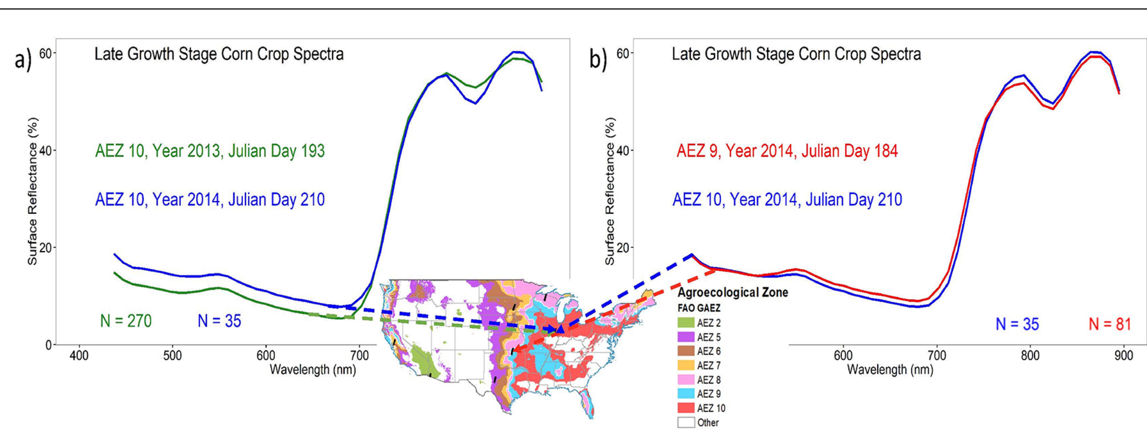

Figure 2. Spectral libraries and spectral matching techniques (SMTs) to analyze hyperspectral data. The spectral libraries of crops are developed by gathering large quantities of ideal spectra of particular crop types and storing them in spectral databank which are then matched with spectra of classes generated during classification of the image. The SMTs help identify and label crops and classes.

The new generation of spaceborne hyperspectral remote sensing sensors by government space agencies (e.g., EnMAP, PRISMA, DESIS) as well as from private enterprise driven hyperspectral micro-satellite or CubeSat constellations (e.g., Tanager-1, GHOSt, Pixxel) have ushered a new-era in remote sensing science. Availability of new generation hyperspectral data offer many opportunities for advancement in remote sensing science, relative to multispectral broadband data, that include:

1. Capturing spectral signatures of objects that help build spectral libraries of features such as minerals, agricultural crops, and plant species, which in-turn can be used in characterizing these features and utilizing them in training machine learning algorithms (MLA's) as well as in testing and validating products produced by MLA's.
2. Improving accuracies in classification, modeling, and mapping such as land cover, and crop types.
3. Enhancing ability to discern and map more classes such as forest types and biomes.
4. Capturing subtle differences in characteristics such as in separating species types, and within field variability in quantities such as biomass more accurately.
5. Helping in development of specific hyperspectral vegetation indices (HVIs) to study specific quantities such as biophysical (e.g., biomass, leaf area index, plant height, plant density), biochemical (e.g., pigments, lignin, cellulose, plant nitrogen content) plant health (e.g., stress), and plant structural (e.g., planophile and erectophile) characteristics with improved accuracies. and
6. Building ideal spectral data-banks through spectral libraries that become knowledge-base for artificial intelligence (AI) foundation models to classify, model, map, and monitor various terrestrial phenomenon.

All of these and many other possibilities offered by the hyperspectral data (Thenkabail *et al.*, 2018) requires substantial more research and publications. A goal advanced by these special issues.

Acknowledgments

Any use of trade, firm, or product names is for descriptive purposes only and does not imply endorsement by the U.S. Government.

References

Aneece, I., and Thenkabail. P. 2022. New generation hyperspectral sensor (DESIS and PRISMA) performances in Agriculture. *Photogrammetric Engineering and Remote Sensing*, 88 (11):715-729. https://doi.org/10.14358/PERS.22-00039R2

Aneece, I., Foley, D., Thenkabail, P., Oliphant, A., Pardhasaradhi, T. 2022. New generation hyperspectral data from DESIS compared and contrasted with hyperspectral resolution Planetscope data for crop type classification. *IEEE Journal of Selected Topics in Applied Earth Observations and Remote Sensing*. Volume: 15 (7846 – 7858). DOI: 10.1109/JSTARS.2022.3204223.

Chen, B.; Liu, L.; Zou, Z.; Shi, Z. 2023. Target Detection in Hyperspectral Remote Sensing Image: Current Status and Challenges. *Remote Sens.* 2023, 15, 3223. https://doi.org/10.3390/rs15133223

Kumar, V., Rajan, S., Perumal, V., Persello, C. 2023. Synergistic Fusion of Spaceborne Polarimetric SAR and Hyperspectral Data for Land Cover Classification. Book Chapter in the Book entitled *Spaceborne Synthetic Aperture Radar Remote Sensing Techniques and Applications* (Editors: Shashi Kumar, Paul Siqueira, Himanshu Govil and Shefali Agrawal). First Edition, https://doi.org/10.1201/9781003204466. Pp. 432. eBook ISBN9781003204466.

Norton, C.L.; Hartfield, K.; Collins, C.D.H.; van Leeuwen, W.J.D.; Metz, L.J. 2022. Multi-Temporal LiDAR and Hyperspectral Data Fusion for Classification of Semi-Arid Woody Cover Species. *Remote Sens.* 2022, 14, 2896. https://doi.org/10.3390/rs14122896.

Thenkabail, P.S., Aneece, I., Teluguntla, P. 2024. Special Issue Introduction: Ushering a New Era of Hyperspectral Remote Sensing to Advance Remote Sensing Science in the Twenty-first Century. PE&RS Special Issue. *Photogrammetric Engineering and Remote Sensing*. 90(8): 467-470. Doi: 10.14358.PERS.90.8.467

Thenkabail, Prasad. 2024a. *Remote Sensing Handbook* (Second Edition, Six Volume Book-set), Volume I: Sensors, Data Normalization, Harmonization, Cloud Computing, and Accuracies. Taylor and Francis Inc.\CRC Press, Boca Raton, London, New York. 978-1-032-89095-1— CAT# T132478. Print ISBN: 9781032890951. eBook ISBN: 9781003541141. Pp. 640.

Thenkabail, Prasad. 2024a. *Remote Sensing Handbook* (Second Edition, Six Volume Book-set), Volume II: Image Processing, Change Detection, GIS, and Spatial Data Analysis. Taylor and Francis Inc.\CRC Press, Boca Raton, London, New York. 978-1-032-89097-5— CAT# T133208. Print ISBN: 9781032890975. eBook ISBN: 9781003541158. Pp. 552.

Thenkabail, Prasad. 2024c. *Remote Sensing Handbook* (Second Edition, Six Volume Book-set), Volume III: Agriculture, Food Security, Rangelands, Vegetation, Phenology, and Soils. Taylor and Francis Inc.\CRC Press, Boca Raton, London, New York. 978-1-032-89101-9—CAT# T133213. Print ISBN: 9781032891019; eBook ISBN: 9781003541165. Pp. 824.

Thenkabail, Prasad. 2024d. *Remote Sensing Handbook* (Second Edition, Six Volume Book-set), Volume IV: Forests, Biodiversity, Ecology, LULC, and Carbon. Taylor and Francis Inc.\CRC Press, Boca Raton, London, New York. 978-1-032-89103-3— CAT# T133215. Print ISBN: 9781032891033. eBook ISBN: 9781003541172. Pp. 568.

Thenkabail, Prasad. 2024e. *Remote Sensing Handbook* (Second Edition, Six Volume Book-set), Volume V: Water, Hydrology, Floods, Snow and Ice, Wetlands, and Water Productivity. Taylor and Francis Inc.\CRC Press, Boca Raton, London, New York. 978-1-032-89145-3— CAT# T133261. Print ISBN: 9781032891453. eBook ISBN: 9781003541400. Pp. 592.

Thenkabail, Prasad. 2024f. *Remote Sensing Handbook* (Second Edition, Six Volume Book-set), Volume VI: Droughts, Disasters, Pollution, and Urban Mapping. Taylor and Francis Inc.\CRC Press, Boca Raton, London, New York. 978-1-032-89148-4 — CAT# T133267. Print ISBN: 9781032891484; eBook ISBN: 9781003541417. Pp. 520.

Thenkabail, P.S., Teluguntla, P.G., Xiong, J., Oliphant, A., Congalton, R.G., Ozdogan, M., Gumma, M.K., Tilton, J.C., Giri, C., Milesi, C., Phalke, A., Massey, R., Yadav, K., Sankey, T., Zhong, Y., Aneece, I., and Foley, D., 2021a, Global cropland-extent product at 30-m resolution (GCEP30) derived from Landsat satellite time-series data for the year 2015 using multiple machine-learning algorithms on Google Earth Engine cloud: U.S. Geological Survey Professional Paper 1868, 63 p., https://doi.org/10.3133/pp1868.

Thenkabail, P.S., Aneece, I., Teluguntla, P., Oliphant, A. 2021b. Hyperspectral Narrowband Data Propel Gigantic Leap in the Earth Remote Sensing. Highlight Article. *Photogrammetric Engineering and Remote Sensing*. http://www.asprs.org/a/publications/pers/2021journals/07-21_July_Flipping_Public.pdf doi: 10.14358/PERS.87.7.461. 87(7): 461-467. IP-127022.

Thenkabail, P.S., J.G. Lyon, A. Huete (Eds.), 2018. *Hyperspectral Remote Sensing of Vegetation*, Second Edition, Four Volume Set (2nd ed.), CRC Press. https://doi.org/10.1201/9781315159287

Yuan, Y.; Meng, X.; Sun, W.; Yang, G.; Wang, L.; Peng, J.; Wang, Y. 2022. Multi-Resolution Collaborative Fusion of SAR, Multispectral and Hyperspectral Images for Coastal Wetlands Mapping. *Remote Sens.* 2022, 14, 3492. https://doi.org/10.3390/rs14143492.

WHO'S WHO IN ASPRS

Founded in 1934, the American Society for Photogrammetry and Remote Sensing (ASPRS) is a scientific association serving thousands of professional members around the world. Our mission is to advance knowledge and improve understanding of mapping sciences to promote the responsible applications of photogrammetry, remote sensing, geographic information systems (GIS) and supporting technologies.

BOARD OF DIRECTORS

BOARD OFFICERS

President
Bandana Kar
U. S. Department of Energy (DOE)

President-Elect
Amr Abd-Elrahman
University of Florida

Vice President
Alvan Karlin, PhD, CMS-L, GISP
Dewberry

Past President
Lorraine B. Amenda, PLS, CP
Towill, Inc

Treasurer
John McCombs
NOAA

Secretary
Harold Rempel
ESP Associates, Inc.

COUNCIL OFFICERS

ASPRS has six councils. To learn more, visit https://www.asprs.org/Councils.html.

Sustaining Members Council
Chair: Paul Badr
Deputy Chair: Melissa Martin

Technical Division Directors Council
Chair: Hope Morgan
Deputy Chair: Tao Liu

Early-Career Professionals Council
Chair: Greg Stamnes

Region Officers Council
Chair: Demetrio Zourarakis
Deputy Chair: Cody Condron

Committee Chairs Council
Chair: David Day

Student Advisory Council
Chair: Oscar Duran
Deputy Chair: Ali Alruzuq

TECHNICAL DIVISION OFFICERS

ASPRS has seven professional divisions. To learn more, visit https://www.asprs.org/Divisions.html.

Geographic Information Systems Division
Director: Jin Lee
Assistant Director: Michael Baranowski

Lidar Division
Director: Matt Bethel
Assistant Director: Nora May

Photogrammetric Applications Division
Director: Hank Theiss
Assistant Director: Jae Sung Kim

Primary Data Acquisition Division
Director: Srini Dharmapuri
Assistant Director: Ravi Soneja

Professional Practice Division
Director: Hope Morgan
Assistant Director: Christian Stallings

Remote Sensing Applications Division
Director: Tao Liu
Assistant Director: Indu Jeyachandran

Unmanned Autonomous Systems (UAS)
Director: Bahram Salehi
Assistant Director: Rebecca Capps

REGION PRESIDENTS

ASPRS has 13 regions to serve the United States. To learn more, visit https://www.asprs.org/regions.html.

Alaska Region
Dave Parret

Cascadia Region
Jimmy Schulz

Eastern Great Lakes Region
Greg Lemke

Florida Region
Matt LaLuzerne

Gulf South
Cody Condron

Heartland Region
Whit Lynn

Mid-South Region
David Hughes

North Atlantic Region
Kurt Lutz

Northeast Region
Trevis Gigliotti

Pacific Southwest Region
Omar Mora

Potomac Region
Jason Brown

Rocky Mountain Region
Trent Casi

Western Great Lakes Region
Adam Smith

Morphology-Based Feature Extraction Network for Arbitrary-Oriented SAR Vehicle Detection

Ting Chen and Xiaohong Huang

Abstract

In recent years, synthetic aperture radar (SAR) vehicle detection has become a research hotspot. However, algorithms using horizontal bounding boxes can lead to redundant detection areas due to the varying aspect ratio and arbitrary orientation of vehicle targets. This paper proposes a morphology-based feature extraction network (MFE-Net), which fully uses the prior shape knowledge of the vehicle targets. Specifically, we adopt rotatable bounding boxes to predict the targets, and a novel rectangular rotation-invariant coordinate convolution (RRICC) is proposed to extract the feature, which can determine more accurately the convolutional sampling location of the vehicles. The adaptive thresholding denoising module (ATDM) is designed to suppress background clutter. Furthermore, inspired by the convolutional neural networks (CNNs) and self-attention, we propose the hybrid representation enhancement module (HREM) to highlight the vehicle target features. The experiment results show that the proposed model obtains an average precision (AP) of 93.1% on the SAR vehicle detection data set (SVDD).

Introduction

Synthetic aperture radar (SAR) is an active sensor based on the imaging mechanism of electromagnetic scattering, which plays a crucial role in modern society (Li *et al.* 2010; Guo *et al.* 2020; Luti *et al.* 2021). Compared with visible light imaging systems, SAR has the ability to effectively penetrate concealed targets and can perform imaging under all weather and all time conditions (Moreira *et al.* 2013). The development of SAR sensors such as *Sentinel-1*, *TerraSAR-X*, *RADARSAT-2*, and *GF-3* has further provided more and more high-quality SAR images. As a common land transportation tool, the detection of SAR vehicle targets in complex backgrounds is of great significance.

Traditional SAR target detection methods mainly include three stages: detection, discrimination, and identification (Robey *et al.* 1992). However, these algorithms require human intervention in designing model parameters, resulting in poor generalization ability. Vehicles are usually located in urban areas with complex backgrounds including trees, buildings, and roads, which severely limits the performance of traditional algorithms.

In recent years, with the development of big data and artificial intelligence, deep learning models have achieved excellent results in the field of target detection (Ren *et al.* 2015; Cai and Vasconcelos 2018; Ge *et al.* 2021). More and more scholars have applied deep learning algorithms to SAR vehicle detection, and the results have demonstrated the excellent performance of deep learning. To address the problem of vehicle detection in complex backgrounds, Wang *et al.* (2023) proposed a multi-scale semantic attention module to extract and fuse different features, which effectively suppresses the interference of background clutter. Zou *et al.* (2021) designed a subaperture decomposition of ResNet-34 to extract target features and used the semantic-context enhancement module to refine context information, achieving high accuracy in complex scenes. Other works have attempted to improve the accuracy and speed of vehicle detection in large scenes. Fan *et al.* (2023) combined traditional algorithms with deep learning algorithms to construct a framework for SAR vehicle target detection in large scenes. Sun *et al.* (2022) introduced the transformer module to obtain global contextual information and achieved large-scale military ground vehicle detection. Song *et al.* (2023) improved the performance and speed of wide-area SAR vehicle detection by combining coarse-grained judgment with fine-grained detection.

Although the aforementioned methods have improved the performance of vehicle detection, the geometric shape information on SAR vehicles is also important and has not yet been integrated with vehicle detection models. Vehicle targets in SAR images often appear as rectangular shapes, as shown in Figure 1a. However, traditional convolutional kernels in deep learning networks are square-shaped. The stacking of convolutional layers can increase the receptive field, but the shape of the receptive field remains square. This results in the convolutional sampling position not being well fitted to the vehicle shape characteristics, which limits the ability of the model to represent vehicle target features. In addition, SAR vehicles have the characteristics of dense distribution and arbitrary orientation, as shown in Figure 1b. Using traditional horizontal bounding boxes (HBBs) can lead to redundant detection areas, introducing more background interference and resulting in false positives or missed detections, and cannot describe the true shape of the target. Furthermore, due to the down-sampling operation and local receptive field of convolutional neural networks (CNNs), the global context information on the target will be missed, and even the small targets will be completely lost, as shown in Figure 1c.

A morphology-based feature extraction network (MFE-Net) is proposed in this article to address the problem of arbitrary-oriented SAR vehicle detection in complex scenes. Unlike the approach of directly applying deep network models to SAR images, MFE-Net fully leverages the shape characteristics of SAR vehicle targets. Specifically, regardless of changes in the scale, aspect ratio, and rotation angle of the target, it always maintains a rectangular shape. First, this paper uses rotatable bounding boxes (RBBoxes) to more accurately depict the true shape of vehicle targets. Additionally, we introduce Kullback-Leibler divergence (KLD) (Yang *et al.* 2022) as the regression loss. The KLD loss has the advantage of dynamically adjusting the parameter gradient and scale invariance, and it performs well on high-precision rotation detection tasks. Second, a vehicle feature extraction module (VFEM) is designed to extract SAR vehicle features in complex scenes. The network first extracts vehicle features through rectangular rotation-invariant coordinate convolution (RRICC). This convolution can adaptively learn the width, height, and rotation angle attributes of different vehicle targets. Its sampling positions are always maintained as rectangular and able to rotate in any direction, which matches the shape of vehicle targets more accurately. After that, an adaptive threshold denoising module (ATDM) is constructed to denoise the extracted features. Inspired by the idea of soft thresholding, ATDM can dynamically learn

Ting Chen and Xiaohong Huang are with the School of Electronics and Communication Engineering, Shenzhen Campus of Sun Yat-sen University.

Corresponding author: Xiaohong Huang (huangxh75@mail.sysu.edu.cn)

Received December 28, 2023, accepted May 10, 2024.

Photogrammetric Engineering & Remote Sensing
Vol. 90, No. 11, November 2024, pp. 665–673.
0099-1112/22/665–673

doi: 10.14358/PERS.24-00014R2

PEER-REVIEWED CONTENT
IS ONLY AVAILABLE TO
ASPRS MEMBERS AND SUBSCRIBERS

FOR MORE INFORMATION VISIT
MY.ASPRS.ORG

PEER-REVIEWED CONTENT
IS ONLY AVAILABLE TO
ASPRS MEMBERS AND SUBSCRIBERS

FOR MORE INFORMATION VISIT
MY.ASPRS.ORG

PEER-REVIEWED CONTENT
IS ONLY AVAILABLE TO
ASPRS MEMBERS AND SUBSCRIBERS

FOR MORE INFORMATION VISIT
MY.ASPRS.ORG

PEER-REVIEWED CONTENT IS ONLY AVAILABLE TO ASPRS MEMBERS AND SUBSCRIBERS

FOR MORE INFORMATION VISIT MY.ASPRS.ORG

PEER-REVIEWED CONTENT
IS ONLY AVAILABLE TO
ASPRS MEMBERS AND SUBSCRIBERS

FOR MORE INFORMATION VISIT
MY.ASPRS.ORG

PEER-REVIEWED CONTENT
IS ONLY AVAILABLE TO
ASPRS MEMBERS AND SUBSCRIBERS

FOR MORE INFORMATION VISIT
MY.ASPRS.ORG

PEER-REVIEWED CONTENT IS ONLY AVAILABLE TO ASPRS MEMBERS AND SUBSCRIBERS

FOR MORE INFORMATION VISIT MY.ASPRS.ORG

Spatial-Spectral Middle Cross-Attention Fusion Network for Hyperspectral Image Superresolution

Xiujuan Lang, Tao Lu, Yanduo Zhang, Junjun Jiang, and Zixiang Xiong

Abstract

The spatial and spectral features of hyperspectral images exhibit complementarity, and neglecting them prevents the full exploitation of useful information for superresolution. This article proposes a spatial-spectral middle cross-attention fusion network to explore the spatial-spectral structure correlation. Initially, we learn spatial and spectral features through spatial and spectral branches instead of single ones to reduce information compression. Then, a novel middle-cross attention fusion block that includes middle features fusion strategy and cross-attention is proposed to fuse spatial-spectral features to enhance their mutual effects, which aims to explore the spatial-spectral structural correlations. Finally, we propose a spectral feature compensation mechanism to provide complementary information for adjacent band groups. The experimental results show that the proposed method outperforms state-of-the-art algorithms in object values and visual quality.

Introduction

Compared with multispectral images or RGB images, hyperspectral images (HSIs) contain more spectral information that can reflect the subtle spectral features of the object precisely. However, due to the limitations of the devices, which make it difficult to acquire high-quality images, the obtained HSIs tend to have a low resolution (LR). The LR will affect the performance of high-level tasks, such as image classification (Wang *et al.* 2018), medical diagnosis (Lin *et al.* 2018), plant detection (Lowe *et al.* 2017), mineral exploration (Sabins 1999), and quantitative monitoring (Shi *et al.* 2023; Sun *et al.* 2023; Zhuang *et al.* 2023; Li *et al.* 2024). Since breaking the hardware limitation is expensive, improving the resolution of images at the software level would be more practical and realistic. Therefore, the HSI superresolution (SR) technique has been developed (Akgun *et al.* 2005; Dong *et al.* 2016; Xie *et al.* 2019; Lu, Zhao, *et al.* 2022; Wang, Lu, Zhang, *et al.* 2023; Xiao *et al.* 2023; Wang, Lu, *et al.* 2024; Wang, Zhou, *et al.* 2024), which aims to reconstruct high-resolution (HR) images with clarity from LR images. With more pixels providing excess information, which enhances the perception quality, the SR technique improves detection and classification accuracy.

Different from RGB images, HSIs have a high degree of similarity in spatial bands, especially in adjacent bands. There are three characteristics: global correlation along spectrum (GCS), nonlocal self-similarity across spatial (NSS), and spatial-spectral structure correlation. According to different characteristics, the HSI SR can be divided into three categories: spatial, spectral, and joint spatial-spectral SR methods. Thanks to the outstanding performance of natural-image SR methods (Lu *et al.* 2020, 2024; Jiang, Wang, *et al.* 2020; Wang, Lu, *et al.* 2021), the researchers applied them to HSI, achieving spatial SR. For example, a nonconvex tensor penalty was used to explore nonlocal self-similarity across the spatial domain (Wang *et al.* 2017). The structural self-similarity (Pan *et al.* 2013) and total variation (Li *et al.* 2016) were introduced for remote sensing images restored. Although these methods perform better with natural images, they ignore the GCS, leading to spectral distortion. Recently, deep learning has presented predominant advantages in different computer vision applications. Convolutional neural networks (CNNs) play a vital role in image SR tasks because of their powerful nonlinear learning capabilities (Lu, Wang, *et al.* 2022; Wang, Lu, Yao, *et al.* 2023; Zhao *et al.* 2024). SRCNN (Dong *et al.* 2015) was the first deep learning–based method for natural image SR tasks. Although it used only three convolutional layers, it performed much better than traditional algorithms. The above works attracted the attention of many scholars to use CNNs for HSI SR. Then Yuan *et al.* (2017) first took advantage of deep CNN to exploit spatial and spectral features of HSIs. Since then, the field of hyperspectral reconstruction based on deep learning has flourished.

As mentioned above, spatial and spectral dimensions play equally important roles in HSI. Thus, some processing tasks attempt to restore the spatial and spectral information simultaneously. A straightforward method is to handle them sequentially in a single branch, followed by spatial and spectral SR, or in reverse order. Li *et al.* (2021) explored the relationship between 2D and 3D convolution for HSI SR, indicating that the analysis of spectrum in horizontal or vertical dimension is by means of 3D units and the exploration of spatial features is with the help of 2D units. Mei *et al.* (2020) proposed a spatial-spectral joint SR (sepSS-JSR) algorithm, in which sepSSJSR1 was conducted in the spatial and spectral domain sequentially. As for sepSSJSR2, the reverse order of sepSSJSR1 was conducted in the spectral and spatial domain. Jiang, Sun, *et al.* (2020) applied the spatial-spectral block to study the spatial and spectral features sequentially. As we all know, with more deep layers functioning, the CNNs will be more prone to compress or even lose their information flow. Consequently, HSI SR tasks cannot completely capture the information of the last domain. For example, performing the HSI SR task in a spatial and spectral order can result in an undesirable effect on the last spectral domain, including spectral distortion, and vice versa. Moreover, the sequential way ignores the critical spatial-spectral structure correlation characteristic in the single HSI SR (SHISR) task.

The spatial-spectral structure correlation is another important characteristic of HSI, on par with NSS and GCS in the HSI SR task. Hence,

Xiujuan Lang is with the Hubei Key Laboratory of Intelligent Robot, Wuhan Institute of Technology, Wuhan, 430073, China; and the School of Computer Science and Information Technology, Daqing Normal University, Daqing 163111, China.

Tao Lu is with the Hubei Key Laboratory of Intelligent Robot, Wuhan Institute of Technology, Wuhan, 430073, China (lutxyl@gmail.com).

Yanduo Zhang is with the Hubei Key Laboratory of Intelligent Robot, Wuhan Institute of Technology, Wuhan, 430073, China; and the Hubei University of Arts and Science, Xiangyang 441053, China.

Junjun Jiang is with the School of Computer Science and Technology, Harbin Institute of Technology, Harbin 150001, China.

Zixiang Xiong is with the Department of Electrical and Computer Engineering, Texas A&M University, College Station, TX 77843.

Fully documented templates are available in the elsarticle package on CTAN.

Corresponding author: Tao Lu (lutxyl@gmail.com)

Received January 9, 2024, accepted May 10, 2024.

Photogrammetric Engineering & Remote Sensing
Vol. 90, No. 11, November 2024, pp. 675–686.
0099-1112/22/675–686

doi: 10.14358/PERS.24-00007R2

PEER-REVIEWED CONTENT
IS ONLY AVAILABLE TO
ASPRS MEMBERS AND SUBSCRIBERS

FOR MORE INFORMATION VISIT
MY.ASPRS.ORG

PEER-REVIEWED CONTENT
IS ONLY AVAILABLE TO
ASPRS MEMBERS AND SUBSCRIBERS

FOR MORE INFORMATION VISIT
MY.ASPRS.ORG

PEER-REVIEWED CONTENT
IS ONLY AVAILABLE TO
ASPRS MEMBERS AND SUBSCRIBERS

FOR MORE INFORMATION VISIT
MY.ASPRS.ORG

PEER-REVIEWED CONTENT
IS ONLY AVAILABLE TO
ASPRS MEMBERS AND SUBSCRIBERS

FOR MORE INFORMATION VISIT
MY.ASPRS.ORG

PEER-REVIEWED CONTENT
IS ONLY AVAILABLE TO
ASPRS MEMBERS AND SUBSCRIBERS

FOR MORE INFORMATION VISIT
MY.ASPRS.ORG

**PEER-REVIEWED CONTENT
IS ONLY AVAILABLE TO
ASPRS MEMBERS AND SUBSCRIBERS**

**FOR MORE INFORMATION VISIT
MY.ASPRS.ORG**

PEER-REVIEWED CONTENT
IS ONLY AVAILABLE TO
ASPRS MEMBERS AND SUBSCRIBERS

FOR MORE INFORMATION VISIT
MY.ASPRS.ORG

PEER-REVIEWED CONTENT
IS ONLY AVAILABLE TO
ASPRS MEMBERS AND SUBSCRIBERS

FOR MORE INFORMATION VISIT
MY.ASPRS.ORG

PEER-REVIEWED CONTENT
IS ONLY AVAILABLE TO
ASPRS MEMBERS AND SUBSCRIBERS

FOR MORE INFORMATION VISIT
MY.ASPRS.ORG

Machine Learning and New-Generation Spaceborne Hyperspectral Data Advance Crop Type Mapping

Itiya Aneece, Prasad S. Thenkabail, Richard McCormick, Haireti Alifu, Daniel Foley, Adam J. Oliphant, Pardhasaradhi Teluguntla

Abstract

Hyperspectral sensors provide near-continuous spectral data that can facilitate advancements in agricultural crop classification and characterization, which are important for addressing global food and water security issues. We investigated two new-generation hyperspectral sensors, Germany's Deutsches Zentrum für Luft- und Raumfahrt Earth Sensing Imaging Spectrometer (DESIS) and Italy's PRecursore IperSpettrale della Missione Applicativa (PRISMA), within California's Central Valley in August 2021 focusing on five irrigated agricultural crops (alfalfa, almonds, corn, grapes, and pistachios). With reference data from the U.S. Department of Agriculture Cropland Data Layer, we developed a spectral library of the crops and classified them using three machine learning algorithms (support vector machines [SVM], random forest [RF], and spectral angle mapper [SAM]) and two philosophies: 1. Full spectral analysis (FSA) and 2. Optimal hyperspectral narrowband (OHNB) analysis. For FSA, we used 59 DESIS four-bin product bands and 207 of 238 PRISMA bands. For OHNB analysis, 9 DESIS and 16 PRISMA nonredundant OHNBs for studying crops were selected. FSA achieved only 1% to 3% higher accuracies relative to OHNB analysis in most cases. SVM provided the best results, closely followed by RF. Using both DESIS and PRISMA image OHNBs in SVM for classification led to higher accuracy than using either image alone, with an overall accuracy of 99%, producer's accuracies of 94% to 100%, and user's accuracies of 95% to 100%.

Highlights

1. **Spectral libraries:** Built spectral libraries of five irrigated crops in California's Central Valley using Deutsches Zentrum für Luft- und Raumfahrt Earth Sensing Imaging Spectrometer (DESIS) and PRecursore IperSpettrale della Missione Applicativa (PRISMA) data.
2. **Intersensor relationships:** Developed an intersensor relationship between DESIS and PRISMA data ($R^2 = 0.97$) in the common spectral range of 403 to 1000 nm.
3. **Full spectral analysis (FSA) versus optimal hyperspectral narrowband (OHNB) analysis:** Compared two philosophies of hyperspectral data analysis. FSA improved crop classification accuracies over OHNB analysis by only 1% to 3%.
4. **Classification performance:** Compared two hyperspectral sensors. DESIS and PRISMA achieved overall accuracies of 96% to 99%, producer's accuracies of 86% to 100%, and user's accuracies of 88% to 100% in classifying five crops, with support vector machines being the best machine learning algorithm closely followed by random forest.

Itiya Aneece , Prasad S. Thenkabail, Richard McCormick, Daniel Foley, and Adam J. Oliphant are with the U.S. Geological Survey, Western Geographic Science Center.

Haireti Alifu is with the Taylor Geospatial Institute.

Pardhasaradhi Teluguntla is with the U.S. Geological Survey, Western Geographic Science Center and the Bay Area Environmental Research Institute.

Corresponding author: Itiya Aneece (ianeece@usgs.gov)

Received February 22, 2024, accepted June 5, 2024.

Introduction

Satellite remote sensing has been playing a key role in understanding, modeling, mapping, and monitoring global croplands that help provide critically important data for assessing food and water security (Thenkabail *et al.* 2021b; Potapov *et al.* 2022; Yu *et al.* 2022; Foley *et al.* 2023; Shi *et al.* 2023; Stanimirova *et al.* 2023; Van Tricht *et al.* 2023). Furthermore, great advances are taking place with the launches of new-generation hyperspectral sensors, for example the Italian Space Agency's (Agenzia Spaziale Italiana, ASI) PRecursore IperSpettrale della Missione Applicativa (PRISMA) and Germany's Deutsches Zentrum für Luft- und Raumfahrt (DLR) Earth Sensing Imaging Spectrometer (DESIS) that can advance our understanding and improve accuracies of agricultural croplands and their characteristics (Campbell *et al.* 2022; Tagliabue *et al.* 2022; Farmonov *et al.* 2023; Ranghetti *et al.* 2023; Shaik *et al.* 2023). There is substantial literature on hyperspectral remote sensing of agricultural crops (Thenkabail *et al.* 2018a, 2018b, 2018c, 2018d; Khan *et al.* 2022; Yu *et al.* 2022), but fewer publications using new-generation sensors and advanced methods like machine learning algorithms and cloud computing.

In this context, the focus of this paper was to evaluate two new-generation hyperspectral sensors (DESIS and PRISMA) for modeling and mapping agricultural crops. These sensors have extensive collections of images throughout the world (Shaik *et al.* 2023). Although they have similar sensor characteristics, they differ primarily in terms of their orbit, spectral range, and bandwidths (Aneece and Thenkabail 2022c). DESIS is mounted on the International Space Station (ISS), whereas PRISMA is polar-orbiting. Both collect data upon tasking, rather than on a continuous basis. DESIS collects data in the visible (VIS) and near-infrared (NIR) regions, whereas PRISMA collects data in the VIS, NIR, and shortwave infrared (SWIR) regions (Peschel *et al.* 2018; Heiden *et al.* 2019; Krutz *et al.* 2019). Lastly, PRISMA data consist of bands that are ≤12 nm wide, whereas DESIS data with 1× binning consist of bands with 2.55-nm bandwidth. Although these narrow bands provide a high volume of data, they can have a lower signal-to-noise ratio, making it difficult to distinguish meaningful features from the noise (Aneece and Thenkabail 2021). The recently available four-bin DESIS product consolidates information into sixty 10-nm narrowbands, which increases the signal-to-noise ratio (Patel *et al.* 2024).

Hyperspectral data analysis is becoming increasingly mature (Thenkabail *et al.* 2018a, 2018b, 2018c, 2018d); however, more exploration of different information extraction methods and classification/regression models is needed (Yu *et al.* 2022). For instance, avenues such as full spectral analysis (FSA) and optimal hyperspectral narrowband (OHNB) analysis warrant deeper investigation. FSA allows the use of

Photogrammetric Engineering & Remote Sensing
Vol. 90, No. 11, November 2024, pp. 687–698.
0099-1112/22/687–698

doi: 10.14358/PERS.24-00026R2

all the data across an entire spectral profile for analyses. For example, the spectral matching technique uses the shape of the entire profile to match endmembers to samples for classification analyses (Thenkabail *et al.* 2007; Gumma *et al.* 2021, 2022; Rejith *et al.* 2022). Further, hyperspectral data provide near-continuous “spectral signatures” along the electromagnetic spectrum as opposed to a few data points provided by broadband sensors. Hyperspectral data can reveal subtle changes at specific spectral ranges (Yu *et al.* 2022). On the other hand, optimal hyperspectral narrowband analyses summarize information across the spectral profile using a few unique, noncorrelated bands, avoiding the curse of high data dimensionality (also known as Hughes’ phenomenon), decreasing the number of samples needed for building a model, decreasing computation resources needed, and often increasing classification/regression accuracies (Aneece and Thenkabail 2021, 2022c; Anand *et al.* 2022; Fernandez-Habas *et al.* 2022; Kuang *et al.* 2023). However, it must be noted that optimal band selection is application-specific (Yu *et al.* 2022). Until now, no comprehensive studies have been conducted on FSA and OHNB analysis of DESIS and PRISMA data sets.

Hyperspectral signatures facilitate the study of specific plant biophysical/biochemical characteristics, biochemical quantities, plant health, plant moisture, and the physical structure of plants (Anand *et al.* 2022; Yu *et al.* 2022; Patel *et al.* 2024). Therefore, we developed the Global Hyperspectral Imaging Spectral-library of Agricultural Crops (GHISA) platform (GHISA, 2024), in which we aim to consolidate hyperspectral data across sensors, countries, agroecological zones, years, months, crop types, and their growth stages to create a robust spectral library for training and validating machine learning classification models. Several data sets are already publicly available (Aneece and Thenkabail 2019a, 2019b, 2022a; Mariotto *et al.* 2020a, 2020b; Aneece *et al.* 2022) and are being explored and used by others (Basener 2022; McGehee 2022; Gross *et al.* 2023; Longchamps and Philpot 2023; You *et al.* 2023). However, there is an urgent need to enrich our publicly available structured spectral libraries of agricultural crops (Borrmann *et al.* 2023). Conducting intersensor comparisons by collecting spectra from the same sample locations across different sensors can greatly facilitate and benefit future research applications.

Machine learning algorithms automatically learn and implement feature learning for building models (Yu *et al.* 2022). Algorithms like support vector machines (SVMs), random forest (RF), and spectral angle mapper (SAM) have been used for multiple applications like land use/land cover classification, crop planting area extraction, and crop classification (Gopinath *et al.* 2020; Tran *et al.* 2022; Zhang *et al.* 2022; Kuang *et al.* 2023). Additionally, SVM and RF regression models have been used to estimate leaf chlorophyll content (Lian *et al.* 2023).

The overarching goal of this paper was to investigate two advanced new-generation hyperspectral sensors for their performance in classifying irrigated agricultural crops in California’s Central Valley (CCV) using three machine learning algorithms (SVM, RF, and SAM) on the Google Earth Engine (GEE) cloud platform. Within this overarching goal, the specific objectives were to:

1. Build DESIS and PRISMA spectral-libraries of five irrigated agricultural crops (alfalfa, almonds, corn, grapes, and pistachios) in the CCV, demonstrate their characteristics and values, and use them in this research.
2. Explore the two overarching philosophies of hyperspectral data analysis with DESIS and PRISMA data using machine learning algorithms on GEE: (a) use of FSA approach uses all narrowbands except those with high noise levels or situated in atmospheric windows; and (b) OHNB analysis eliminates redundant or noisy narrowbands and uses only those that summarize meaningful information across the spectral profile.
3. Establish the strengths and limitations of FSA and OHNB analysis for classifying agricultural crops.
4. Highlight the advances one can make using new-generation hyperspectral data from DESIS and PRISMA in agricultural cropland studies.

Materials and Methods

Study Area

The study area near Fresno, California, within the CCV was selected because of the importance of the Central Valley for issues of global food security (Aneece and Thenkabail 2022b) and the availability of several globally dominant crops. Two overlapping August DESIS and PRISMA images (Figure 1; Table 1), of close dates during similar growth stages of crops in August, were used to classify alfalfa, almonds, corn, grapes, and pistachios. We selected these crop types because of their prevalence, global importance for food security and/or high water demands.

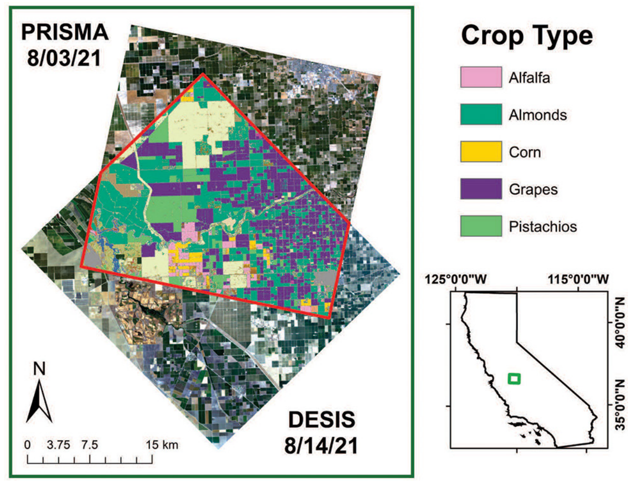

Figure 1. Study area. Location of the study area showing PRecursore IperSpettrale della Missione Applicativa (PRISMA) and Deutsches Zentrum für Luft- und Raumfahrt (DLR) Earth Sensing Imaging Spectrometer (DESIS) image footprints. The red outline indicates the overlapping area across image pairs. Within the outline is the U.S. Department of Agriculture (USDA) National Agricultural Statistics Service (NASS) Cropland Data Layer (CDL), showing study crop type distributions for the 2021 growing season. (Source: USDA National Agricultural Statistics Service Cropland Data Layer 2022).

Table 1. Study area and dates of images from PRISMA and DESIS used for this study, along with dominant crop types.

Study Area	Dominant Crop Types	Sensor	Image Date
Fresno, CA	Alfalfa, almonds, corn, grapes, pistachios	PRISMA	3 August 2021
		DESIS	14 August 2021

DESIS = DLR Earth Sensing Imaging Spectrometer; DLR = Deutsches Zentrum für Luft- und Raumfahrt; PRISMA = PRecursore IperSpettrale della Missione Applicativa.

Data

Reference Data for Training, Testing, and Validation

The U.S. Department of Agriculture (USDA) National Agricultural Statistics Service (NASS) Cropland Data Layer (CDL) 2021 crop type and confidence data were used as a reference for crop type information. The CDL is often used in agricultural remote sensing research because of its high levels of accuracy, annual data, and wall-to-wall coverage of the contiguous United States (CONUS) (Aneece and Thenkabail 2018; Tran *et al.* 2022; Zhang *et al.* 2022; Kraatz *et al.* 2023). The overall accuracy for all Farm Service Agency crops for California in 2021 was 78.4%, and the producer’s and user’s accuracies of study crops were 68.5% to 97.4% and 69.4% to 99.0%, respectively (Table 2). For the classification analysis, we smoothed the CDL 2021 crop type layer (kernel size of 2) to reduce the misclassification speckle (Kraatz *et al.* 2023). Other methods of cropland mapping are being developed, like the radar-based crop area method discussed by Kraatz *et al.* (2023), that may provide higher accuracies for future studies. The California Department of Water Resources (2024) statewide crop mapping data set is also available for California, but not for the rest of CONUS

Hyperspectral Remote Sensing Data from DESIS and PRISMA

To compare classification results across sensors, we selected a cloud-free PRISMA image from 3 August 2021 and a cloud-free DESIS image from 14 August 2021 in the study area (Table 1). Both images were available as surface reflectance products. These overlapping images were acquired less than 2 weeks apart, allowing us to compare spectra and classification results across sensors. Table 3 illustrates the variations in several characteristics between DESIS and PRISMA (Labate *et al.* 2009; Pignatti *et al.* 2013, 2015; Loizzo *et al.* 2016; Peschel *et al.* 2018; Alonso *et al.* 2019; Heiden *et al.* 2019; Krutz *et al.* 2019). In this study, we used DESIS data with 4× binning, for a 10-nm bandwidth, comparable to that of PRISMA. Moreover, Patel *et al.* (2024) found that the optimal bandwidth for estimating plant nitrogen concentrations was between 10 and 40 nm.

We geo-registered the two images in ArcGIS (Environmental Systems Research Institute 2022) and then ingested them as assets in GEE. We used GEE for analysis because it leverages Google's computing power, facilitates code sharing, and has several classification algorithms available (Tamiminia *et al.* 2020).

Spectral Libraries of Irrigated Agricultural Crops

Several spectral libraries exist for soils (Hong *et al.* 2022; Ma *et al.* 2023), minerals (Kokaly *et al.* 2017; Cardoso-Fernandes *et al.* 2023), rocks (Xie *et al.* 2022), and vegetation (Davies *et al.* 2023; Wijewardane *et al.* 2023). There are even a few agricultural spectral libraries other than GHISA, for example, the Multi-crop Spectral Library (MISPEL) (Borrmann *et al.* 2023). These spectral libraries provide much-needed training data for machine learning model development.

In this research, we further developed the GHISA spectral library for irrigated agricultural crops in the CCV. To do this, we further masked the image overlap area in GEE using the CDL confidence values (threshold = 60%, selected to maximize sample sizes while minimizing chances of mislabeled samples); normalized difference vegetation index (NDVI, threshold = 0.45), and crop type (only study crops) to ensure the model was trained on high-quality data; and validated accordingly. Note, the NDVI masks for DESIS, PRISMA, and a combination of the two are different because NDVI values for the same locations differed across sensors. We sampled the masked image overlap area at 90-m intervals to capture within-crop variability while reducing the potential of spatial autocorrelation. After further filtering samples by visual inspection of the spectra, we used them to generate spectral libraries (Table 4). The sample locations were the same for DESIS and PRISMA images to facilitate intersensor comparisons.

Intersensor Comparisons between DESIS and PRISMA

Intersensor comparisons are important for ensuring the continuity of legacy data sets (Roy *et al.* 2016), establishing cross-sensor workflows (Tripathi and Garg 2023), assessing potentials for data fusion (Aneece and Thenkabail 2022b, 2022c; Marshall *et al.* 2022), and comparing sensor characteristics for specific applications (Aneece and Thenkabail 2022b; Marshall *et al.* 2022; Davies *et al.* 2023; Muthusamy *et al.* 2023). For the comparisons in this study, we used PRISMA bands that most closely matched the DESIS four-bin product band centers. We ran correlation analyses by crop type and across all crop types. We excluded alfalfa from the correlation analysis because although the images were only 2 weeks apart, there was a substantial difference in the alfalfa growth. This was probably due to the differences in alfalfa cutting schedules across farms.

Full Spectral Analysis (FSA)

Not only are FSAs often used for classification analyses (Thenkabail *et al.* 2007; Gumma *et al.* 2021, 2022; Rejith *et al.* 2022), the spectral matching technique has also been used to evaluate PRISMA data (Cogliati *et al.* 2021). For the FSA, we used 59 DESIS bands of 60, removing band 1 due to predominantly negative reflectance values

Table 2. Classification accuracies by crop type obtained by the U.S. Department of Agriculture (USDA) National Agricultural Statistics Service (NASS) Cropland Data Layer (CDL) for California, 2021. Source: USDA NASS (2022)

Crop	Producer's Accuracy (%)	User's Accuracy (%)
Alfalfa	86.5	81.7
Almonds	90.1	87.5
Corn	69.9	77.5
Grapes	82.5	74.2
Pistachios	89.1	89.7

Source: USDA NASS (2022)
CDL = Cropland Data Layer; NASS = National Agricultural Statistics Service; USDA = U.S. Department of Agriculture.

Table 3. Characteristics of hyperspectral data used in this study: DESIS and PRISMA.

	DESIS One-Bin	DESIS Four-Bin	PRISMA
Sensor type	Spaceborne, on ISS	Spaceborne, on ISS	Spaceborne, polar-orbiting
Spectral range	402–1000 nm	403–1000 nm	407–2497 nm
Number of bands	235	60	238
Spectral resolution	2.55 nm	10 nm	≤12 nm
Spatial resolution	30 m	30 m	30 m; 5 m for panchromatic band
Swath width	30 km	30 km	30 km

Sources: Heiden et al. (2019); Loizzo et al. (2016).
DESIS = Earth Sensing Imaging Spectrometer; DLR = Deutsches Zentrum für Luft- und Raumfahrt; ISS = International Space Station; PRISMA = PRecursore IperSpettrale della Missione Applicativa.

Table 4. Sample sizes by crop types.

	GHISA	Classification Sample Sizes			
Crop Type	Sample Size	Training	Testing	Validation	Total
Alfalfa	336	120	40	40	200
Almonds	8646	120	40	40	200
Corn	205	120	40	40	200
Grapes	5329	120	40	40	200
Pistachios	2065	120	40	40	200

For classification, all sample sizes were randomly subset to 200 samples/crop type.
GHISA = Global Hyperspectral Imaging Spectral-library of Agricultural Crops.

(mostly noise). Of the 238 PRISMA bands, 207 were retained for FSA; bands from 1400 nm to 1450 nm and from 1800 nm through 1950 nm were removed due to atmospheric noise, because many of them had 0% surface reflectance across all samples.

Optimal Hyperspectral Narrowband (OHNB) Analysis

To select OHNBs for this study, we compared OHNBs across National Aeronautics and Space Administration's (NASA's) Earth Observing-1 Hyperion, DESIS, and PRISMA in our previous work (Aneece and Thenkabail, 2018, 2021, 2022c) to determine which band centers were often deemed optimal regardless of sensor. The OHNBs are often associated with various crop biophysical and biochemical characteristics like pigment content, stress, nitrogen content, biomass/yield, moisture content, and lignin/cellulose content and can be useful for classifying crop types and their growth stages (Serrano *et al.* 2002; Mobasheri and Rahimzadegan 2012; Mariotto *et al.* 2013; Thenkabail *et al.* 2013, 2014, 2021a; Salem *et al.* 2017; Roberts *et al.* 2018; Aneece and Thenkabail 2018, 2021; Hatfield *et al.* 2019; Ma *et al.* 2019; Deng *et al.* 2020; Hennessy *et al.* 2020; Mudereri *et al.* 2020; Ren *et al.* 2020).

Machine Learning Algorithms and Cloud Computing

Of the samples used to compile spectral libraries, we randomly selected 200 samples per crop type for classification analyses. The sample subset for classification analysis were then again randomly split into independent training (60%), testing (20%), and validation (20%) data sets. Training data were used to build an initial model, testing data were used to optimize model parameters through grid search, and validation data were used to assess the performance of the tuned model.

We selected SVM (Abdi 2020; Sheykhmousa *et al.* 2020; Kaul and Raina 2022), RF (Brovelli *et al.* 2020; Tyralis *et al.* 2020), and spectral angle mapper (SAM) (Gopinath *et al.* 2020; Chakravarty *et al.* 2021; Rejith *et al.* 2022) classification algorithms for their strong performances in remote sensing research and ease of implementation in GEE. Indeed, SVM is the most frequently used machine learning algorithm for hyperspectral agricultural research, and RF has been found to be the most accurate classification machine learning algorithm (Khan *et al.* 2022). RF can handle large data sets and missing values and will select the most important predictors from a large set of variables (Khan *et al.* 2022). It is also robust to noise, easy to parallelize, and fast to implement (Datta *et al.* 2022). SAM, which compares angles of reference spectra with those of target spectra, has successfully been used for PRISMA data classification (Alicandro *et al.* 2022).

For SVM, the decision procedure (voting, margin), type of kernel (linear, radial basis function, polynomial, sigmoid), shrinking (true, false), and cost (0.00001 to 1000) parameters were optimized by grid search. For RF, the number of trees (50 to 700), variables per split (1 to 55), minimum leaf population (1 to 200), out-of-bag fraction (0.1 to 0.95), and maximum nodes (10 to 200) parameters were similarly optimized through grid search. We used the spectral distance algorithm in GEE to run SAM. First, the average spectra were obtained from the training data set by crop type to serve as the crop type endmembers. Then, distances from each sample to the endmember spectra were calculated. If the distance to one crop type was sufficiently lower than the distances to all other crop types (difference thresholds optimized using testing data, 0.000001 to 0.15), the sample was labeled that crop type. The kernel size for smoothing classification results (2 to 15) was also optimized using testing data and grid search.

Classifications were run for DESIS and PRISMA separately using FSAs and OHNB analyses with each of the three classification algorithms for a total of 12 runs. DESIS and PRISMA OHNBs were also combined and run with each algorithm for another three runs, for a grand total of fifteen runs. Both DESIS bands and PRISMA bands were used for creating the NDVI masks for the combined image analysis. Only OHNB analyses were conducted when combining data from both images to avoid overfitting from FSA using all 266 (59 + 207) bands. Classification results across sensors, band selections, and classification algorithms were compared using error matrices, including overall accuracies, producer's accuracies (100% − errors of omission), and user's accuracies (100% − errors of commission).

Data Availability

The data used in this study are available online (doi: 10.5066/P14CQACU).

Results

Spectral Libraries of Irrigated Agricultural Crops

In all, 336 alfalfa, 8646 almond, 205 corn, 5329 grape, and 2065 pistachio samples were selected for compilation into the GHISA spectral libraries (Figure 2). The average spectra by crop type are shown in Figure 2 for PRISMA (Figure 2a) and DESIS (Figure 2b). Despite within-crop variability, the average spectral profiles between crops were visually separable for both sensors. Some, like the pistachio and almond averages, appeared similar in shapes and magnitudes. However, a closer inspection revealed that almonds absorbed substantially more in the red portion of the spectrum and reflected substantially more in the NIR portion of the spectrum relative to pistachios. This characteristic of high absorption in red and high reflectance in NIR led to higher NDVI for almonds compared to pistachios. Corn spectra had lower reflectance in the VIS range but higher reflectance in the NIR range and thus higher NDVI values for both sensors. Grape reflectance values were higher than the other crops in the VIS range; in the NIR region, grape reflectance values were greater than those of almonds and pistachios and lower than those of corn. However, alfalfa spectra in relation to other crops varied by sensor. This is likely due to the 2-week difference between image acquisition dates (3 August for PRISMA versus 14 August for the DESIS), in which time some of the alfalfa fields may have been cut.

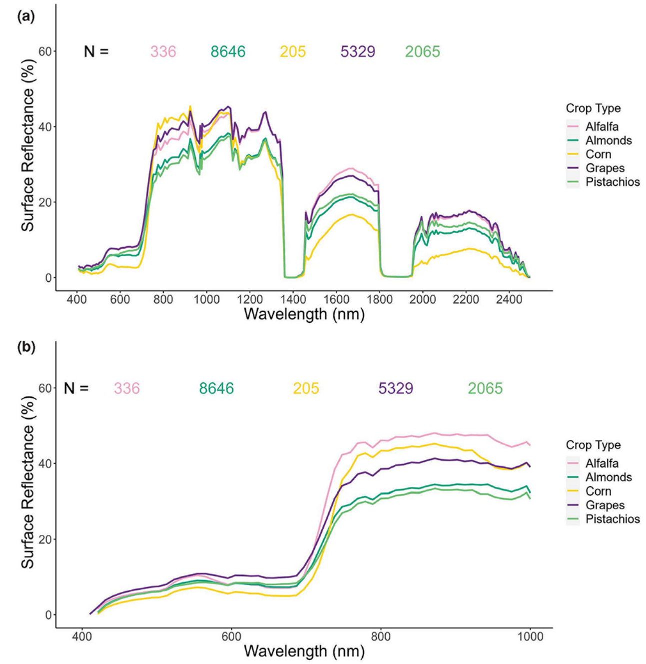

Figure 2. Average spectra by crop type. Average spectra by crop type for PRecursore IperSpettrale della Missione Applicativa (PRISMA) images (a) and Deutsches Zentrum für Luft- und Raumfahrt (DLR) Earth Sensing Imaging Spectrometer (DESIS) (b). N is the number of samples used to calculate the average.

Intersensor Comparisons between DESIS and PRISMA

Spectral data from four crops (almonds, corn, grapes, and pistachios) were pooled for correlation analysis, from which we obtained an overall R^2 of 0.97 (Figure 3). Several alfalfa fields may have been cut even during the short gap between images; hence, alfalfa was not considered in the intersensor relationship analysis. Similar R^2 values were found for individual crops: almonds (0.97), corn (0.96), grapes (0.96), and pistachios (0.97) (Figure 4). In all of the correlation analyses (Figures 3 and 4), there was a slight nonlinearity at higher reflectances, with PRISMA images (3 August) showing slightly higher reflectivity compared to DESIS (14 August). This 10-day gap between images naturally has crop growth effects in the relationships. Same-day images are needed for a perfect comparison but are extremely difficult to acquire. Nevertheless, the two images used here were from very close dates, and crops were in the critical growth phases on both dates.

Full Spectral Analysis (FSA)

When visually comparing spectral averages of each crop type from the two sensors (Figure 5), we found that the averages for almonds, corn, grapes, and pistachios were similar across sensors, especially in the NIR region. However, there was greater absorption in the water absorption portion (900 to 1000 nm) of the PRISMA spectra. As can be seen in Figure 5, the absorption features in this portion of the spectrum were more prominent in PRISMA than in DESIS, indicating a greater sensitivity of the PRISMA sensor to subtle differences in plant moisture. At the same time, the spectral behavior in the green portion (500 to 600 nm), where healthy/vigorous plants reflect higher than stressed/nonvigorous plants, was the opposite. In the green portion, DESIS reflected more energy than PRISMA, showing that DESIS was more sensitive to reflective characteristics in that spectral range.

Optimal Hyperspectral Narrowbands (OHNBs)

Upon comparing OHNBs across Hyperion (Aneece and Thenkabail 2018), DESIS (Aneece and Thenkabail 2021, 2022c), and PRISMA

(Aneece and Thenkabail 2022c), we selected 9 VIS to NIR and 16 VIS to SWIR bands for DESIS and PRISMA, respectively (Table 5). These band centers are often correlated with plant biophysical and biochemical characteristics as listed in Table 5.

Classification Results from Machine Learning Algorithms

Classification results varied across sensor, band selection method, and classification algorithm (Table 6). SVM performed the best, closely followed by RF (Table 6). The SAM classification accuracies were substantially poor, and hence, we will discuss only the SVM and RF results.

For DESIS, SVM classified the five crops with an overall accuracy of 97% using FSA and 96% using OHNBs. For FSA, the producer's accuracies were 88% to 100% (errors of omission, 0% to 12%), and user's accuracies were 93% to 100% (errors of commission, 0% to 7%). For OHNB analysis, the producer's accuracies were 91% to 100%, and user's accuracies were 90% to 100%. Also for DESIS, the RF classified the five crops with an overall accuracy of 92% using FSA and 89% using OHNBs. For FSA, the producer's accuracies were 79% to 100%, and user's accuracies were 83% to 96%. For OHNB analysis, the producer's accuracies were 76% to 100%, and user's accuracies were 83% to 95%.

For PRISMA, SVM classified the five crops with an overall accuracy of 96% using FSA and 97% using OHNBs. For FSA, the producer's accuracies were 86% to 100%, and user's accuracies were 88% to 100%. For OHNB analysis, the producer's accuracies were 92% to 100%, and user's accuracies were 92% to 100%. Also for PRISMA, RF classified the five crops with an overall accuracy of 95% using FSA and 93% using OHNBs. For FSA, the producer's accuracies were 86% to 100%, and user's accuracies were 88% to 100%. For OHNB analysis, the producer's accuracies were 86% to 100%, and user's accuracies were 84% to 100%.

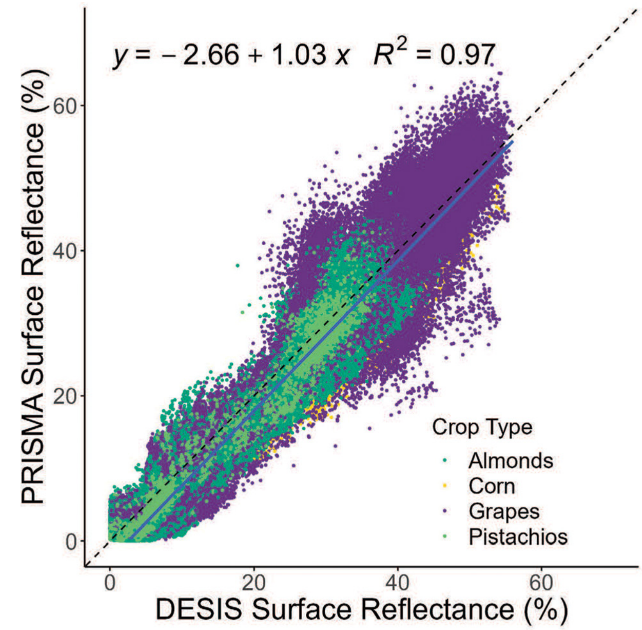

Figure 3. Correlation analysis. The figure shows a linear correlation analysis between a 3 August 2021 PRecursore IperSpettrale della Missione Applicativa (PRISMA) image and a 14 August 2021 Deutsches Zentrum für Luft- und Raumfahrt (DLR) Earth Sensing Imaging Spectrometer (DESIS) image. Reflectances are from all DESIS four-bin product bands, except band 1 and the PRISMA bands that most closely matched the DESIS band centers.

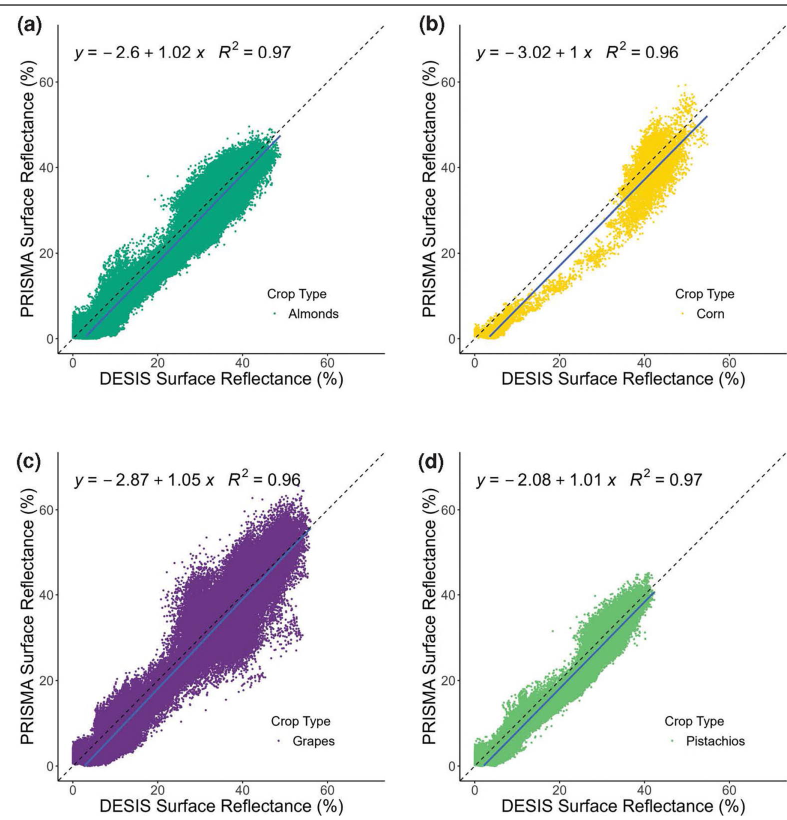

Figure 4. Correlation analyses by crop type. The figure shows linear correlation analyses by crop type for spectra from a 3 August 2021 PRecursore IperSpettrale della Missione Applicativa (PRISMA) image and a 14 August 2021 Deutsches Zentrum für Luft- und Raumfahrt (DLR) Earth Sensing Imaging Spectrometer (DESIS) image. (a) Almonds. (b) Corn. (c) Grapes. (d) Pistachios. Reflectances are from all DESIS four-bin product bands, except band 1 and the PRISMA bands that most closely matched the DESIS band centers.

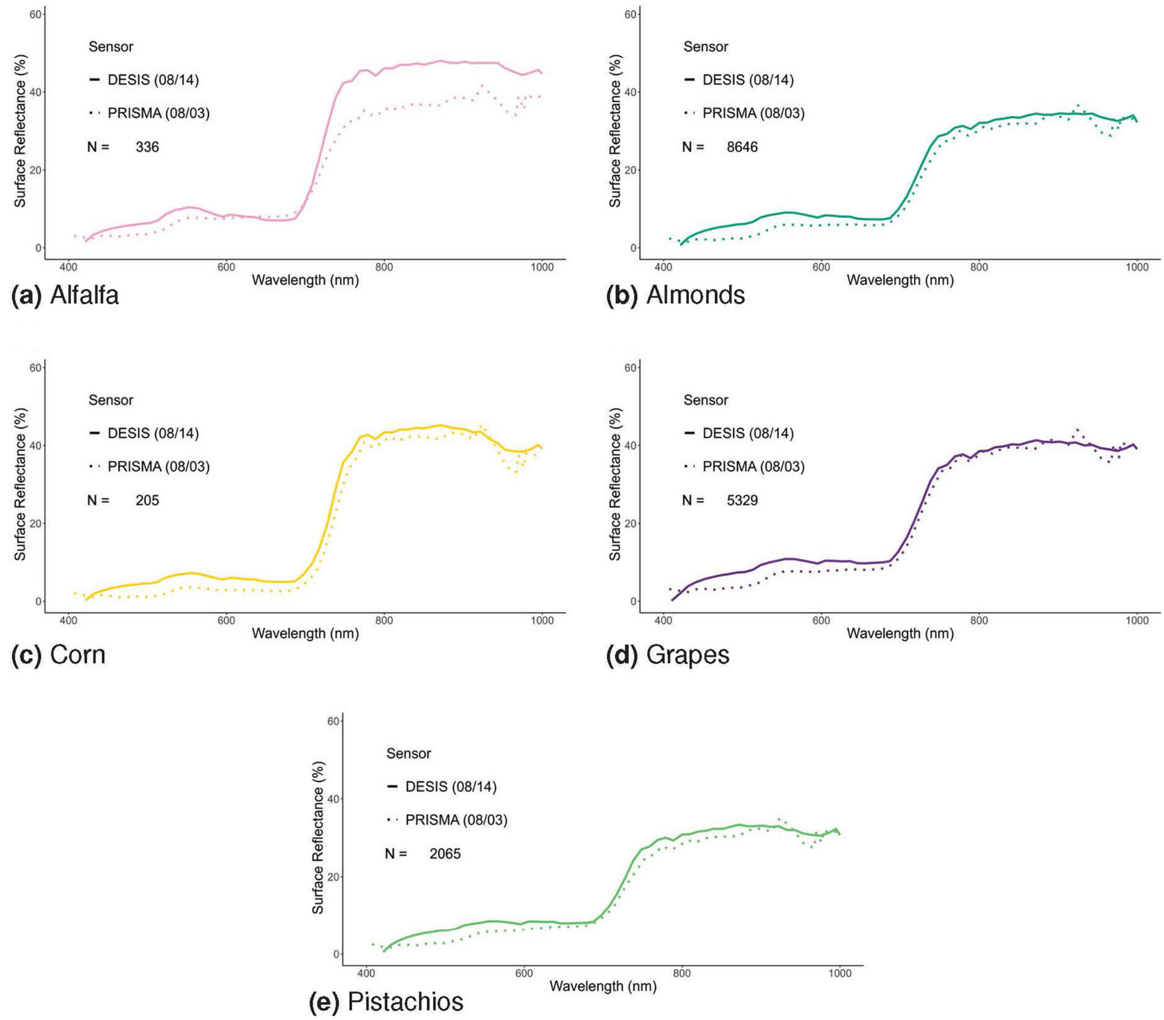

Figure 5. Average spectra by sensor. The figure shows the average spectra from Deutsches Zentrum für Luft- und Raumfahrt (DLR) Earth Sensing Imaging Spectrometer (DESIS) and PRecursore IperSpettrale della Missione Applicativa (PRISMA) in the visible and near-infrared range. (a) Alfalfa. (b) Almonds. (c) Corn. (d) Grapes. (e) Pistachios. N is the number of samples used to calculate the average.

Table 5. OHNBs used in this study for DESIS and PRISMA image analysis.

OHNB (nm)		Relevance	References
DESIS	PRISMA		
493	497	Carotenoids, LUE, stress	Aneece and Thenkabail (2018); Hennessy et al. (2020); Thenkabail et al. (2014, 2013)
534	527	LUE, stress, disease, growth stage	Aneece and Thenkabail (2021); Deng et al. (2020); Hennessy et al. (2020); Ma et al. (2019); Ren et al. (2020); Roberts et al. (2018); Thenkabail et al. (2014, 2013)
565	567	Nitrogen, growth stage, weeds, pigments	Aneece and Thenkabail (2021); Hennessy et al. (2020); Ma et al. (2019); Mudereri et al. (2020); Ren et al. (2020); Salem et al. (2017); Thenkabail et al. (2021a)
717	714	Stress, pigments, growth stage	Aneece and Thenkabail (2018, 2021); Ma et al. (2019); Thenkabail et al. (2014, 2013)
769	775	Biomass/yield, pigments	Aneece and Thenkabail (2018, 2021); Ren et al. (2020); Salem et al. (2017); Thenkabail et al. (2013)
810	807	Crop classification	Mariotto et al. (2013)
830	839	Biomass/yield	Aneece and Thenkabail (2021); Mariotto et al. (2013)
912	913	Moisture, biomass, proteins	Thenkabail et al. (2021a)
986	989	Moisture, biomass/yield, starch	Hatfield et al. (2019); Mobasheri and Rahimzadegan (2012); Roberts et al. (2018); Serrano et al. (2002); Thenkabail et al. (2021a)
-	1175	Biomass/yield, moisture	Mariotto et al. (2013); Roberts et al. (2018)
-	1240	Water sensitivity	Thenkabail et al. (2021a)
-	1295	Biomass/yield	Mariotto et al. (2013)
-	1717	Biomass/yield, lignin, starch, protein	Mariotto et al. (2013); Mobasheri and Rahimzadegan (2012); Serrano et al. (2002)
-	2078	Moisture, nitrogen, protein	Aneece and Thenkabail (2018); Mobasheri and Rahimzadegan (2012); Serrano et al. (2002)
-	2191	Lignin, cellulose, sugar, starch, protein	Aneece and Thenkabail (2018); Roberts et al. (2018); Thenkabail et al. (2014, 2013)
-	2343	Cellulose, protein, nitrogen	Mobasheri and Rahimzadegan (2012); Thenkabail et al. (2021a)

DESIS = DLR Earth Sensing Imaging Spectrometer; DLR = Deutsches Zentrum für Luft- und Raumfahrt; LUE = light-use efficiency; OHNB = optimal hyperspectral narrowband; PRISMA = PRecursore IperSpettrale della Missione Applicativa.

Table 6. Classification results using OHNB analysis and FSA from DESIS and PRISMA images using three MLAs: SVM, RF, and SAM.

				Accuracies (%)										
					Alfalfa		Almonds		Corn		Grapes		Pistachios	
Sensor	MLA	Bands	Kappa	OA	PA	UA	PA	UA	PA	UA	PA	UA	PA	UA
DESIS	SVM	FSA	0.97	97	100	97	100	93	100	100	88	97	97	100
		OHNB	0.95	96	97	100	95	90	100	100	91	97	97	95
	RF	FSA	0.90	92	100	95	92	83	100	95	79	96	90	95
		OHNB	0.86	89	100	95	76	83	100	93	76	90	92	86
	SAM	FSA	0.64	71	77	77	58	86	100	95	48	42	64	55
		OHNB	0.53	63	63	75	70	43	100	95	23	32	48	78
PRISMA	SVM	FSA	0.95	96	100	100	97	88	100	100	86	94	98	100
		OHNB	0.97	97	100	97	92	97	100	100	97	92	98	100
	RF	FSA	0.93	95	100	97	92	88	100	100	86	89	95	100
		OHNB	0.91	93	97	97	87	87	100	100	86	84	93	95
	SAM	FSA	0.42	54	71	81	51	35	97	73	3	100	46	40
		OHNB	0.57	66	84	91	63	45	100	100	20	44	52	49
Both	SVM	OHNB	0.99	99	100	100	100	95	100	100	94	100	100	100
	RF	OHNB	0.88	90	97	97	82	82	100	100	82	90	90	83
	SAM	OHNB	0.62	70	91	97	71	49	100	97	38	62	36	43

DESIS = DLR Earth Sensing Imaging Spectrometer; DLR = Deutsches Zentrum für Luft- und Raumfahrt; FSA = full spectral analysis; MLA = machine learning algorithm; OA = overall accuracy; OHNB = optimal hyperspectral narrowband; PA = producer's accuracy; PRISMA = PRecursore IperSpettrale della Missione Applicativa; RF = random forest; SAM = spectral angle mapper; SVM = support vector machine; UA = user's accuracy.

When OHNBs from both DESIS and PRISMA were used, SVM classified the five crops with an overall accuracy of 99%, producer's accuracies of 94% to 100%, and user's accuracies of 95% to 100%. RF classified the five crops with the overall accuracy of 90%, and producer's and user's accuracies of 82% to 100%. Across all SVM and RF runs, overall accuracies were 89% to 99%, producer's accuracies were 76% to 100%, and user's accuracies were 82% to 100%.

Visual inspection of the classification results (Figures 6 and 7) using the best classifier (SVM) shows a close match with the reference data. In Figure 6, the DESIS SVM classification results for the five crops is shown for FSA (Figure 6b) and OHNB analysis (Figure 6c) and compared with the reference USDA NASS CDL product (Figure 6a). In Figure 7, the PRISMA SVM classification results for the five crops are shown for FSA (Figure 7b) and OHNB analysis (Figure 7c) and compared with the reference USDA NASS CDL product (Figure 7a).

The DESIS SVM FSA result (overall accuracy [OA] = 97%) closely matched the masked CDL layer, although some grape fields were incorrectly classified as alfalfa and almonds (Figure 6b). In addition to similar misclassifications in the DESIS RF FSA result (OA = 92%), we also see many grape fields misclassified as corn. The DESIS OHNB analysis results (OA for SVM and RF, respectively = 96% and 89%) (Figure 6c) show similar errors as the FSA results.

The PRISMA SVM FSA result (OA = 96%) looks similar to the masked CDL layer, although some grape fields are misclassified as alfalfa (Figure 7b). The PRISMA RF FSA result (OA = 95%) similarly shows more grape fields and fields misclassified as alfalfa. Similar misclassifications are found in the PRISMA OHNB analysis results (OA for SVM and RF, respectively = 97% and 93%) (Figure 7c).

When using OHNBs from both images, the overall accuracies increased for SVM OHNB analysis (by 3% from DESIS and by 2% from PRISMA). The overall accuracy also increased for RF OHNB analysis from DESIS (by 1%) but decreased from PRISMA (by 3%). The results (not shown) still show similar misclassifications as when OHNBs from the two images were used separately.

Discussion

In this study, we compared two philosophies of hyperspectral remote sensing (FSA and OHNB analysis) using data from two new-generation hyperspectral spaceborne sensors (DESIS and PRISMA) and three machine learning algorithms (SVM, RF, and SAM) to classify five irrigated agricultural crops (alfalfa, almonds, corn, grapes, and pistachios) in the CCV.

We began by compiling spectral libraries for the crops using DESIS and PRISMA data and using those libraries to establish intersensor comparisons. We found that DESIS and PRISMA spectra were similar by crop types for almonds, corn, grapes, and pistachios; however, alfalfa spectra differed substantially, especially in the NIR region. Correlation analyses between similar bands from the VIS to NIR region show strong relationships between DESIS and PRISMA spectral reflectances for all crops except alfalfa. Alicandro *et al.* (2022) did similar spectral signature comparisons between PRISMA and *Sentinel-2* and found strong agreement between the two; the extra detail provided by PRISMA made this sensor more advantageous for their application. Although spectral libraries were generated for several intersensor comparison studies, the data were available by request instead of being published and easily accessible to other researchers as we have done in this study (Alicandro *et al.* 2022; Bresciani *et al.* 2022; Muthusamy *et al.* 2023).

We also compared the two sensors in their abilities to classify crop types. DESIS and PRISMA performed similarly in terms of overall classification accuracies, and combining information from both images increased overall accuracies when using SVM and SAM. In contrast, Muthusamy *et al.* (2023) found PRISMA slightly outperformed DESIS for mapping peatland vegetation due to additional information in the PRISMA SWIR bands. This may be because of differences in the vegetation background of mostly soil for agricultural crops and mostly water or water-saturated soil for peatland vegetation.

For both DESIS and PRISMA data, FSAs generally had higher overall accuracies than corresponding OHNB analyses, but only by 1% to 3%. This supports previous studies that achieved high classification accuracies even with 15 to 30 OHNBs (Aneece and Thenkabail 2018, 2021, 2022c). We used 207 PRISMA bands for FSA analysis; however, Alicandro *et al.* (2022) removed other bands as well (throughout the 407- to 2497-nm spectral range) due to their contributions to salt-and-pepper noise. Removing these additional bands may further increase FSA classification accuracies in future studies.

SVM and RF resulted in high classification accuracies, as supported in previous work (Aneece and Thenkabail 2021). They both outperformed SAM, supporting findings by Gopinath *et al.* (2020). However, Alicandro *et al.* (2022) were able to use SAM to classify archeological sites. Kuang *et al.* (2023) found similar classification accuracies between SVM/RF and several neural network (NN) models. They noted that the NN models had less salt-and-pepper noise; however, we addressed this problem by smoothing the classification results.

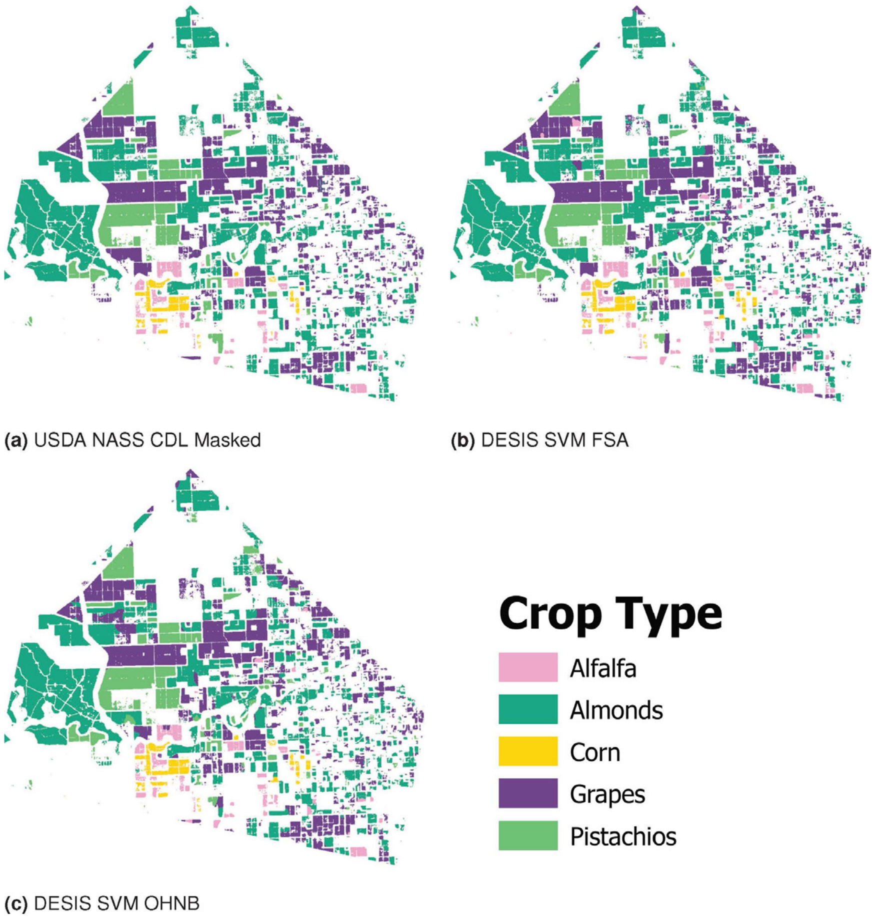

Figure 6. DESIS SVM FSA- and OHNB-derived maps compared with USDA NASS CDL reference map. The figure shows comparisons of U.S. Department of Agriculture (USDA) National Agricultural Statistics Service (NASS) Cropland Data Layer (CDL) (a), Deutsches Zentrum für Luft- und Raumfahrt (DLR) Earth Sensing Imaging Spectrometer (DESIS) Support Vector Machine (SVM) Full Spectral Analysis (FSA) (b), and DESIS SVM Optimal Hyperspectral Narrowband (OHNB) (c) analysis.

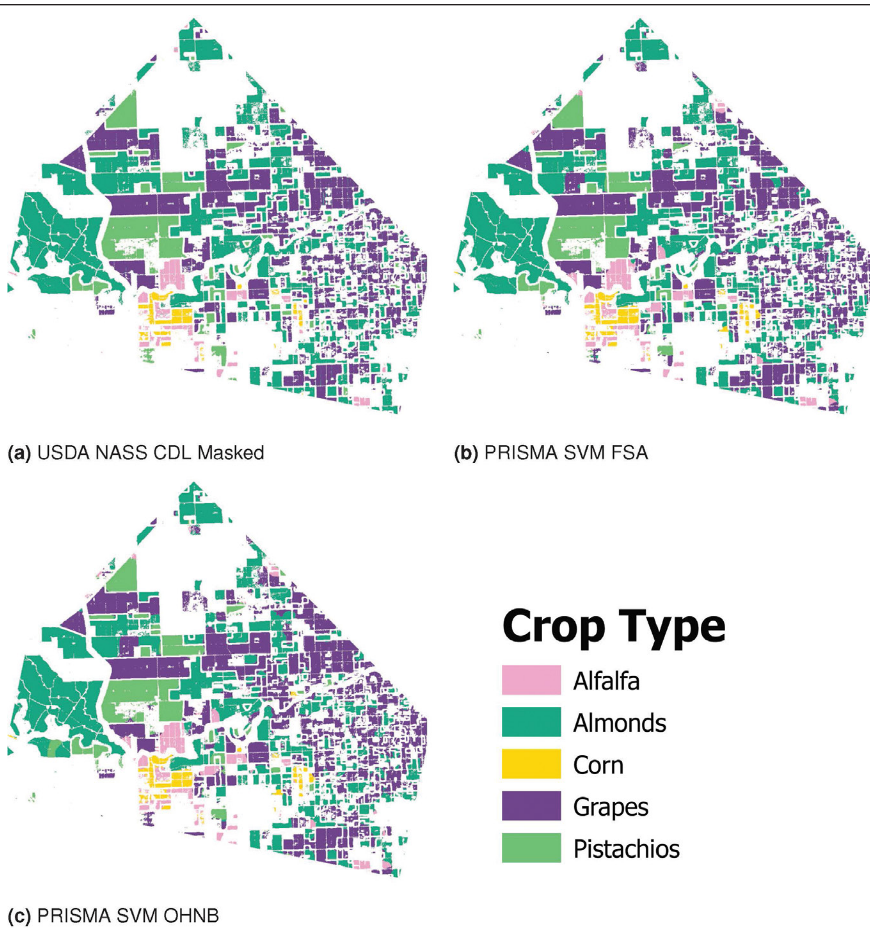

Figure 7. PRISMA SVM FSA- and OHNB-derived maps compared with USDA NASS CDL reference map. Comparisons of a) United States Department of Agriculture (USDA) National Agricultural Statistics Service (NASS) Cropland Data Layer (CDL), b) PRecursore IperSpettrale della Missione Applicativa (PRISMA) Support Vector Machine (SVM) Full Spectral Analysis (FSA), and c) PRISMA SVM Optimal Hyperspectral Narrowband (OHNB) analysis.

This work can be furthered by validating the models for different locations/years. Comparison with other hyperspectral sensors would also be helpful. Using a different reference data set like the CADWR statewide crop mapping data set (California Department of Water Resources 2024) may also improve results. Pansharpening of hyperspectral images, like PRISMA, may also improve classification accuracies (Vivone *et al.* 2023). In addition, using deep learning models may vastly improve classification accuracies over traditional machine learning algorithms (Datta *et al.* 2022). Convolutional neural networks have frequently and successfully been used in hyperspectral agricultural, and classification applications (Chang *et al.* 2022; Kaul and Raina 2022; Khan *et al.* 2022). Farmonov *et al.* (2023) found that CNN outperformed SVM and RF for crop type classification using DESIS imagery. There are also deep learning versions of traditional machine learning algorithms like SVM and RF (Datta *et al.* 2022). Time-series multispectral data can also be used to classify crops (Tran *et al.* 2022; Zhang *et al.* 2022; Rußwurm *et al.* 2023; You *et al.* 2023) and to quantitatively observe the temporal variability of crop spectral profiles (Yu *et al.* 2022).

Conclusions

This study evaluated two new-generation hyperspectral sensors, DESIS and PRISMA, in classifying and mapping five irrigated crops (alfalfa, almonds, corn, grapes, and pistachios) in a study area in California's Central Valley. First, we developed spectral libraries of five irrigated crops using both sensors (Aneece *et al.*, 2024). These spectral libraries were used as input for training machine learning algorithms and for testing and validating the cropland products. The spectral libraries have been released through the existing Global Hyperspectral Imaging Spectral-library of Agricultural crops (GHISA) platform (GHISA, 2024) and will be invaluable for building machine learning and artificial intelligence models using remote sensing data. Second, intersensor comparisons of DESIS and PRISMA provided a linear relationship with a high R^2 value of 0.97. This shows that the hyperspectral sensor data from instruments like DESIS and PRISMA can be used across sensors to maximize data collection over any given area. Third, using the best machine learning algorithm, support vector machine (SVM), five irrigated crops were classified with overall accuracies of 96% to 97% using full spectral analysis (FSA) and optimal hyperspectral narrowband (OHNB) analysis across sensors. For FSA, the producer's accuracies were 86% to 100% (errors of omission, 0% to 14%) and user's accuracies were 88% to 100% (errors of commission, 0% to 12%) across sensors. For OHNB analysis, the producer's accuracies were 91% to 100% (errors of omission, 0% to 9%) and user's accuracies were 90% to 100% (errors of commission, 0% to 10%) across sensors. SVM performed the best closely followed by RF. SAM provided significantly lower accuracies. When both DESIS and PRISMA sensors were combined in the analysis, there was an ~2% to 3% increase in accuracies using SVM. Fourth, the FSAs only provided 1% to 3% higher accuracies relative to OHNBs using SVM and RF. This implies that optimal classification accuracies of crops can be achieved with the best 9 to 25 OHNBs. Nevertheless, the full spectrum will still be needed for classifying more complex land cover types with many more crops and/or in the study of other specific crop biophysical, biochemical, plant health, plant stress, or plant structural characteristics. These findings will be important for the design and analysis of data from many current and upcoming hyperspectral sensors such as Germany's DLR's Environmental Mapping and Analysis Program (EnMAP) and NASA's Surface Biology and Geology (SBG) mission, alongside NASA's and U.S. Geological Survey's (USGS's) Landsat Next superspectral sensor.

Acknowledgments

This research was supported by the National Land Imaging (NLI) Program, Land Change Science (LCS) program, and the Core Science Systems (CSS) of the United States Geological Survey (USGS). The research was conducted in the science facilities of the USGS Western Geographic Science Center (WGSC). Any use of trade, firm, or product names is for descriptive purposes only and does not imply endorsement by the U.S. Government. Data used in this study are available online (Aneece *et al.*, 2024)

References

Abdi, A. 2020. Land cover and land use classification performance of machine learning algorithms in a boreal landscape using *Sentinel-2* data. *GIScience and Remote Sensing* 57:1–20.

Alicandro, M., E. Candigliota, D. Dominici, F. Immordino, F. Masin, N. Pascucci, R. Quaresima and S. Zollini. 2022. Hyperspectral PRISMA and *Sentinel-2* preliminary assessment comparison in Alba Fucens and Sinuessa archaeological sites (Italy). *Land* 11(11):2070.

Alonso, K., M. Bachmann, K. Burch, E. Carmona, D. Cerra, R. de los Reyes, D. Dietrich, U. Heiden, A. Holderlin, J. Ickes, U. Knodt, D. Krutz, H. Lester, R. Muller, M. Pagnutti, P. Reinartz, R. Richter, R. Ryan, I. Sebastian and M. Tegler. 2019. Data products, quality and validation of the DLR Earth Sensing Imaging Spectrometer (DESIS). *Sensors* 19(4471):1–44.

Anand, A., R. Malhi, P. Srivastava, P. Singh, A. Mudaliar, G. Petropoulos and G. Kiran. 2022. Optimal band characterization in reformation of hyperspectral indices for species diversity estimation. *Physics and Chemistry of the Earth* 126(103040):1–13.

Aneece, I., D. Foley, P. Thenkabail, A. Oliphant and P. Teluguntla. 2022. PlanetScope and DESIS spectral library of agricultural crops in California's Central Valley for the 2020 growing season. U.S. Geological Survey data release.

Aneece, I. and P. Thenkabail. 2018. Accuracies achieved in classifying five leading world crop types and their growth stages using optimal Earth Observing-1 Hyperion hyperspectral narrowbands on Google Earth Engine. *Remote Sensing* 10:1–29.

Aneece, I. and P. Thenkabail. 2019a. Global Hyperspectral Imaging Spectral-library of Agricultural crops (GHISA) for the Conterminous United States (CONUS). Algorithm Theoretical Basis Document (ATBD). In *NASA Land Processes Distributed Active Archive Center (LP DAAC)*, pp. 1–25.

Aneece, I. and P. Thenkabail. 2019b. Global Hyperspectral Imaging Spectral-library of Agricultural crops (GHISA) for the Conterminous United States (CONUS). User Guide. In *NASA Land Processes Distributed Active Archive Center (LP DAAC)*, pp. 1–7.

Aneece, I. and P. Thenkabail. 2021. Classifying crop types using two generations of hyperspectral sensors (Hyperion and DESIS) with machine learning on the cloud. *Remote Sens*ing 13(4704):1–24.

Aneece, I. and P. Thenkabail. 2022a. DESIS and PRISMA spectral library of agricultural crops in California's Central Valley in the 2020 Growing Season. U.S. Geological Survey data release.

Aneece, I. and P. Thenkabail. 2022b. New generation hyperspectral data from DESIS compared to high spatial resolution PlanetScope data for crop type classification. *IEEE Journal of Selected Topics in Applied Earth Observations and Remote Sensing* 15:7846–7858.

Aneece, I. and P. Thenkabail. 2022c. New generation hyperspectral sensors DESIS and PRISMA provide improved agricultural crop classifications. *Photogrammetric Engineering and Remote Sensing* 88:715–729.

Aneece, I., P. Thenkabail, R. McCormick, P. Teluguntla, A. Oliphant, and D. Foley. 2024. DESIS and PRISMA spectral library of agricultural crops for California's Central Valley in August 2021, https://doi.org/10.5066/P14CQACU.

Basener, B. 2022. Classifying crop types Using Gaussian Bayesian models and neural networks on Ghisaconus USGS Data from NASA Hyperspectral Satellite Imagery. In *2022 12th Workshop on Hyperspectral Imaging and Signal Processing: Evolution in Remote Sensing (WHISPERS)*, 13–16 September 2022, Rome, Italy, pp. 1–6.

Borrmann, P., P. Brandt and H. Gerighausen. 2023. MISPEL: A multi-crop spectral library for statistical crop trait retrieval and agricultural monitoring. *Remote Sensing* 15(14):3664.

Bresciani, M., C. Giardino, A. Fabbretto, A. Pellegrino, S. Mangano, G. Free and M. Pinardi. 2022. Application of new hyperspectral sensors in the remote sensing of aquatic ecosystem health: Exploiting PRISMA and DESIS for four Italian lakes. *Resources* 11(8):1–17.

Brovelli, M., Y. Sun and V. Yordanov. 2020. Monitoring forest change in the Amazon using multi-temporal remote sensing data and machine learning classification on Google Earth Engine. *ISPRS International Journal of Geo-information* 9(10):580.

California Department of Water Resources. 2024. Statewide Crop Mapping. <https://data.cnra.ca.gov/dataset/statewide-crop-mapping> (last date accessed 20 February 2024).

Campbell, P., K. Huemmrich, E. Middleton, J. Alfieri, C. van der Tol and C. Neigh. 2022. Using DESIS and EO-1 Hyperion reflectance time series for the assessment of vegetation traits and gross primary production (GPP). *International Archives of the Photogrammetry, Remote Sensing and Spatial Information Sciences* XLVI-1/W1-2021:1–9.

Cardoso-Fernandes, J., D. Santos, C. Rodrigues de Almeida, A. Lima, A. C. Teodoro and GREENPEG project team. 2023. Spectral library of European pegmatites, pegmatite minerals and pegmatite host-rocks – the GREENPEG project database. *Earth System Science Data* 15(7):3111–3129.

Chakravarty, S., B. Paikaray, R. Mishra and S. Dash. 2021. Hyperspectral image classification using spectral angle mapper. *IEEE International Women in Engineering Conference on Electrical and Computer Engineering*, 4-5 December 2021, Dhaka, Bangladesh, pp. 87–90.

Chang, Y., T. Tan, W. Lee, L. Chang, Y. Chen, K. Fan and M. Alkhaleefah. 2022. Consolidated convolutional neural network for hyperspectral image classification. *Remote Sensing*, 14(1571):1–16.

Cogliati, S., F. Sarti, L. Chiarantini, M. Cosi, R. Lorusso, E. Lopinto, F. Miglietta, L. Genesio, L. Guanter, A. Damm, S. Pérez-López, D. Scheffler, G. Tagliabue, C. Panigada, U. Rascher, T. Dowling, C. Giardino and R. Colombo. 2021. The PRISMA imaging spectroscopy mission: Overview and first performance analysis. *Remote Sensing of Environment* 262:112499.

Datta, D., P. Mallick, A. Bhoi, M. Ijaz, J. Shafi and J. Choi. 2022. Hyperspectral image classification: Potentials, challenges, and future directions. *Hindawi Computational Intelligence and Neuroscience* 20122(3854635):1–36.

Davies, B. F. R., Gernez, P., Geraud, A., Oiry, S., Rosa, P., Zoffoli, M. L. and Barillé, L. 2023. Multi- and hyperspectral classification of soft-bottom intertidal vegetation using a spectral library for coastal biodiversity remote sensing. *Remote Sensing of Environment*, 290:113554.

Deng, X., Z. Zhu, J. Yang, Z. Zheng, Z. Huang, X. Yin, S. Wei and Y. Lan. 2020. Detection of citrus huanglongbing based on multi-input neural network model of UAV hyperspectral remote sensing. *Remote Sensing* 12(2678):1–20.

Environmental Systems Research Institute. 2022. ArcGIS Desktop: Release 10.8.1. Redlands, CA: Environmental Systems Research Institute.

Farmonov, N., K. Amankulova, J. Szatmari, A. Sharifi, D. Abbasi-Moghadam, S. Nejad and L. Mucsi. 2023. Crop type classification by DESIS hyperspectral imagery and machine learning algorithms. *IEEE Journal of Selected Topics in Applied Earth Observations and Remote Sensing* 16:1576–1588.

Fernandez-Habas, J., M. Canada, A. Moreno, J. Leal-Murillo, M. Gonzalez-Dugo, B. Oar, P. Gomez-Giraldez and P. Fernandez-Rebollo. 2022. Estimating pasture quality of Mediterranean grasslands using hyperspectral narrow bands from field spectroscopy by Random Forest and PLS regressions. *Computers and Electronics in Agriculture* 192(106614):1–15.

Foley, D., P. Thenkabail, A. Oliphant, I. Aneece and P. Teluguntla. 2023. Crop water productivity from cloud-based Landsat helps assess California's water savings. *Remote Sensing*, 15(4894):1–23.

GHISA (2024). Global Hyperspectral Imaging Spectral-library of Agricultural-Crops & Vegetation (GHISA), https://www.usgs.gov/centers/western-geographic-science-center/science/globalhyperspectral-imaging-spectral-library.

Gopinath, G., N. Sasidharan and U. Surendran. 2020. Landuse classification of hyperspectral data by spectral angle mapper and support vector machine in humid tropical region of India. *Earth Science Information* 13:633–640.

Gross, G., D. Helder and L. Leigh. 2023. Extended cross-calibration analysis using data from the Landsat 8 and 9 underfly event. *Remote Sensing* 15:1788.

Gumma, M., M. Kadiyala, P. Panjala, S. Ray, V. Akuraju, S. Dubey, A. Smith, R. Das and A. Whitbread. 2021. Assimilation of remote sensing data into crop growth model for yield estimation: A case study from India. *Journal of the Indian Society of Remote Sensing* 50(5):1–15.

Gumma, M., K. Tummala, S. Dixit, F. Collivignarelli, F. Holecz, R. Kolli and A. Whitbread. 2022. Crop type identification and spatial mapping using *Sentinel-2* satellite data with focus on field-level information. *Geocarto International* 37(7):1833–1849.

Hatfield, J., J. Prueger, T. Sauer, C. Dold, P. O'Brien and K. Wacha. 2019. Applications of vegetative indices from remote sensing to agriculture: Past and future. *Inventions* 4(71):1–17.

Heiden, U., M. Bachmann, K. Alonso, E. Carmona, D. Cerra, D. Dietrich, D., M. Langheinrich, R. de los Reyes, R. Mueller, N. Pinnel and V. Ziel. 2019. DESIS imaging spectrometer data access and synergistic use with other ISS earth observing instruments. In *Workshop on International Cooperation in Spaceborne Imaging Spectroscopy*, ESA-ESRIN, 9–11 July 2019, Frascati, Italy, https://elib.dlr.de/129175/.

Hennessy, A., K. Clarke and M. Lewis. 2020. Hyperspectral classification of plants: A review of waveband selection generalisability. *Remote Sensing* 12(113):1–27.

Hong, Y., Y. Chen, S. Chen, R. Shen, B. Hu, J. Peng, N. Wang, L. Guo, Z. Zhuo, Y. Yang, Y. Liu, A. M. Mouazen and Z. Shi. 2022. Data mining of urban soil spectral library for estimating organic carbon. *Geoderma* 426:116102.

Kaul, A. and S. Raina. 2022. Support vector machine versus convolutional neural network for hyperspectral image classification: A systematic review. *Concurrency and Computation Practice and Experience* 34:e6945.

Khan, A., A. Vibhute, S. Mali and C. Patil. 2022. A systematic review on hyperspectral imaging technology with a machine and deep learning methodology for agricultural applications. *Ecological Informatics* 69(101678):1–12.

Kokaly, R., R. Clark, G. Swayze, K. Livo, T. Hoefen, N. Pearson, R. Wise, W. Benzel, H. Lowers, R. Driscoll and A. Klein. 2017. USGS Spectral Library Version 7 Data: U.S. Geological Survey data release.

Kraatz, S., B. Lamb, W. Hively, J. Jennewein, F. Gao, M. Cosh and P. Siqueira. 2023. Comparing NISAR (using *Sentinel-1*), USDA/NASS CDL, and ground truth crop/non-crop areas in an urban agricultural region. *Sensors* 23(8595):1–26.

Krutz, D., R. Muller, U. Knodt, B. Gunther, I. Walter, I. Sebastian, T. Sauberlich, R. Reulke, E. Carmona, A. Eckardt, H. Venus, C. Fischer, B. Zender, S. Arloth, M. Lieder, M. Neidhardt, U. Grote, F. Schrandt, S. Gelmi and A. Wojtkowiak. 2019. The instrument design of the DLR Earth Sensing Imaging Spectrometer (DESIS). *Sensors* 19(1622):1–16.

Kuang, X., J. Guo, J. Bai, H. Geng and H. Wang. 2023. Crop-planting area prediction from multi-source *Gaofen* satellite images using a novel deep learning model: A case study of Yangling District. *Remote Sensing* 15(3792):1–20.

Labate, D., M. Ceccherini, A. Cisbani, V. De Cosmo, C. Galeazzi, L. Giunti, M. Melozzi, S. Pieraccini and M. Stagl. 2009. The PRISMA payload optomechanical design, a high performance instrument for a new hyperspectral mission. *Acta Astronautica* 65:1429–1436.

Lian, S., L. Guan, Z. Peng, G. Zeng, M. Li and Y. Xu. 2023. Retrieval of leaf chlorophyll content in Gannan navel orange based on fusing hyperspectral vegetation indices using machine learning algorithms. *Ciencia Rural* 53(3):1–9.

Loizzo, R., C. Ananasso, R. Guarini, E. Lopinto, L. Candela and A. Pisani. 2016. The PRISMA hyperspectral mission. In *Workshop on Living Planet Symposium*, 9–13 May 2019, Prague, Czech Republic. https://lps16.esa.int/.

Longchamps, L. and W. Philpot. 2023. Full-season crop phenology monitoring using two-dimensional normalized difference pairs. *Remote Sensing* 15(5565):1–16.

Ma, H., K. Zhao, X. Jin, J. Ji, Z. Qiu and S. Gao. 2019. Spectral difference analysis and identification of different maturity blueberry fruit based on hyperspectral imaging using spectral index. *International Journal of Agriculture and Biological Engineering* 134(3):134–140.

Ma, Y., P. Roudier, K. Kumar, T. Palmada, G. Grealish, S. Carrick, L. Lilburne and J. Triantafilis. 2023. A soil spectral library of New Zealand. *Geoderma Regional* 35:e00726.

Mariotto, I., P. Thenkabail and I. Aneece. 2020a. Global Hyperspectral Imaging Spectral-library of Agricultural crops (GHISA) Area of Study: Central Asia. Algorithm Theoretical Basis Document (ATBD). In *NASA Land Processes Distributed Active Archive Center (LP DAAC)*, pp. 1–28.

Mariotto, I., P. Thenkabail and I. Aneece. 2020b. Global Hyperspectral Imaging Spectral-library of Agricultural crops (GHISA) Area of Study: Central Asia. User Guide. In *NASA Land Processes Distributed Active Archive Center (LP DAAC)*, pp. 1–7.

Mariotto, I., P. Thenkabail, A. Huete, T. Slonecker and A. Platonov. 2013. Hyperspectral versus multispectral crop-productivity modeling and type discrimination for the HyspIRI mission. *Remote Sensing of Environment* 139:291–305.

Marshall, M., M. Belgiu, M. Boschetti, M. Pepe, A. Stein and A. Nelson. 2022. Field-level crop yield estimation with PRISMA and *Sentinel-2*. *ISPRS Journal of Photogrammetry and Remote Sensing* 187:191–210.

McGehee, R. 2022. *Nonpoint Source Pollutant Modeling in Small Agricultural Watersheds with the Water Erosion Prediction Project*. Ph.D. dissertation, Purdue University, West Lafayette, Indiana.

Mobasheri, M. and M. Rahimzadegan. 2012. Introduction to protein absorption lines index for relative assessment of green leaves protein content using EO-1 Hyperion datasets. *Journal of Agricultural Science and Technology* 14:135–147.

Mudereri, B., T. Dube, S. Niassy, E. Kimathi, T. Landmann, Z. Khan and E. Abdel-Rahman. 2020. Is it possible to discern Striga weed (*Striga hermonthica*) infestation levels in maize agro-ecological systems using in-situ spectroscopy? *International Journal of Applied Earth Observation and Geoinformation* 85(102008):1–14.

Muthusamy, A., F. Thiel, V. Pham, C. Hellmann and S. van der Linden. 2023. Mapping vegetation cover on rewetted fen peatlands using hyperspectral spaceborne images from DESIS and PRISMA. *European Geosciences Union General Assembly*, EGU23-5352, 23–28 April 2023, Vienna, Austria, pp. 1–2.

Patel, M., D. Ryu, A. Western, G. Fitzgerald, E. Perry, H. Suter and I. M. Young. 2024. A new multispectral index for canopy nitrogen concentration applicable across growth stages in ryegrass and barley. *Precision Agriculture* 25:486–519.

Peschel, T., M. Beier, C., Damm, J. Hartung, R. Jende, S. Muller, M. Rohde, A. Gebhardt, S. Risse, I. Walter, I. Sebastian and D. Krutz. 2018. Integration and testing of an imaging spectrometer for earth observation. In *International Conference on Space Optics*, 9–12 October 2018, Chania, Greece, pp. 1–7.

Pignatti, S., N. Acito, U. Amato, R. Casa, F. Castaldi, R. Coluzzi, R. De Bonis, M. Diani, V. Imbrenda, G. Laneve, S. Matteoli, A. Palombo, S. Pascucci, F. Santini, T. Simoniello, C. Ananasso, G. Corsini and V. Cuomo. 2015. Environmental products overview of the Italian hyperspectral PRISMA mission: The SAP4PRISMA project. In *IEEE International Geoscience and Remote Sensing Symposium*, 13–18 July 2015, Milan, Italy, pp. 1–5.

Pignatti, S., A. Palombo, S. Pascucci, F. Romano, F. Santini, T. Simoniello, U. Amato, V., Cuomo, N. Acito, M. Diani, S. Matteoli, G. Corsini, R. Casa, R. De Bonis, G. Laneve and C. Ananasso. 2013. The PRISMA hyperspectral mission: Science, activities and opportunities for agriculture and land monitoring. In *IEEE International Geoscience and Remote Sensing Symposium*, 21–26 July 2013, Melbourne, Australia, pp. 1–5.

Potapov, P., S. Turubanova, M. Hansen, A. Tyukavina, V. Zalles, A. Khan, X. Song, A. Pickens, Q. Shen and J. Cortez. 2022. Global maps of cropland extent and change show accelerated cropland expansion in the twenty-first century. *Nature Food* 3:19–28.

Ranghetti, M., M. Boschetti, L. Ranghetti, G. Tagliabue, C. Panigada, M. Gianinetto, J. Verrelst and G. Candiani. 2023. Assessment of maize nitrogen uptake from PRISMA hyperspectral data through hybrid modelling. *European Journal of Remote Sensing* 56(1):1–18.

Rejith, R., M. Sundararajan, L. Gnanappazham and V. Loveson. 2022. Satellite-based spectral mapping (ASTER and Landsat data) of mineralogical signatures of beach sediments: A precursor insight. *Geocarto International* 37(9):2580–2603.

Ren, J., R. Wang, G. Liu, R. Feng, Y. Wang and W. Wu. 2020. Partitioned relief-F method for dimensionality reduction of hyperspectral images. *Remote Sensing* 12(1104):1–21.

Roberts, D., K. Roth, E. Wetherley, S. Meerdink and R. Perroy. 2018. Hyperspectral vegetation indices. In *Hyperspectral Remote Sensing of Vegetation*, volume II: Hyperspectral Indices and Image Classifications for Agriculture and Vegetation. Taylor and Francis Inc., CRC Press: Boca Raton, FL, pp. 1–24.

Roy, D., V. Kovalskyy, H. Zhang, E. Vermote, L. Yan, S. Kumar and A. Egorov. 2016. Characterization of *Landsat-7* to *Landsat-8* reflective wavelength and normalized difference vegetation index continuity. *Remote Sensing of Environment* 185:57–70

Rußwurm, M., N. Courty, R. Emonet, S. Lefèvre, D. Tuia and R. Tavenard. 2023. End-to-end learned early classification of time series for in-season crop type mapping. *ISPRS Journal of Photogrammetry and Remote Sensing* 196:445–456.

Salem, S., H. Higa, K. Kim, H. Kobayashi, K. Oki and T. Oki. 2017. Assessment of chlorophyll-a algorithms considering different trophic statuses and optimal bands. *Sensors* 17(1746):1–24.

Serrano, L., J. Penuelas, and S. Ustin. 2002. Remote sensing of nitrogen and lignin in Mediterranean vegetation from AVIRIS data: Decomposing biochemical from structural signals. *Remote Sensing of Environment* 81:355–364.

Shaik, R., S. Periasamy and W. Zeng. 2023. Potential assessment of PRISMA hyperspectral imagery for remote sensing applications. *Remote Sensing* 15(1378):1–14.

Sheykhmousa, M., M. Mahdianpari, H. Ghanbari, F. Mohammadimanesh, P. Ghamisi and S. Homayouni. 2020. Support vector machine vs. random forest for remote sensing image classification: A meta-analysis and systematic review. *IEEE Journal of Selected Topics in Applied Earth Observations and Remote Sensing* 13:6308–6325.

Shi, Q., D. He, Z. Liu, X. Liu and J. Xue. 2023. Globe230k: A benchmark dense-pixel annotation dataset for global land cover mapping. *Journal of Remote Sensing* 3:0078.

Stanimirova, R., K. Tarrio, K. Turlej, K. McAvoy, S. Stonebrook, K. Hu, P. Arevalo, E. Bullock, Y. Zhang, C. Woodcock, P. Olofsson, Z. Zhu, C. Barber, C. Souza, S. Chen, J. Wang, F. Mensah, M. Calderon-Loor, M. Hadjikakou, B. Bryan, J. Graesser, D. Beyene, B. Mutasha, S. Siame, A. Siampale and M. Friedl. 2023. A global land cover training dataset from 1984 to 2020. *Scientific Data* 10(879):1–12.

Tagliabue, G., M. Boschetti, G. Bramati, G. Candiani, R. Colombo, F. Nutini, L. Pompilio, J. P. Rivera-Caicedo, M. Rossi, M. Rossini, J. Verrelst and C. Panigada. 2022. Hybrid retrieval of crop traits from multi-temporal PRISMA hyperspectral imagery. *ISPRS Journal of Photogrammetry and Remote Sensing* 187:362–377.

Tamiminia, H., B. Salehi, M. Mahdianpari, L. Quackenbush, S. Adeli and B. Brisco. 2020. Google Earth Engine for geo-big data applications: A meta-analysis and systematic review. *ISPRS Journal of Photogrammetry and Remote Sensing* 164:152–170.

Thenkabail, P., I. Aneece, P. Teluguntla and A. Oliphant. 2021a. Hyperspectral narrowband data propel gigantic leap in the earth remote sensing, highlight article. *Photogrammetric Engineering and Remote Sensing* 87(7):461–467.

Thenkabail, P., Teluguntla, P., Biggs, T., Krishna, M. and Turral, H. 2007. Spectral matching techniques to determine historical land-use/land-cover (LULC) and irrigated areas using time-series 0.1-degree AVHRR Pathfinder datasets. *Photogrammetric Engineering and Remote Sensing* 73(9):1029–1040.

Thenkabail, P., M. Gumma, P. Telaguntla and I. Mohammed. 2014. Hyperspectral remote sensing of vegetation and agricultural crops. *Photogrammetric Engineering and Remote Sensing* 80(4):697–709.

Thenkabail, P., G. Lyon and A. Huete. 2018a. Hyperspectral remote sensing of vegetation. In *Volume I: Fundamentals, sensor systems, spectral libraries, and data mining for vegetation*, pp. 1–449. Taylor and Francis Inc., CRC Press: New York.

Thenkabail, P., G. Lyon and A. Huete. 2018b. Hyperspectral remote sensing of vegetation. In *Volume II: Hyperspectral indices and image classifications for agriculture and vegetation*, pp. 1–296. Taylor and Francis Inc., CRC Press: New York.

Thenkabail, P., G. Lyon. and A. Huete. 2018c. Hyperspectral remote sensing of vegetation. In *Volume III: Biophysical and biochemical characterization and plant species studies*, pp. 1–348. Taylor and Francis Inc., CRC Press: New York.

Thenkabail, P., G. Lyon and A. Huete. 2018d. Hyperspectral remote sensing of vegetation. In *Volume IV: Advanced applications in remote sensing of agricultural crops and natural vegetation*, pp. 1–386. Taylor and Francis Inc., CRC Press: New York.

Thenkabail, P., I. Mariotto, M. Gumma, E. Middleton, D. Landis and K. Huemmrich. 2013. Selection of hyperspectral narrowbands (HNBs) and composition of hyperspectral two band vegetation indices (HVIs) for biophysical characterization and discrimination of crop types using field reflectance and Hyperion/EO-1 data. *IEEE Journal of Selected Topics in Applied Earth Observations and Remote Sensing* 6(2):427–439.

Thenkabail, P., P. Teluguntla, J. Xiong, A. Oliphant, R. Congalton, M. Ozdogan, M. Gumma, J. Tilton, C. Giri, C. Milesi, A. Phalke, M. Massey, K. Yadav, C. Milesi, T. Sankey, Y. Zhong, I. Aneece and D. Foley. 2021b. Global cropland extent product at 30m (GCEP30) derived using Landsat satellite time-series data for the year 2015 through multiple machine learning algorithms on Google Earth Engine (GEE) cloud. In *United States Geological Survey (USGS) Research Paper*, in press.

Tran, K., H. Zhang, J. McMaine, X. Zhang and D. Luo. 2022. 10 m crop type mapping using *Sentinel-2* reflectance and 30 m cropland data layer product. *International Journal of Applied Earth Observations and Geoinformation* 107(102692):1–16.

Tripathi, P. and R. Garg. 2023. Potential of DESIS and PRISMA hyperspectral remote sensing data in rock classification and mineral identification: A7. *Environmental Monitoring and Assessment* 195(5):575.

Tyralis, H. G. Papacharalampous and A. Langousis. 2020. A brief review of random forests for water scientists and practitioners and their recent history in water resources. *Water* 11:1–37.

USDA National Agricultural Statistics Service. 2022. 2021 California Cropland Data 20 Layer — NASS/USDA, Technical report, United States Department of Agriculture, National Agricultural Statistics Service. https://www.nass.usda.gov/ (last date accessed 20 February 2024).

USDA National Agricultural Statistics Service Cropland Data Layer. 2022. Published crop-specific data layer. https://nassgeodata.gmu.edu/CropScape/ (last date accessed 9 June 2022).

Van Tricht, K., J. Degerickx, S. Gilliams, D. Zanaga, M. Battude, A. Grosu, J. Brombacher, M. Lesiv, J.C.L. Bayas, S. Karanam, S. Fritz, I. Becker-Reshef, B. Franch, B. Mollà-Bononad, H. Boogaard, A. K. Pratihast, B. Koetz and Z. Szantoi. 2023. WorldCereal: A dynamic open-source system for global-scale, seasonal, and reproducible crop and irrigation mapping. *Earth System Science Data* 15(12):5491–5515.

Vivone, G., A. Garzelli, Y. Xu, W. Liao and J. ChanussotJ. 2023. Panchromatic and hyperspectral image fusion: Outcome of the 2022 WHISPERS hyperspectral pansharpening challenge. *IEEE Journal of Selected Topics in Applied Earth Observations and Remote Sensing* 16:166–179.

Wijewardane, N. K., H. Zhang, J. Yang, J. C. Schnable, D. P., Schachtman and Y. Ge. 2023. A leaf-level spectral library to support high-throughput plant phenotyping: Predictive accuracy and model transfer. *Journal of Experimental Botany* 74(14):4050–4062.

Xie, B., L. Wu, W. Mao, S. Zhou and S. Liu. 2022. An open integrated Rock Spectral Library (RockSL) for a global sharing and matching service. *Minerals* 12(2):191–211.

You, N., J. Dong, J. Li, J. Huang and Z. Jin. 2023. Rapid early-season maize mapping without crop labels. *Remote Sensing of Environment* 290:113496.

Yu, H., B. Kong, Y. Hou, X. Xu, T. Chen and X. Liu. 2022. A critical review on applications of hyperspectral remote sensing in crop monitoring. *Experimental Agriculture* 58(e26):1–18.

Zhang, C., L. Di, L. Lin, H. Li, L. Guo., Z. Yang, E. Yu, Y. Di and A. Yang. 2022. Towards automation of in-season crop type mapping using spatiotemporal crop information and remote sensing data. *Agricultural Systems* 201:103462.

In-Press Articles

Remote sensing tailing pond image detection method based on YOLOv8-RVSW
ZhengJun Dang and Kun Li

Monitoring LULC Changes in Babil Province for Sustainable Development Purposes Within the Period 2004–2023
Hayder Hameed Jassoom and Rabab Saadoon Abdoon

Spatiotemporal Behavior of Active Forest Fires Using Time-Series MODIS C6 Data
Syed Azimuddin and R.S. Dwivedi

Landslide Evolution Assessment Based on Sequential InSAR Methods in the Kunming Transmission Line Corridor
Gang Wen, Yizuo Li, Chuhang Xie, Zezhong Zheng, Yi Ma, Fangrong Zhou, Baiyan Su, and Huahui Tang

A Variable-Iterative Fully Convolutional Neural Network for Sparse Unmixing

Fanqiang Kong, Zhijie Lv, Kun Wang, Xu Fang, Yuhan Zheng, and Shengjie Yu

Abstract

Neural networks have greatly promoted the development of hyperspectral unmixing (HU). Most data-driven deep networks extract features of hyperspectral images (HSIs) by stacking convolutional layers to achieve endmember extraction and abundance estimation. Some model-driven networks have strong interpretability but fail to mine the deep feature. We propose a variable-iterative fully convolutional neural network (VIFCNN) for sparse unmixing, combining the characteristics of these two networks. Under the model-driven iterative framework guided by sparse unmixing by variable splitting and augmented lagrangian (SUnSAL), a data-driven spatial-spectral feature learning module and a spatial information updating module are introduced to enhance the learning of data information. Experimental results on synthetic and real datasets show that VIFCNN significantly outperforms several traditional unmixing methods and two deep learning–based methods. On real datasets, our method improves signal-to-reconstruction error by 17.38%, reduces abundance root-mean-square error by 25.24%, and reduces abundance spectral angle distance by 31.40% compared with U-ADMM-BUNet.

Introduction

Hyperspectral remote sensing combines imaging and spectral technologies, using many narrow and continuous spectral bands to generate 3D hyperspectral images (HSIs). HSIs have been widely used in mineral exploration (Peyghambari and Zhang 2021), target detection (Shang *et al.* 2021), agricultural monitoring (Lu *et al.* 2020), and military surveillance (Tu *et al.* 2022). Compared with visible light image, which only records information in the range of 0.38–0.76 μm, HSIs usually include hundreds or thousands of bands, which means the spectral resolution of HSIs is very high. However, the limitations of optical components make the spatial resolution of HSIs low, resulting in one pixel containing the reflection spectra of multiple objects (Villa *et al.* 2011), which makes it difficult to distinguish the types of objects spatially. Such a pixel containing the reflectance spectra of multiple ground materials is called a mixed pixel. Hyperspectral unmixing (HU) technology is designed to decompose mixed pixels into endmember spectral curves and corresponding abundance coefficients.

According to different mixing modes of mixed pixels, hyperspectral mixing models can be divided into linear mixing models (LMMs) and nonlinear mixing models (NLMMs). The NLMM considers each mixed-pixel spectrum as a nonlinear combination of related endmember spectra, which is more in line with the realistic situation (Dobigeon *et al.* 2014). It is suitable for fine spectral analysis but is difficult to model. The LMM assumes that the spectra of the mixed pixels are all linear combinations of the spectra of each endmember. It is the most widely used unmixing model for mixed pixels because of its simplicity and clear physical meaning (Dobigeon *et al.* 2009). In addition, the abundance coefficients in LMM usually satisfy the abundance nonnegativity constraints (ANC) and abundance sum-to-one constraints (ASC). The HU process based on the LMM involves two tasks: endmember extraction and abundance estimation. Many endmember extraction algorithms have been proposed, such as vertex component analysis (Nascimento and Dias 2005) based on pure pixel assumptions, and simplex volume maximization (Heylen *et al.* 2011) based on data clustering. Subsequently, abundance estimation methods such as fully constrained least squares (FCLS) (Heinz and Chang 2001) and sparse unmixing by variable splitting and augmented Lagrangian (SUnSAL) (Bioucas-Dias and Figueiredo 2010) are used to calculate the proportion of each endmember contained in the mixed pixel.

HU is divided into sparse unmixing and blind unmixing according to whether there is an a priori spectral library. Blind unmixing enables simultaneous endmember extraction and abundance estimation (Palsson *et al.* 2022). For example, the popular nonnegative matrix factorization (NMF) (Lee and Seung 1999) maps the unmixing problem to the matrix factorization problem by imposing nonnegative constraints on endmembers and abundances. However, if pure pixels do not exist in HSI, NMF may extract virtual endmembers, leading to distortion of abundance estimation. In sparse unmixing, the use of spectral libraries avoids the problem of inaccurate endmember extraction (Chen *et al.* 2024).

Typically, the sparse regression method describes the unmixing problem as an optimization problem of a convex function, and then uses the alternating direction method of multipliers (ADMM) (Boyd *et al.* 2011) or the alternating least squares method (Lin 2007) for solution. Convex relaxation-based methods approximate the l0-norm combinatorial optimization problem to the l_1-norm convex optimization problem. This transformation converts the non-deterministic polynomial-time hard (NP-hard) (Natarajan 1995) problem into a convex optimization problem that is easy to solve. Representative convex optimization algorithms include the SUnSAL algorithm with l_1 regularization on the abundance matrix, the collaborative SUnSAL with $l_{2,1}$ regularization (Iordache *et al.* 2014), the SUnSAL-TV (Iordache *et al.* 2012), which integrates spatial information using total variation regularization, and spectral-spatial weighted sparse unmixing (S^2WSU) (Zhang *et al.* 2018), which uses both spatial and spectral weighting factors. The convex optimization method obtains an approximate solution to the sparse unmixing problem rather than an exact solution, and the sparsity of the abundance results obtained is not the best. Therefore, some scholars have proposed greedy algorithm–based sparse unmixing methods. This approach reduces the redundancy of the spectral library, making the estimated abundances sparser. Classical greedy algorithms include subspace matching pursuit

Fanqiang Kong, Yuhan Zheng, and Shengjie Yu are with the College of Astronautics, Nanjing University of Aeronautics and Astronautics, Nanjing, China.

Zhijie Lv is with the College of Astronautics, Nanjing University of Aeronautics and Astronautics, Nanjing, China.

Kun Wang is with the First Military Representative Office of Empty Equipment, Wuxi, China.

Xu Fang is with AVIC Leihua Electronic Technology Research, Wuxi, China.

Corresponding author: Zhijie Lv (zhijie_2022@nuaa.edu.cn)

Received March 25, 2024, accepted June 20, 2024.

Photogrammetric Engineering & Remote Sensing
Vol. 90, No. 11, November 2024, pp. 699–706.
0099-1112/22/699–706

doi: 10.14358/PERS.24-00038R2

PEER-REVIEWED CONTENT
IS ONLY AVAILABLE TO
ASPRS MEMBERS AND SUBSCRIBERS

FOR MORE INFORMATION VISIT
MY.ASPRS.ORG

PEER-REVIEWED CONTENT
IS ONLY AVAILABLE TO
ASPRS MEMBERS AND SUBSCRIBERS

FOR MORE INFORMATION VISIT
MY.ASPRS.ORG

PEER-REVIEWED CONTENT
IS ONLY AVAILABLE TO
ASPRS MEMBERS AND SUBSCRIBERS

FOR MORE INFORMATION VISIT
MY.ASPRS.ORG

PEER-REVIEWED CONTENT
IS ONLY AVAILABLE TO
ASPRS MEMBERS AND SUBSCRIBERS

FOR MORE INFORMATION VISIT
MY.ASPRS.ORG

PEER-REVIEWED CONTENT IS ONLY AVAILABLE TO ASPRS MEMBERS AND SUBSCRIBERS

FOR MORE INFORMATION VISIT MY.ASPRS.ORG

PEER-REVIEWED CONTENT
IS ONLY AVAILABLE TO
ASPRS MEMBERS AND SUBSCRIBERS

FOR MORE INFORMATION VISIT
MY.ASPRS.ORG

PEER-REVIEWED CONTENT
IS ONLY AVAILABLE TO
ASPRS MEMBERS AND SUBSCRIBERS

FOR MORE INFORMATION VISIT
MY.ASPRS.ORG

SUSTAININGMEMBERS

Applanix
Richmond Hill, Ontario, Canada
http://www.applanix.com
Member Since: 7/1997

Ayres Associates
Madison, Wisconsin
www.AyresAssociates.com
Member Since: 1/1953

Dewberry
Fairfax, Virginia
www.dewberry.com
Member Since: 1/1985

Digital Mapping, Inc.(DMI)
Huntington Beach, California
www.admap.com
Member Since: 4/2002

Environmental Research Incorporated
Linden, Virginia
www.eri.us.com
Member Since: 8/2008

Esri
Redlands, California
www.esri.com
Member Since: 1/1987

GeoCue Group
Madison, Alabama
http://www.geocue.com
Member Since: 10/2003

GeoDyn GmbH
Munich, Germany
www.geodyn.com/index
Member Since: 3/2024

Geographic Imperatives LLC
Centennial, Colorado
Member Since: 12/2020

GPD Group
Columubs, Ohio
https://gpdgroup.com/
Member Since: 7/2024

GPI Geospatial Inc.
Orlando, Florida
www.aca-net.com
Member Since: 1/1994

Halff Associates, Inc.
Richardson, Texas
https://halff.com/
Member Since: 8/2020

Keystone Aerial Surveys, Inc.
Philadelphia, Pennsylvania
http://www.kasurveys.com
Member Since: 1/1985

Kucera International
Willoughby, Ohio
www.kucerainternational.com
Member Since: 1/1992

L3Harris Technologies
Broomfield, Colorado
www.l3harris.com
Member Since: 6/2008

Leica Geosystems AG
Heerbrugg, Switzerland
https://leica-geosystems.com/en-us/
Member Since: 1/1990

Merrick & Company
Greenwood Village, Colorado
www.merrick.com
Member Since: 4/1995

Miller Creek Associates
SeaTac Washington
www.mcamaps.com
Member Since: 12/2014

NV5 Geospatial
Sheboygan Falls, Wisconsin
www.quantumspatial.com
Member Since: 1/1974

Pickett and Associates, Inc.
Bartow, Florida
www.pickettusa.com
Member Since: 4/2007

PixElement
Belmont, Michigan
https://pixelement.com
Member Since: 2/2017

Riegl USA, Inc.
Orlando, Florida
https://www.rieglusa.com
Member Since: 11/2004

Sanborn Map Company
Colorado Springs, Colorado
www.sanborn.com
Member Since: 10/1984

Surdex Corporation
(a Bowman company)
Chesterfield, Missouri
www.surdex.com
Member Since: 12/2011

Surveying And Mapping, LLC (SAM)
Austin, Texas
www.sam.biz
Member Since: 12/2005

T3 Global Strategies, Inc.
Bridgeville, Pennsylvania
https://t3gs.com/
Member Since: 6/2020

Towill, Inc.
San Francisco, California
www.towill.com
Member Since: 1/1952

U.S. Dept. of Commerce/NOAA/NOS/ National Geodetic Survey
Chesapeake, Virginia
https://www.ngs.noaa.gov/
Member Since: 7/2009

U.S. Geological Survey
Reston, Virginia
https://www.usgs.gov/
Member Since: 4/2002

Woolpert LLP
Dayton, Ohio
www.woolpert.com
Member Since: 1/1985

***PE&RS* READERSHIP HIGHLIGHTS**

ASPRS is in the Top 10!

In March, April, and May, 2024, *PE&RS* ranked 9th, 8th, and 9th, respectively, out of over 11,000 journals for full-text downloads with Ingenta Connect.

Circulation: 2,500

Total audience: 5,000*

Digital Edition Monthly Unique Views: 2,000+

Professional Demographics

Work Setting	% Composition
Corporate	30%
Academia	30%
Government	26%
Sole Proprietor	13%

Education	% Composition
Doctorate degree	32%
Post graduate degree	45%
4-year college degree	19%
2-year college degree	4%

ASPRS Certifications	Amount
ASPRS Certified Photogrammetrists	290+
ASPRS Certified Mapping Scientists†	130+
ASPRS Certified Technologists	40+

†Includes our new and fast-growing Lidar certification

asprs THE IMAGING & GEOSPATIAL INFORMATION SOCIETY

Founded in 1934, the American Society for Photogrammetry and Remote Sensing (ASPRS) is a scientific association serving professional members throughout the world. Our mission is to advance knowledge and improve understanding of mapping sciences to promote the responsible applications of photogrammetry, remote sensing, geographic information systems (GIS), and supporting technologies.

Our members are analysts/specialists, educators, engineers, managers/administrators, manufacturers/ product developers, operators, technicians, trainees, marketers, and scientists/ researchers. Employed in the disciplines of the mapping sciences, they work in the fields of Agriculture/Soils, Archeology, Biology, Cartography, Ecology, Environment, Forestry/ Range, Geodesy, Geography, Geology, Hydrology/Water Resources, Land Appraisal/ Real Estate, Medicine, Transportation, and Urban Planning/Development.

*Based on 2 readers per copy as well as online views| Source: *PE&RS* Readership Survey, Summer 2023

PE&RS Media Kit

PE&RS 2025 Advertising Rates & Specs

THE MORE YOU ADVERTISE THE MORE YOU SAVE! PE&RS offers frequency discounts. Invest in a three-times per year advertising package and receive a 5% discount, six-times per year and receive a 10% discount, 12-times per year and receive a 15% discount off the cost of the package.

	Sustaining Member Exhibiting at a 2025 ASPRS Conference	**Sustaining Member**	**Exhibitor**	**Non Member**
All rates below are for four-color advertisments				
Cover 1	$1,850	$2,000	$2,350	$2,500
In addition to the cover image, the cover sponsor receives a half-page area to include a description of the cover (maximum 500 words). The cover sponsor also has the opportunity to write a highlight article for the journal. Highlight articles are scientific articles designed to appeal to a broad audience and are subject to editorial review before publishing.				
Cover 2	$1,500	$1,850	$2,000	$2,350
Cover 3	$1,500	$1,850	$2,000	$2,350
Cover 4	$1,850	$2,000	$2,350	$2,500
Advertorial	1 Complimentary Per Year	1 Complimentary Per Year	$2,150	$2,500
Full Page	$1,000	$1,175	$2,000	$2,350
2 page spread	$1,500	$1,800	$3,200	$3,600
2/3 Page	$1,100	$1,160	$1,450	$1,450
1/2 Page	$900	$960	$1,200	$1,200
1/3 Page	$800	$800	$1,000	$1,000
1/4 Page	$600	$600	$750	$750
1/6 Page	$400	$400	$500	$500
1/8 Page	$200	$200	$250	$250
Other Advertising Opportunities (see page 5 for full descriptions)				
Employment Promotion	$500 (30 day web + 1 email) $300 (30 day web)	$500 (30 day web + 1 email) $300 (30 day web)	$500 (30 day web + 1 email) $300 (30 day web)	$500 (30 day web + 1 email) $300 (30 day web)
Dedicated Content Email blast	$2,500	$2,500	$2,500	$2,500
Newsletter Display Advertising	1 Complimentary Per Year	1 Complimentary Per Year	$500	$500
PE&RS Announcement E-Mail	$1000	$1000	$1000	$1000

A 15% commission is allowed to recognized advertising agencies

Ad Size	Width	Height
Cover	8.625”	11.25”
Full Page	8.375”	10.875”
2/3 Page Horizontal	7.125”	6.25”
2/3 Page Vertical	4.58”	9.625”
1/2 Page Horizontal	7.125”	4.6875”
1/2 Page Vertical	3.4375”	9.625”
1/3 Page Horizontal	7.125”	3.125”
1/3 Page Vertical	2.29”	9.625”
1/4 Page Horizontal	7.125”	2.34”
1/4 Page Vertical	3.4375”	4.6875”
1/8 Page Horizontal	7.125”	1.17”
1/8 Page Vertical	1.71875”	4.6875”

Send ad materials to:
Rae Kelley (rkelley@asprs.org)

- Publication Size: 8.375” × 10.875” (W x H)
- Live area: 1/2” from gutter and 3/8” from all other edges
- Software Used: PC InDesign
- Supported formats: TIFF, EPS, BMP, JPEG, PDF, PNG PC InDesign, Illustrator, and Photoshop

For more information, contact Bill Spilman at bill@innovativemediasolutions.com | (877) 878-3260 toll-free | (309) 483-6467 direct | (309) 483-2371 fax

Special Advertising Opportunities

FRONT COVER SPONSORSHIP

A PE&RS cover sponsorship is a unique opportunity to capture the undivided attention of your target market through three premium points of contact.

1— *PE&RS* FRONT COVER

(Only twelve available, first-come, first-served)
PE&RS is world-renowned for the outstanding imagery displayed monthly on its front cover—and readers have told us they eagerly anticipate every issue. This is a premium opportunity for any company, government agency, university or non-profit organization to provide a strong image that demonstrates their expertise in the geospatial information industry.

2— FREE ACCOMPANYING "HIGHLIGHT" ARTICLE

A detailed article to enhance your cover image is welcome but not a condition of placing an image. Many readers have asked for more information about the covers and your article is a highly visible way to tell your story in more depth for an audience keenly interested in your products and services. No article is guaranteed publication, as it must pass ASPRS editorial review. For more information, contact Rae Kelley at rkelley@asprs.org.

3— FREE TABLE OF CONTENTS COVER DESCRIPTION

Use this highly visible position to showcase your organization by featuring highlights of the technology used in capturing the front cover imagery. Limit 200-word description.

Terms: Fifty percent nonrefundable deposit with space reservation and payment of balance on or before materials closing deadline.

Cover Specifications: 8 3/8" × 10 7/8"

PRICING

	Sustaining Member Exhibiting at a 2025 ASPRS Conference	Sustaining Member	Exhibitor	Non Member
Cover 1	$1,850	$2,000	$2,350	$2,500

VENDOR SEMINARS

ASPRS Sustaining Members now have the opportunity to hold a 1-hour informational session as a Virtual Vendor Seminar that will be free to all ASPRS Members wishing to attend. There will be one opportunity per month to reach out to all ASPRS Members with a demonstration of a new product, service, or other information. ASPRS will promote the Seminar through a blast email to all members, a notice on the ASPRS web site home page, and ads in PE&RS.

The Virtual Seminar will be hosted by ASPRS through its Zoom capability and has the capacity to accommodate 500 attendees.

Vendor Seminars	
Fee	$2,500 (no discounts)

DIGITAL ADVERTISING OPPORTUNITIES

EMPLOYMENT PROMOTION

When you need to fill a position right away, use this direct, right-to-the-desktop approach to announce your employment opportunity. The employment opportunity will be sent once to all ASPRS members in our regular Wednesday email newsletter to members, and will be posted on the ASPRS Web site for one month. This type of advertising gets results when you provide a web link with your text.

Employment Opportunity	Net Rate
30-Day Web + 1 email	$500/opportunity
Web-only (no email)	$300/opportunity

Do you have multiple vacancies that need to be filled? Contact us for pricing details for multiple listings.

NEWSLETTER DISPLAY ADVERTISING

Your vertical ad will show up in the right hand column of our weekly newsletter, which is sent to more than 3,000 people, including our membership and interested parties. **Open Rate: 32.9%**

Newsletter vertical banner ad	Net Rate
180 pixels x 240 pixels max	$500/ opportunity

DEDICATED CONTENT EMAIL BLAST

Send a dedicated email blast to the ASPRS email list. Advertiser supplies HTML (including images). Lead time: 14 days.

Materials	Net Rate
Advertiser supplies HTML, including images.	$3000/ opportunity

Digital Edition Announcement E-Mail: 5,800+
PE&RS is available online in both a public version that is available to anyone but does not include the peer-reviewed articles, and a full version that is available to ASPRS members only upon login.

The enhanced version of PE&RS contains hot links for all ASPRS Sustaining Member Companies, as well as hot links on advertisements, ASPRS Who's Who, and internet references.

Become a sponsor today!
The e-mail blast sponsorship opportunity includes a **180 x 240 pixel ad** in the email announcement that goes out to our membership announcing the availability of the electronic issue.

Digital Edition Opportunities	Net Rate
E-mail Blast Sponsorship*	$1,000

For more information, contact Bill Spilman at bill@innovativemediasolutions.com | (877) 878-3260 toll-free | (309) 483-6467 direct | (309) 483-2371 fax

PE&RS Media Kit

Conference Advertising Opportunities

Every year ASPRS holds an **Annual Conference** as an in-person event, in addition to a **Virtual Technical Symposium**. There are exciting advertising opportunites available for each.

Our Attendees are people you need to reach! You'll meet face-to-face with decision makers who have budget authority from top organizations utilizing your products and services. Land remote sensing data users, researchers, applications scientists, producers, managers and policymakers participate in this important conference.

Maximize the benefits of your participation by becoming a conference sponsor. Your company can make its mark and gain visibility before, during and after the event. Choose from our list of Unique Sponsorships for the events or items that best showcase your company. If you are interested in a sponsorship not shown here, speak with our sales representative and he will be happy to work with your needs and desires for a mutually beneficial opportunity.

ANNUAL CONFERENCE at GEO WEEK ADVERTISING OPPORTUNITIES

Sponsor an ASPRS Workshop

Sponsoring an ASPRS Workshop is an excellent way to reach a targeted audience of attendees seeking professional development.

Your support for an ASPRS workshop shows your commitment to promote unbiased educational materials to the professional community. Your support also helps ASPRS offset a portion of cost of the A/V equipment for the workshop and provide a small honorarium for the workshop instructors who volunteer their preparation time and travel.

Each workshop sponsor will receive:

1. Recognition on ASPRS website
2. Recognition in ASPRS enewsletter
3. Recognition in ASPRS conference program (printed handout)
4. Session moderator thanks sponsor in introductory remarks with logo on screen
5. Logo and sponsorship noted in workshop handouts
6. Area in workshop classroom for promotional materials

Day Sponsor

Each Day Sponsor opportunity will include

1. Logo on program website
2. eBlast announcement to all conference attendees on sponsored day. Announcement will include a 50-word description and logo.
3. 30-second video at the beginning of sponsored day.
4. Logo on opening slide of all 4-5 sessions throughout the sponsored day and sponsor acknowledgement.

Single Session Sponsor

Each Single Session Sponsor opportunity will include

1. Logo on program website
2. Logo on opening slide of the session and sponsor acknowledgement.

Break Sponsorship

Coffee and sodas will be available for workshop participants. Take this time, as the workshop participants enjoy a break, to promote your company and products.

VIRTUAL TECHNICAL SYMPOSIUM ADVERTISING OPPORTUNITIES

This format is an attractive, convenient presentation venue for remote sensing professionals globally who are unable to travel. This year, ASPRS will be offering a select number of Vendor Spotlight opportunities. "This is an excellent opportunity to reach ASPRS Conference attendees and to invite non-attendees to participate in a vendor product demonstration," said Karen Schuckman, Managing Director, ASPRS.

Vendor Spotlight/Product Demo

Each Vendor Spotlight/Product Demo will include

1. 30-minute time slot available during conference week
2. Vendor Spotlight/Product Demo listed in the conference program
3. Free for conference and non-conference attendees. There will be separate URL for each Vendor Spotlight/Product Demo
4. List of Vendor Spotlight/Product Demo attendees supplied to vendor at the end of the conference.

Day Sponsor

Each Day Sponsor opportunity will include

1. Logo on program website
2. eBlast announcement to all conference attendees on sponsored day. Announcement will include a 50-word description and logo.
3. 30-second video at the beginning of sponsored day.
4. Logo on opening slide of all 4-5 sessions throughout the sponsored day and sponsor acknowledgement.

Single Session Sponsor

Each Single Session Sponsor opportunity will include

1. Logo on program website
2. Logo on opening slide of the session and sponsor acknowledgement.

For more prices & a full list of opportunities,
contact Bill Spilman at bill@innovativemediasolutions.com
(877) 878-3260 toll-free, (309) 483-6467 direct, (309) 483-2371 fax